

ORNL/TM--9920

DE86 012605

MASTER

ORNL/TM-9920

ENVIRONMENTAL SCIENCES DIVISION

DETrital MICROBIAL COMMUNITY DEVELOPMENT AND PHOSPHORUS
DYNAMICS IN A STREAM ECOSYSTEM¹

R. E. Perkins,² J. W. Elwood, and G. S. Sayler³

Environmental Sciences Division
Publication No. 2643

¹Submitted as a thesis by R. E. Perkins to the Graduate Council of the University of Tennessee in partial fulfillment of the requirements for the degree of Doctor of Philosophy in Microbiology.

²Present address: Department of Microbiology, School of Medicine, East Carolina University, Greenville, North Carolina 27834.

³University of Tennessee, Knoxville, Tennessee 37916.

Date Published - June 1986

Prepared for the
National Science Foundation Ecosystem Studies Program

Prepared by the
OAK RIDGE NATIONAL LABORATORY
Oak Ridge, Tennessee 37831
operated by
MARTIN MARIETTA ENERGY SYSTEMS, INC.
for the
U.S. DEPARTMENT OF ENERGY
under Contract No. DE-AC05-84OR21400

DISTRIBUTION OF THIS DOCUMENT IS UNLIMITED

EP

TABLE OF CONTENTS

SECTION	PAGE
I. LITERATURE REVIEW	1
Decomposition of Leaf Litter.	2
Phosphorus Dynamics	7
II. OBJECTIVES.	29
III. EXPERIMENTAL APPROACH	30
IV. MATERIALS AND METHODS	32
Miscellaneous Materials	32
Radionuclides	32
Preliminary Studies	33
Closed-system phosphorus uptake	33
Homogenization time course study.	34
Bacterial removal efficiency.	34
Analytical recovery of cellular components.	35
Microbial Biomass and Cell Density.	36
Adenosine triphosphate (ATP).	36
Acridine orange direct counts (AODC).	37
Colonization Study.	38
Heterotrophic activity determination.	38
Fixation method for scanning electron microscopy observation	41
Analysis of Phosphorus Tracer Labeled Cellular Pools.	41
Whole cell radioactivity.	41
Phospholipid extraction procedure	42
Fractionation of intracellular phosphorus components.	42
Radioactivity Quantitation.	46
Phosphorus Dynamics of a Detrital Microbial Community	47
Laboratory streams description.	51
Radiolabeled phosphate release.	53
Stream sampling for fractionation of CPOM	54
Phosphate analysis.	54
Leaf mass	55
Data analysis	55
V. RESULTS	57
Preliminary Studies	57
Analytical Recovery Efficiencies for Intracellular Phosphorus Pools.	64
Microbial Colonization of Leaf CPOM	67
Glucose metabolism and metabolic activity of CPOM associated microbial communities.	67
CPOM mass (organic content)	75
Scanning electron microscopy of CPOM.	77

SECTION	PAGE
Dogwood CPOM.	77
Maple CPOM.	79
Oak CPOM.	83
Phosphorus Dynamics of CPOM Associated Microbial Communities	90
Phosphorus Dynamics of a Red Maple CPOM Microbial Community	94
Microbial Biomass	94
Phosphorus Incorporation Rates.	97
Area-specific rates	97
ATP-specific phosphorus incorporation rates	97
³³ P Distribution in the Intracellular Pools	105
Phosphorus Turnover Rate Constants.	107
ATP-specific phosphorus turnover rate constants	111
Area-specific phosphorus turnover rate constants.	111
Phosphorus Turnover Rate.	111
Phosphorus Dynamics in an Ungrazed and Grazed Oak CPOM Microbial Community	116
CPOM Organic Content.	116
Stream Orthophosphate Concentration	118
Stream Water Temperature.	118
Microbial Biomass and Bacterial Cell Density.	118
Physiological Activity of an Ungrazed and Grazed Microbial Community	124
Phosphorus Incorporation Rates.	124
Comparison of Phosphate Accumulation for an Ungrazed and Grazed Oak CPOM Microbial Community	128
Distribution of ³³ P in the Intracellular Pools.	128
Phosphorus Turnover Kinetics for an Oak CPOM Microbial Community	131
Phosphorus Turnover Rate Constants for Synthesis.	131
Area-specific phosphorus turnover rate constants for synthesis	138
Cell-specific phosphorus turnover rate constants for synthesis	139
ATP-specific phosphorus turnover rate constants for synthesis	140
Turnover Rates.	140
Area-specific turnover rates.	140
Cell-specific turnover rate	141
ATP-specific turnover rates	144
VI. DISCUSSION	146
Microbial Community Development and Activity	147
Physiological Status	151
Detrital Community Phosphorus Dynamics	153
Influence of Grazing	158
Contribution to Phosphorus Spiraling	162

SECTION	PAGE
VII. SUMMARY	166
VIII. CONCLUSIONS	169
LIST OF REFERENCES	171

DISCLAIMER

This report was prepared as an account of work sponsored by an agency of the United States Government. Neither the United States Government nor any agency thereof, nor any of their employees, makes any warranty, express or implied, or assumes any legal liability or responsibility for the accuracy, completeness, or usefulness of any information, apparatus, product, or process disclosed, or represents that its use would not infringe privately owned rights. Reference herein to any specific commercial product, process, or service by trade name, trademark, manufacturer, or otherwise does not necessarily constitute or imply its endorsement, recommendation, or favoring by the United States Government or any agency thereof. The views and opinions of authors expressed herein do not necessarily state or reflect those of the United States Government or any agency thereof.

LIST OF FIGURES

FIGURE	PAGE
1. Schematic Representation of Nutrient Cycling Models.	20
2. Schematic Representation of Nutrient Spiraling in a Stream Ecosystem.	22
3. Glucose Uptake System.	39
4. Fractionation Scheme for Microbial Phosphorus Pools.	43
5. Experimental Protocol Used for Phosphorus Dynamics Studies .	48
6. Schematic Representation of the Phosphorus Dynamics Associated with a Microbial Community.	50
7. Artificial Streams at Oak Ridge National Laboratory, Environmental Sciences Division.	52
8. Phosphate Uptake by Microbiota Associated with Decomposing Red Maple CPOM Established for 19 Days	59
9. Kinetics of Phosphate Removal by Microbiota Associated with Red Maple CPOM Established for 19 Days	61
10. Phosphorus Uptake by Microbiota Associated with Red Maple CPOM Established for 31 Days	62
11. Incorporation of Phosphate into Phospholipid	65
12. Temporal Patterns of Glucose Uptake (i.e., Assimilated Plus Mineralized) Rates by Decomposing Leaf CPOM.	70
13. Temporal Pattern for Glucose Assimilation Rates by Decomposing Leaf CPOM	71
14. Temporal Pattern for Glucose Mineralization Rates for Decomposing Leaf CPOM.	72
15. Temporal Pattern for CPOM of Percentage of Glucose Uptake Which Was Mineralized.	73
16. Temporal Pattern of Leaf CPOM Organic Content as Measured by Ash-Free Dry Weight (AFDW).	76
17. Dogwood Leaf CPOM, Day 0 to Day 3.	78

FIGURE	PAGE
18. Dogwood Leaf CPOM, Days 7 to 22.	80
19. Dogwood Leaf CPOM, Days 22 to 29	81
20. Dogwood Leaf CPOM, Days 22 to 44	82
21. Maple Leaf CPOM, Days 0 to 7	84
22. Maple Leaf CPOM, Days 3 to 10.	85
23. Maple Leaf CPOM, Days 15 to 29	86
24. Maple Leaf CPOM, Days 36 to 56	87
25. Oak Leaf CPOM, Days 0 to 10.	88
26. Oak Leaf CPOM, Days 15 to 22	89
27. Oak Leaf CPOM, Days 29 to 36	91
28. Oak Leaf CPOM, Days 36 to 56	92
29. Temporal Pattern of ATP Biomass for Maple Leaf CPOM Microbial Community.	95
30. Area-Specific Incorporation of Phosphorus into Whole Cell Phosphorus (WC-P) Pool of an Ungrazed Microbial Community Associated with Maple CPOM	99
31. Area-Specific Incorporation of Phosphorus into Metabolite Pool Phosphorus (MP-P) and Lipid Phosphorus (L-P) Pools of an Ungrazed Microbial Community Associated with Maple CPOM.	100
32. Area-Specific Incorporation of Phosphorus into the Deoxyribonucleic Acid Phosphorus (DNA-P) and Ribonucleic Acid Phosphorus (RNA-P) Pools of an Ungrazed Microbial Community Associated with Maple CPOM.	101
33. ATP-Specific Phosphorus Incorporation into Lipid Phosphorus (L-P) and Whole Cell Phosphorus (WC-P) Pools of an Ungrazed Microbial Community Associated with Maple CPOM	102
34. ATP-Specific Incorporation of Phosphorus into Deoxyribonucleic Acid Phosphorus (DNA-P) and Metabolite Pool Phosphorus (MP-P) Pools of an Ungrazed Microbial Community Associated with Maple CPOM	103

FIGURE	PAGE
35. ATP-Specific Incorporation of Phosphorus into Ribonucleic Acid Phosphorus (RNA-P) Pool by an Ungrazed Microbial Community Associated with Maple CPOM	104
36. Incorporation of ^{33}P (as ng P cm^{-2}) into the Whole Cell Phosphorus (WC-P) Pool of an Ungrazed Maple CPOM Microbial Community Before and After Isotopic Equilibrium Was Achieved	108
37. Incorporation of ^{33}P (as ng P cm^{-2}) into the Lipid Phosphorus (L-P) Pool of an Ungrazed Microbial Community Associated with Maple CPOM Before and After Isotopic Equilibrium Was Achieved	109
38. Phosphorus Turnover Kinetics for WC-P pool for ^{33}P and ^{32}P of an Ungrazed Maple CPOM Microbial Community.	113
39. Phosphorus Turnover Kinetics of the L-P pool for ^{33}P and ^{32}P (as ng P cm^{-2}) for an Ungrazed Maple CPOM Microbial Community.	114
40. Temporal Pattern of ATP Biomass for an Ungrazed and a Grazed Oak CPOM Microbial Community.	122
41. Temporal Pattern of Bacterial Cell Density for an Ungrazed and a Grazed Oak CPOM Microbial Community.	123
42. Incorporation of ^{33}P (as ng P cm^{-2}) into L-P Pool of a Grazed Microbial Community Associated with Oak CPOM Before and After Isotopic Equilibrium Was Achieved.	132
43. Incorporation of ^{33}P (as ng P cm^{-2}) in WC-P Pool of a Grazed Microbial Community Associated with Oak CPOM Before and After Isotopic Equilibrium Was Achieved.	133
44. Incorporation of ^{33}P (as ng P cm^{-2}) into L-P Pool of an Ungrazed Microbial Community Associated with Oak CPOM Before and After Isotopic Equilibrium Was Achieved.	134
45. Incorporation of ^{33}P (as ng P cm^{-2}) into WC-P Pool of an Ungrazed Microbial Community Associated with Oak CPOM Before and After Isotopic Equilibrium Was Achieved.	135
46. Postulated Effects of Different Interactions Between Nutrient Spiraling and Biological Activity	163

LIST OF TABLES

TABLE	PAGE
1. Dissolved Phosphorus Forms of Possible Significance in Natural Waters	9
2. Solid Phase Forms of Phosphorus of Possible Significance in Natural Water Systems	10
3. Comparison of Stomacher Homogenation Times for the Removal of Bacteria from the Leaf Surface.	58
4. Abiotic Adsorption of Phosphate to Maple Leaf CPOM in Closed Systems.	66
5. Recovery of Standards During CPOM Fractionation.	68
6. Glucose Metabolism by Microbes Associated with Decomposing Dogwood, Maple, and Oak CPOM	69
7. Comparison of Initial Phosphorus Incorporation Rates for a Maple Leaf Detrital Microbial Community.	98
8. ^{33}P Distribution for the Period of Isotopic Equilibrium in the Intracellular Phosphorus Pools (as % of WC-P) for Maple CPOM Microbial Community	106
9. Comparison of Phosphorus Turnover Rate Constants for Synthesis for a Maple Detrital Microbial Community	110
10. Comparison of Phosphorus Turnover Rates for Degradation for a Maple Leaf Detrital Microbial Community.	115
11. Comparison of the Organic Content of Oak CPOM for an Ungrazed and a Grazed Stream	117
12. Comparison of SRP Concentration in Water in the Ungrazed and Grazed Stream	119
13. Comparison of Microbial Biomass Associated with Oak CPOM in an Ungrazed and Grazed Stream Channel.	121
14. Comparison of Calculated ATP Content Per Cell for an Ungrazed and a Grazed Oak CPOM Microbial Community	125
15. Comparison of Initial Phosphorus Incorporation Rates for an Ungrazed and a Grazed Oak Leaf Detrital Microbial Community. .	126

TABLE	PAGE
16. Comparison of Phosphorus Accumulation in Phosphorus Pools for an Ungrazed and a Grazed Microbial Community	129
17. Distribution of ^{33}P at Isotopic Equilibrium for the Intra- cellular Pools as % of WC-P.	130
18. Comparison of Phosphorus Turnover Rate Constants for Synthesis for an Ungrazed and a Grazed Oak Leaf Detrital Microbial Community. .	136
19. Comparison of Phosphorus Turnover Rates for Degradation for an Ungrazed and a Grazed Oak Leaf Detrital Microbial Community. .	142
20. Comparison of Phosphorus Turnover Rates for Degradation for an Ungrazed and a Grazed Oak Leaf Detrital Microbial Community. .	143

ACKNOWLEDGMENTS

We wish to extend our appreciation to Drs. Gary Stacy, Jeff Becker, and Raymond Beck, all of whom were members of the senior author's graduate committee at The University of Tennessee, Knoxville, for reviewing this manuscript. We also thank Leigh Ann Ferren for her help in collecting samples.

Thanks are also extended to Barbara Perkins, the senior author's wife, for her editorial corrections and her assistance in the preparation of drafts of this manuscript, and to Marilyn Caponetti for typing the final copy of this manuscript.

This research was supported by the National Science Foundation's Ecosystem Studies Program under Interagency Agreement No. BSR-8103181, A02 with the U.S. Department of Energy.

ABSTRACT

Detrital microbial community development and phosphorus dynamics in a lotic system were investigated in non-recirculating laboratory streams containing leaf detritus. Temporal patterns of microbial colonization, as determined by scanning electron microscopy, indicate leaf species dependency and that bacteria were the first colonizers followed by fungi. An extensive glycocalyx layer developed.

Phosphorus incorporation rates of both the whole community and intracellular components were determined by time-course measurements of $^{33}\text{P}\text{O}_4$ or $^{32}\text{P}\text{O}_4$. The phosphorus incorporation rate for the maple community was $1.67 \text{ ng P h}^{-1} \text{ cm}^{-2}$ and the rate for intracellular components ranged from $0.28 \text{ ng P h}^{-1} \text{ cm}^{-2}$ to $0.74 \text{ ng P h}^{-1} \text{ cm}^{-2}$. The rates for the oak microbiota were $0.159 \text{ ng P h}^{-1} \text{ cm}^{-2}$ and $0.163 \text{ ng P h}^{-1} \text{ cm}^{-2}$ and that for intracellular components ranged from $0.020 \text{ ng P h}^{-1} \text{ cm}^{-2}$ to $0.073 \text{ ng P h}^{-1} \text{ cm}^{-2}$ and $0.022 \text{ ng P h}^{-1} \text{ cm}^{-2}$ to $0.069 \text{ ng P h}^{-1} \text{ cm}^{-2}$ for the ungrazed and grazed microbiota, respectively.

Phosphorus turnover rates were determined by a sequential double-labeling procedure using $^{33}\text{P}\text{O}_4$ and $^{32}\text{P}\text{O}_4$, in which the microbiota were labeled with ^{33}P until in isotopic equilibrium, then ^{32}P was added. The turnover rate was determined by time-course measurements of the ratio ^{32}P to ^{33}P . The turnover rate for the maple community was $0.319\% \text{ h}^{-1}$ and ranged from $0.379\% \text{ h}^{-1}$ to $0.577\% \text{ h}^{-1}$ for the intracellular components. The turnover rates for the ungrazed and

grazed oak microbiota were $0.126\% \text{ h}^{-1}$ and $0.131\% \text{ h}^{-1}$, respectively, and ranged between $0.096\% \text{ h}^{-1}$ to $0.194\% \text{ h}^{-1}$ and $0.111\% \text{ h}^{-1}$ to $0.245\% \text{ h}^{-1}$ respectively for the intracellular components.

Snail grazing resulted in an increase in phosphorus metabolism per unit microbial biomass; however, per unit area of leaf surface no increase was observed. Grazing also caused a two-fold reduction in microbial biomass.

The results of this investigation indicate that microbiota associated with decomposing leaves slowly recycle phosphorus, are slowly growing, and have a low metabolic activity. The spiraling length is shortened by microbiota on a short-term basis; however, it may increase on a long-term basis due to hydrological transport of detritus downstream.

I. LITERATURE REVIEW

The interrelationship between the carbon and phosphorus cycles makes it necessary to have an understanding of each before a complete comprehension of stream ecosystems can be achieved. Of the two cycles, carbon dynamics is best understood, however the importance of phosphorus can not be overlooked.

Small woodland stream ecosystems in temperate zones, particularly headwater streams, are heterotrophic (Nelson and Scott, 1962; Minshall, 1967; Fisher and Likens, 1972; Hynes, 1963; Petersen and Cummins, 1974; Cummins, 1974). The heterotrophic nature of stream systems is due in part to the high ratio of land to water surface and the input of allochthonous organic matter and elemental nutrients from the surrounding watershed. The input of nutrients into streams is continuous; however, two pulses of nutrients can occur during the year. One pulse occurs in the autumn which is the period of maximum leaf fall, and the other occurs, in northern latitudes, during the spring due to runoff from melting snow.

Small streams are characterized by rhithron reaches in which the stream bottom is rocky or stoney with gravel and sand, the water flow is turbulent, and the flow volume is small with high dissolved oxygen levels and low water temperature (<20°C) (Hynes, 1963; Hawkes, 1975). The primary consumers in the rhithron are benthic invertebrates of which the great majority in woodland streams are detritivores. Hynes (1961) has reported the activity of both herbivorous and

carnivorous invertebrates was highest in the winter which suggests the importance of the seasonal pulse of organic matter.

Decomposition of Leaf Litter

Upon entering a stream, leaf litter is converted to living biomass, dissolved organic matter and CO₂. The initial event of this conversion is the leaching, which occurs rapidly, of soluble nutrients, both organic and inorganic (Meyer, 1980; Petersen and Cummins, 1974; Kaushik and Hynes, 1971). Cowen and Lee (1973) studied leaching of soluble phosphorus from oak and poplar leaves. They found that 82% and 86% of the phosphorus leachate of poplar and oak leaves, respectively, was soluble reactive phosphorus. The leaves yielded 54 µg to 270 µg P g⁻¹ of leaf. Oak leaves which were cut into small pieces leached approximately three-fold more phosphorus than intact leaves. Total soluble phosphorus from leaves in the littoral area of Lake Mendota were about three-fold lower than leaves collected on shore. These data indicate leaves are a source of phosphorus for aquatic ecosystems. Petersen and Cummins (1974) found a mean weight loss for a 24 h period, due to leaching, of 15% for all of the leaf species examined. Triska et al. (1975) observed low concentrations of phosphorus in decomposing leaf litter, relative to litter prior to placement in the stream. The major loss of phosphorus, due to leaching, occurred within a few days. Following the initial leaching period, the phosphorus concentration stabilized and increased slightly with time in the stream.

During and following the leaching period, microbial colonization and growth, referred to as conditioning, occurs on leaf litter.

Microbial activity on the litter increases with time up to a maximum and then declines (Boling et al., 1975). Fungi, at least initially, seem to be more important than bacteria in leaf decomposition (Kaushik and Hynes, 1968, 1971; Suberkropp and Klug, 1974).

Aquatic hyphomycetes are the dominant members of the fungal population associated with leaf litter in streams (Suberkropp and Klug, 1976). This dominance is partly due to their ability to sporulate underwater, whereas most terrestrial fungi do not (Bärlocher and Kendrick, 1974).

Bacteria replace the fungi during later stages of conditioning (Suberkropp and Klug, 1976a; Paul et al., 1977). Microbial colonization occurs rapidly on veins and on areas near the stomates. This pattern of colonization was suggested to be due to leaching of dissolved organic matter from these areas as a result of insect damage while the leaves were still on the tree (Paul et al., 1977).

During late stages of colonization, fungal activity is associated with the interior portion of the leaf while bacterial activity is associated with the leaf surface (Suberkropp and Klug, 1974). An increase in organic debris on the leaf surface is also associated with leaf conditioning (Paul et al., 1977), which is probably due to both biotic production (Paerl, 1974) and external accumulation.

Aquatic hyphomycetes have the necessary enzymes for cellulose degradation and some can also break down hemicellulose (Suberkropp and Klug, 1980). In pure culture studies, these fungi cause the softening of leaf tissue and the loss of parenchyma tissue from

leaves suggesting that maceration of leaves by fungi may be an important component in detrital processing (Suberkropp and Klug, 1980).

It is important to note that these studies were bacterial-free, thus any interaction between the extracellular polysaccharide produced by bacteria and the leaf tissue was not occurring.

Bacterial exopolysaccharides may act as a cementing agent, slowing down the loss of leaf tissue due to maceration, thus reducing the rate of fine particulate organic matter (FPOM) production.

Bacteria attached to surfaces in streams have been studied by Geesey et al. (1977, 1978). Bacterial populations associated with the slime layer on submerged surfaces were predominantly Gram negative bacteria. Similar results were also reported by Suberkropp and Klug (1976) for bacteria on leaves. The slime layer aids in micro-colony formation by preventing cell dispersal as well as acting as an anchor holding the bacteria firmly to the surface preventing the bacteria from being washed down stream. The polysaccharide slime may also behave in an ion exchange capacity removing nutrients from solution (Lock et al., 1984; Lange, 1976).

The entrapment of bacteria by the slime layer may have a degradative role with respect to the site of attachment. Slime material aids in the attachment of Ruminococcus abus to cellulose (Patterson et al., 1975) and myxobacteria to cyanobacteria (Shilo, 1970). Thus, the polysaccharide slimes seem to play several roles: 1) anchor bacteria to surfaces, 2) allow surface-associated enzymes to come into close proximity to their insoluble substrates (Shilo,

1970; Berg, 1975), and 3) form an ion exchange to concentrate nutrients.

The chemical composition of leaf litter changes during processing in streams. Kaushik and Hynes (1968, 1971) observed an increase in protein content of decaying leaves and speculated that the increase was due to fungal biomass. It has been assumed that increases in nitrogen content of decaying litter is due to protein. Odum et al. (1979), however, suggest that a portion of the nitrogen increase may be due to chitin, a cell wall component of fungi. Suberkropp and Klug (1976b) observed a rapid loss of reducing sugars and polyphenols within 2 weeks, followed by loss of lipids, cellulose and hemicellulose. Lignin was found to be the most recalcitrant component of leaves. They also postulated that plant phenolics interact with nitrogen-containing compounds in leaves to form recalcitrant complexes. Triska et al. (1975) observed increases in the nitrogen and phosphorus content of leaves undergoing decomposition. Elwood et al. (1981) observed that during phosphorus enrichment of a stream, the nitrogen content of decomposing leaf litter increased significantly more in the P-enriched section than in the control, thus linking nitrogen accumulation and phosphorus cycling.

The input of leaf litter into streams not only affects the biotic components of stream systems, but also abiotic factors. Slack and Feltz (1968) observed decreases in dissolved oxygen and pH, and increases in water color, conductivity, iron, bicarbonate, and manganese levels as the amount of litter in the stream increased.

The rate of leaf decomposition is species specific (Kaushik and Hynes, 1971; Suberkropp and Klug, 1976; Petersen and Cummins, 1974). The differential rate of decomposition is attributed to differences in the rate of microbial colonization of leaf types. It should also be noted that not all parts of the leaf are decomposed at the same rate. Petioles, midribs, and major veins persist much longer than the cellulosic leafy tissue of leaves in streams.

Leaf detritus in streams is unevenly distributed. Clumps or aggregates of leaves accumulate at debris dams. The distribution of leaf clumps depends upon the current patterns and the physical structure of the stream bed. The stream bed structure also affects the rate at which leaves are decomposed (Reice, 1974; Meyer, 1980). Leaf decomposition is slower in stream habitats with high sediment deposition than in habitats with low sediment deposition. Meyer (1980) also observed the slowest decomposition rates occurred at debris dams in comparison to pools and riffle habitats, shallow areas where water flow is swift and broken into waves by submerged obstructions.

Other factors also influence leaf processing, such as the size of the leaf clump which affects water movement and oxygen availability within the leaf clump. Leaf clumps are continuously forming and redistributing, thus the stability of the clump will affect the rate of leaf processing. Water flow is important, causing physical abrasion and fragmentation of leaf detritus (Meyer, 1980), and increasing microbial activity (Whitford and Schumacher, 1961, 1964;

Schumacher and Whitford, 1965). Water temperature is an important factor controlling the processing rate (Kaushik and Hynes, 1971). It is interesting that the temperature at which maximal leaf processing occurs does not coincide with the maximum stream temperature. The size of the detrital particle is also important. Hargrave (1972) demonstrated an increase in mass-specific microbial activity with a decrease in detrital particle size.

Microorganisms associated with leaf detritus are not only important in a decomposer role, but are also important as food sources to higher organisms in the streams. Many stream invertebrates (detritivores) have a preference for detritus which has been colonized by microorganisms (Kaushik and Hynes, 1971; Petersen and Cummins, 1977; Bärlocher and Kendrick, 1973). Rodina (1963) considers the accumulated bacteria as components of detritus. Microbial biomass may, therefore, be an important regulator of stream productivity. The microorganisms in woodland temperate streams may be envisaged as the "primary" producer, in which detritus is the primary energy source for microorganisms (fungi and bacteria) and the microorganisms are the energy source for the animals.

Phosphorus Dynamics

Phosphorus dynamics in stream ecosystems, as in all ecosystems, consists of both biotic and abiotic components, neither of which are independent of the other. Phosphate is fully oxidized with an oxidation number of V and a coordination number of 4. Phosphate exists as orthophosphate in all known minerals with the ionic form

of PO_4^{3-} . The dissolved phosphate in natural water comes from weathering and dissolution of phosphate minerals, biological inputs, and atmospheric inputs (Peters, 1977). Organic phosphates and condensed inorganic phosphates found in waters are products of biological growth. The predominant dissolved orthophosphate species between pH 5 and pH 9 are $\text{H}_2\text{PO}_4^{1-}$ and HPO_4^{2-} (Stumm and Morgan, 1970). Table 1 shows some dissolved phosphorus forms and Table 2 shows solid phosphorus forms of importance in natural waters.

The role of sediments in phosphorus dynamics will be dependent on the concentration of phosphate, pH, complexing metals (Fe, Al, Ca), and other ligands (carbonates, organic matter) (Stumm and Morgan, 1970). The complexing of phosphates and metal ions can affect the distribution of phosphate, the metal ion, or both (Wetzel, 1975). Jackson and Schindler (1975) using ^{32}P as a tracer, found phosphorus was associated with iron and aluminum, the highest radioactivity was associated with the fraction highest in humic matter. Thus, they concluded that phosphorus was bound to Fe and Al complexes of humic matter. They also noted that on a per μmole of Fe and Al, more ^{32}P was bound in the fulvic acid fraction than in the humic acid fraction. Francko and Heath (1979, 1982) observed that 60% to 90% of the dissolved phosphorus fraction in bog water was associated with a high molecular weight fraction which was unreactive with acid molybdate reagents or alkaline phosphatase, and co-chromatographed with dissolved high molecular weight humic matter. Soluble reactive phosphorus, however, was released from phosphate-iron complexes

Table 1. Dissolved phosphorus forms of possible significance in natural waters.

Form	Representative Compounds or Species
Orthophosphate	$H_2PO_4^-$, HP_04^{2-} , P_04^{3-} , $FeHPO_4^+$, $CaH_2PO_4^+$
Inorganic condensed phosphates	
pyrophosphate	$H_2P_2O_7^{2-}$, $HP_2O_7^{3-}$, $P_2O_7^{4-}$, $CaP_2O_7^{2-}$, $MnP_2O_7^{2-}$
tripolyphosphate	$H_2P_3O_10^{3-}$, $HP_3O_10^{4-}$, $P_3O_10^{5-}$, $CaP_3O_10^{3-}$
trimetaphosphate	$HP_3O_9^{2-}$, $P_3O_9^{3-}$, $CaP_3O_9^-$
Organic orthophosphates	
sugar phosphates	Glucose-1-phosphate, Adenosine monophosphate
inositol phosphates	Inositol monophosphate, Inositol hexaphosphate
phospholipids	Glycerophosphate, Phosphatidic acids, Phosphatidylcholine
phosphoamides	Phosphocreatine, Phosphoarginine
phosphoproteins	
Organic condensed phosphates	Adenosine-5'-triphosphate, Coenzyme A

Taken from Stumm and Morgan, 1970.

Table 2. Solid phase forms of phosphorus of possible significance in natural water systems.

Form	Representative Compounds/Substances
Soil and Rock Mineral Phases	
hydroxylapatite	$\text{Ca}_{10}(\text{OH})_2(\text{PO}_4)_6$
brushite	$\text{CaHPO}_4 \cdot 2\text{H}_2\text{O}$
carbonate fluorapatite	$(\text{Ca}, \text{H}_2\text{O})_{10}(\text{F}, \text{OH})_2(\text{PO}_4, \text{CO}_3)_6$
variscite, strengite	$\text{AlPO}_4 \cdot 2\text{H}_2\text{O}$, $\text{FePO}_4 \cdot 2\text{H}_2\text{O}$
wavellite	$\text{Al}_3(\text{OH})_3(\text{PO}_4)_2$
Mixed Phases, Solid Solutions, Sorbed Species, etc.	
clay-phosphate	$[\text{Si}_2\text{O}_5\text{Al}_2(\text{OH})_4 \cdot (\text{PO}_4)]$
metal hydroxide-phosphate	$[\text{Fe}(\text{OH})_x(\text{PO}_4)_{1-x/3}]$
	$[\text{Al}(\text{OH})_x(\text{PO}_4)_{1-x/3}]$
clay-organophosphate	$[\text{Si}_2\text{O}_5\text{Al}_2(\text{OH})_4 \cdot \text{ROP}]$ clay-pesticide, etc.
metal hydroxide-inositol phosphate	$[\text{Fe}(\text{OH})_3 \cdot \text{inositol hexaphosphate}]$
Suspended or Insoluble Organic Phosphorus	
bacterial cell material	Inositol hexaphosphate or phytin,
plankton material	phospholipid, phosphoprotein,
plant debris	nucleic acids, polysaccharide
proteins	phosphate

Taken from Stumm and Morgan, 1970.

upon exposure to low level ultraviolet light due to the photoreduction of iron.

McCallister and Logan (1978) attributed phosphorus adsorption capacity of a river sediment to the high content of amorphous iron and aluminum components. They pointed out that even though sediments have a high phosphorus adsorption capacity, the capacity was not saturated. The adsorption of phosphorus by sediments has been implicated as an important mechanism for phosphorus retention and control of soluble phosphate concentration (Meyer, 1979; Hill, 1982). Green et al. (1978) observed that the total phosphorus in suspended sediments was greater than in the bottom sediments.

Phosphorus dynamics in lakes is better understood than in streams. Lean (1973a,b), using radioactive phosphate in conjunction with gel chromatography, examined the biologically important forms of phosphorus in lake water. He observed rapid establishment of a steady-state between radioactive phosphate and four components of phosphorus in the lake water: a particulate fraction ($>0.45 \mu\text{m}$) which contained the majority of the phosphorus, a low molecular weight organic phosphorus, colloidal phosphorus ($>5 \times 10^6 \text{ MW}$), and soluble inorganic phosphate. He demonstrated that the small molecular weight organic phosphate and colloidal phosphate are produced only in the presence of bacteria, algae, and other particulate matter. Both small molecular weight compounds and colloidal phosphate were found to be negatively charged as determined by anion exchange. Jackson and Schindler (1975) confirmed Lean's conclusion that the

formation of colloidal phosphate is due to microorganisms. They found that within 14 hours of adding $^{32}\text{P}_\text{O}_4$, all of the dissolved ^{32}P was in colloidal form (>5000 MW).

Lean and Nalewajko (1976) examined the flux of phosphate using axenic algal cultures. They found that the major flux was between the cells and the medium. All of the algal species examined produced colloidal phosphorus in the medium. The excretion of dissolved organic phosphorus occurred when the phosphate was nearly depleted from the medium. Fuhs and Canelli (1970) studied diatoms with the use of ^{33}P microautoradiography and observed hot spots associated with an unknown extracellular component; no cells were associated with this material. The material may be similar to Lean's colloidal matter. Paerl and Lean (1976) examined the movement of phosphorus between algae, bacteria, and abiotic particles in lake water by microautoradiography. They showed that bacteria were, initially, much more densely labeled than the algae; however, since the algal biomass was much greater than that of the bacteria, the algal uptake of phosphorus was the more important path. The accumulation of ^{33}P in detritus and the extracellular polysaccharide surrounding Anabaena was also demonstrated. Upon further examination of the sites of accumulation, they observed material of colloidal nature. They speculated that extracellular slime of microorganisms may be an important storage site of phosphorus for microorganisms which can not produce polyphosphates.

Downes and Paerl (1978) separated two dissolved reactive phosphorus fractions in lake water; a reactive high molecular weight

phosphorus fraction (RHMW-P, >5000 MW) which probably contributes to the overestimation of orthophosphate, and a small molecular weight phosphorus fraction corresponding to orthophosphate. The biological availability of these phosphorus pools was determined using phosphorus starved Chlorella. The results indicated free orthophosphate is preferred; however, the RHMW-P fraction can be utilized upon longer incubations (96 h) (Paerl and Downes, 1978). The RHMW-P fraction, therefore, is less available on a short-term basis, but 97% was utilized by 96 hours. This suggests that once the orthophosphate pool is depleted, other phosphorus pools (organic phosphate) will be utilized. White and Payne (1980) using a modification of the chromatography technique of Downes and Paerl examined the distribution and biological availability of RHMW-P in natural waters. They found that eutrophic lakes and streams (pastoral agricultural catchments) contained dissolved reactive phosphorus which corresponded to orthophosphate and RHMW-P. Orthophosphate accounted for 63% to 100% of the dissolved reactive phosphorus in some lakes in the summer. They also observed that 40% to 50% of the RHMW-P was utilized in contrast to Paerl and Downes (1978) who found that 97% was utilized.

Minear (1972) characterized naturally occurring dissolved organic phosphate compounds. He found that 20% of the organic phosphorus in algal culture media was a high molecular weight fraction (>50,000 MW) and that as much as 50% of this high molecular weight fraction was DNA (probably large oligonucleotides). DNA released due to cell death is accumulated in solution rather than being

hydrolyzed. Lorenz et al. (1981) found that DNA-sediment interactions protected the DNA from nuclease activity. They also described a procedure for determining DNA content in marine sediments. Holm-Hansen (1968) showed that DNA, in substantial amounts, was bound to detritus.

An interesting approach used in the characterization of phosphorus has been performed by Newman and Tate (1980). Using ^{31}P -nuclear magnetic resonance, they found that in soils inorganic orthophosphate and orthophosphate monoesters are the predominant forms of phosphorus. It would be valuable to use such an approach in aquatic systems to characterize phosphorus.

Phosphorus turnover times in lake water can range from seconds to hours (White et al., 1981; Paerl and Lean, 1976; Rigler, 1956; Pomeroy, 1960). Phosphate turnover times for algal cultures varying from about 3 minutes to 11,000 minutes, depending upon growth stage of the culture, and algal-phosphorus turnover times ranging from 115 minutes to about 10,000 minutes have been reported by Lean and Nalewajko (1976). Paerl and Downes (1978) found turnover times for P in water were variable, depending upon the size of phosphate (PO_4) and RHMW-P pools. Lake water with large PO_4 pools (88% of total reactive phosphorus was PO_4) had no detectable turnover within 4 hours; however, when the majority of reactive phosphorus was RHMW-P, relatively short PO_4 turnover times occurred, 3.7 hours. Thus, the smaller the pool size of orthophosphate, the faster the turnover rate. Factors affecting phosphorus turnover times have been examined.

Turnover time was found to be negatively correlated to biomass, positively related to the dissolved phosphate concentration, and short in instances of phosphorus limitation (White et al., 1982).

Streams also have a dissolved reactive high molecular weight phosphorus fraction. White and Payne (1980) found streams in New Zealand that contained a small proportion of dissolved reactive phosphorus as RH MW-P. The water from five streams arising as springs did not contain RH MW-P, suggesting that groundwater does not have RH MW-P material. Peters (1978) studied the phosphorus fraction in streams entering Lake Memphremagog. He found that the total phosphorus concentration varied from 18 μg to 64 $\mu\text{g L}^{-1}$, however the proportion of phosphorus in each fraction (RH MW-P and PO_4) remained relatively constant. Soluble phosphorus accounted for about one-third of the total phosphorus, and orthophosphate, as determined by a radioactive bioassay, was less than 10% of the total phosphorus pool. The soluble phosphorus pool was equally divided between RH MW-P (>5000 MW) and a small molecular weight fraction (<400 MW) containing orthophosphate and some small organic phosphate compounds. Tracer studies indicated all of the phosphorus fractions were involved in phosphorus exchange with orthophosphate which indicated biological availability. It was also found that the percent of total P for the soluble phosphorus pool and orthophosphate increased during periods of low stream flow.

Phosphorus dynamics in stream systems has been studied to a lesser extent than that in lake systems. The understanding of

phosphorus dynamics has been aided by the fact that the radioactive isotopes of this element (^{32}P and ^{33}P) have a relatively short half-life (14.3 days and 25.2 days, respectively). $^{32}\text{P}\text{O}_4$ has been added at tracer levels to streams and the phosphorus dynamics followed.

Using such an approach, Ball and Hooper (1963) were able to follow the translocation of phosphorus in a river ecosystem. They were able to estimate the distance phosphorus traveled before being lost from the water (411 to 10,274 meters). Their travel distance may be overestimated due to the way in which the ^{32}P was introduced into the stream. These workers used a drum which was filled with unfiltered stream water into which the ^{32}P was diluted. Depending upon the microbes in the stream water a certain portion of the ^{32}P may have been assimilated and not available (until cycled) for uptake upon entry into the stream. It is likely that the general trends observed by Ball and Hooper concerning the sites of ^{32}P accumulation will hold true. These investigators observed that most of the uptake of ^{32}P was due to aufwuchs (attached microorganisms) and aquatic macrophytes.

Nelson et al. (1969) extended the ^{32}P release technique to a mass balance approach to estimate the standing crop of aufwuch and the effective surface area of a stream reach. They observed that about 75% of ^{32}P released was accumulated by the aufwuchs with the remaining being transported downstream of the 100 m reach studied. The standing crop of aufwuch and the surface area were estimated to be 1.5 kg AFDW and 560 m^2 , respectively. They also showed that

comparatively little ^{32}P was adsorbed by sediments and fresh leaves. The ^{32}P concentration of the aufwuch demonstrated habitat dependency, the ^{32}P concentration in the riffle sites being greater than in pools as a result of current effects.

Elwood and Nelson (1972) used the material balance method to estimate aufwuch production and grazing rates. These workers found: 1) recycling of ^{32}P within the aufwuch community; 2) ^{32}P sorption onto leaves from the stream was a function of aufwuch growth; 3) snails in the stream were grazing on the labeled aufwuch; and 4) grazing limited aufwuch production rates by controlling the standing crop of aufwuch.

Gregory (1978) examined the physical and biological sorption processes of phosphorus onto inorganic and organic substrates in a laboratory stream system. Sorption of phosphorus onto sterile stream substratum (alder leaves, conifer needles, fractioned sediment) was less than that sorbed by non-sterile substratum. He also demonstrated that the longer the residence time of leaves and needles in the stream, the more ^{32}P accumulation occurred, and that uptake per unit mass onto the maple leaves was greater than that of the conifer needles. Examination of ^{32}P adsorption by aquatic primary producers indicated that epilithic algae were responsible for the greatest amount of phosphorus accumulation following ^{32}P release into the stream. He concluded that the uptake of phosphorus is predominantly a biological process.

The transport and transformation of phosphorus has also been studied using a mass balance approach (input-output). Meyer and

Likens (1979) used such an approach to study phosphorus retention and processing of three size classes of phosphorus in a forested stream in New Hampshire. The phosphorus input budget was: tributary stream (62%); falling and blown-in litter (23%); sub-surface water (10%); and precipitation (5%). Mass balance data indicated that phosphorus retention in the stream occurs, annual inputs exceeding outputs. They found that inputs of dissolved and coarse particulate phosphorus exceeded the outputs of these phosphorus classes; however, the output of fine particulate matter exceeded its input. They concluded that processing of phosphorus to fine particulate phosphorus occurs and that fine particulate phosphorus is the major form (67% of total phosphorus) exported downstream.

Meyer (1979) examined the role of sediments and bryophytes in stream phosphorus dynamics. She reported that increased phosphorus adsorption to stream sediment was a function of particle size (increased adsorption with decreasing particle size) and organic matter and aluminum content (increased adsorption with increasing content). Sediments had less adsorptive capacity for leaf-leachate phosphorus than orthophosphate. She states that the microbial community plays a minor role in the retention of phosphorus in the sediment. These data may be biased due to the extremely high concentration of phosphates used (1000x in situ concentration). Under this condition, saturation of the adsorptive sites of sediment probably occurred and may have exceeded the capacity for uptake by the microbial component, thus over emphasizing the importance of sediments.

Phosphorus is an essential nutrient and often limits productivity in aquatic ecosystems. Phosphorus dynamics of lotic ecosystems are complicated by the downstream flux of phosphorus. Nutrient spiraling, a concept which couples the cycling and the downstream flux of the nutrient, has been described by Webster (1975). Concurrent with the completion of a nutrient cycle is a downstream displacement which stretches the nutrient cycle into a continuous spiral. Spiraling can be viewed as a nutrient cycle which is both closed and open. It is closed in the sense that during the residence time in the stream a nutrient can go through the same ecosystem compartment or trophic level many times. The cycle is open in the sense that upon completion of a cycle the nutrient is displaced spatially downhill, thus the cycle is not completed in place.

Figure 1 compares the concept of nutrient cycling in a closed and open system with that of spiraling in an open, spatially distributed system. Nutrients cycle indefinitely in a closed system (Figure 1a). In an open system, nutrients move into, through, and out of the system (Figure 1b), thus nutrients in an open system are cycled a specific number of times before leaving the system. Nutrient spiraling in open systems differs from the other cycling model in that spiraling emphasizes the downhill translocation of a nutrient within the system, the spatial dimension of the model (Figure 1c).

The concept of nutrient spiraling has been advanced by the nutrient spiraling group at the Oak Ridge National Laboratory,

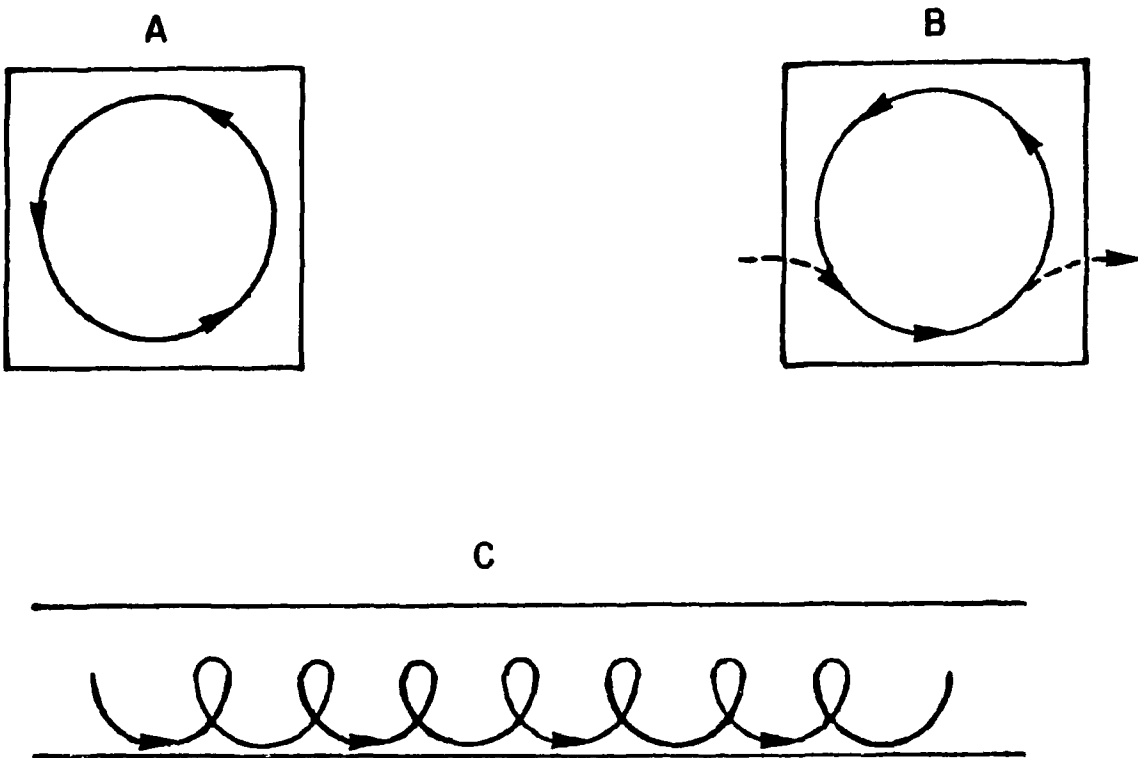
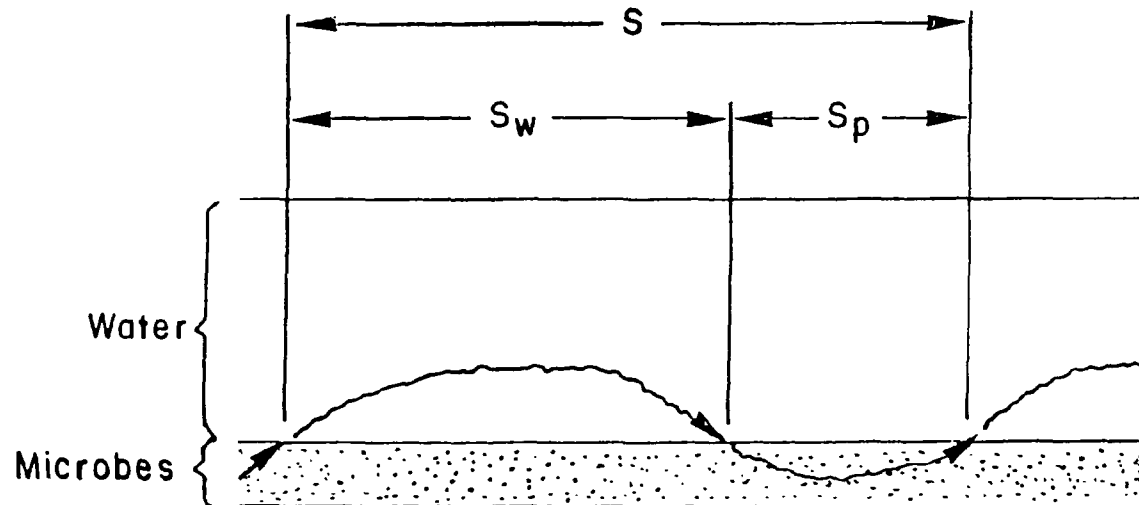


Figure 1. Schematic representation of nutrient cycling models.
a) Cycling in closed systems.
b) Cycling in open systems.
c) Spiraling in open systems.
(See text for discussion.)

Environmental Sciences Division (ORNL-ESD) (Newbold et al., 1981, 1983; Elwood et al., 1983). These workers have developed specific indices to describe nutrient spiraling in lotic ecosystems (Figure 2). Spiraling length (S) is defined by the expression: $S = S_w + S_p$; where S_w , the average uptake length, is the distance traveled by a nutrient before it is taken up by the stream benthos, and S_p , the turnover length, is the average distance a nutrient travels in the particulate state before returning to the water. The spiraling length of a reach of stream is an index of the efficiency with which a nutrient is utilized relative to the downstream flux. The shorter the spiraling length, the greater the number of times a nutrient is utilized within a given reach of stream. Spiraling length measurements are independent of the stream length over which they are measured so they can be compared between streams of different sizes.

Phosphorus spiraling studies in Walker Branch, a small woodland stream in Oak Ridge National Laboratory Environmental Research Park, revealed a spiraling length of about 193 m in July (Newbold et al., 1981) and that the uptake length (the distance a nutrient travels in the water before being sorbed), a component of the spiraling length, varies seasonally with a measurement of 164 m in the summer to 6 m in the autumn after the forest canopy litter fall (Elwood et al., 1982). Phosphorus spiraling in Walker Branch is associated with the microbial component of the stream (90% of phosphorus spiraling due to microbes) (Elwood et al., 1981), whereas macroinvertebrates account for 3% (Newbold et al., 1983).

ORNL-DWG 86-9436



22

Figure 2. Schematic representation of nutrient spiraling in a stream ecosystem. Shown are the components of the spiraling length (S). The uptake length (S_w) is the average distance a nutrient atom travels in the water before being taken up by particulates (microbes). The turnover length (S_p) is the average distance traveled by the nutrient in the particulate component before returning to the water.

Mulholland et al. (1985) examined seasonal patterns of phosphorus spiraling and found that coarse particulate organic matter (CPOM), defined as particulate organic matter greater than 1 mm in size, plays an important role in regulating phosphorus spiraling. They found a rapid uptake of phosphate and shortest spiraling length in autumn after leaf fall. The removal of CPOM resulted in longer spiraling lengths. Phosphorus uptake rates were lowest during the summer when the standing crop of CPOM is at its annual minimum.

Examining the uptake of phosphorus by the attached microbial community to leaves, Mulholland et al. (1984) found that the microbial activity on the leaves is more important than the biomass with respect to phosphate utilization. They also found three cellular pools of phosphorus, each with a characteristic turnover rate. Mulholland et al. (1983) have also examined the effect of grazing on phosphorus spiraling in an autotrophic stream and found that the presence of snails reduced aufwuchs biomass and primary productivity, increased the spiraling length, and increased the weight-specific uptake of phosphorus by aufwuch. The area-specific uptake of phosphorus, however, decreased.

Paerl and Merkel (1982) studied the phosphorus assimilation by attached and unattached bacteria using microautoradiography. They observed that attached bacteria had higher phosphate uptake on a per cell basis than free-living bacteria. They also observed the extent to which attached bacteria were more active was greatest under oligotrophic conditions and least under eutrophic conditions.

Thus, the availability of P and surfaces for attachment are important in phosphorus cycling.

Barsdate et al. (1974) examined the effect of bacterial grazers on phosphorus cycling in microcosms consisting of plant litter. They found that phosphorus uptake per cell, on the average, was about four times higher for the system with grazers than for the nongrazer system (9.38×10^{-7} μ g phosphorus per bacterium and 2.32×10^{-7} μ g phosphorus per bacterium, respectively). They also found that stimulation of detritus mineralization was enhanced in the presence of grazers.

Phosphorus is an essential nutritional element for micro-organisms, and upon its entry into the cell phosphorus is used in the biosynthesis of cellular components. The cellular distribution of phosphorus reveals five sites of accumulation: deoxyribonucleic acid (DNA), ribonucleic acid (RNA), phospholipids, polyphosphates, and a small molecular weight soluble pool (Roberts et al., 1957; Mitchell and Moyle, 1953, 1954; Bolton et al., 1955; Fuhs, 1969). The incorporation of ^{32}P into the acid-soluble pool occurs rapidly and subsequently is incorporated into phospholipids and nucleic acids (Bolton et al., 1955). The incorporation of phosphorus into polyphosphate occurs only after growth ceases and nucleic acid synthesis has stopped. Once nucleic acid synthesis begins again a rapid degradation of polyphosphate occurs with the incorporation of the phosphorus into RNA (Harold, 1963a). It has also been shown that the accumulation of polyphosphate is dependent on the growth medium (Harold, 1963b), under high phosphate conditions polyphosphate accumulates.

Phosphorus metabolism in Escherichia coli has been studied (Robert et al., 1957). The distribution pattern of ^{32}P in labeled cells showed that 20% was in the metabolite pool, 15% associated with phospholipids, and 63% was in the nucleic acids. The distribution was dependent on the conditions and the duration of time that cells were exposed to the tracer. For short pulses, most of the tracer was found in the metabolite pool. Cells grown in the presence of tracer and then allowed to grow in tracer-free medium had low levels of tracer in the metabolite pool.

Mitchell and Moyle (1953) studied the transfer of phosphorus through Micrococcus pyogenes (now commonly referred to as Staphylococcus aureus) under various physiological states. Resting cells (no substrate present) exhibited a reciprocal exchange (influx and efflux) of phosphorus between the cells and the medium with a $T_{1/2}$ of 70 minutes; however, respiring (glucose present) and growing cells had the same rate of phosphorus accumulation (influx) as resting cells, but no efflux occurred. The principle components of phosphorus accumulation were the metabolite pool and phospholipids (90%) in respiring cells, but all fractions (RNA, DNA, phospholipid, etc.) were labeled during growth. They observed a rapid turnover of the phospholipid-phosphorus and metabolite inorganic phosphate in respiring and growing cells with little or no turnover of RNA or DNA phosphate with the other phosphate fractions.

Cuhel and coworkers (1983, 1984) studied microbial growth and metabolism by using inorganic nutrient uptake and subcellular

incorporation patterns. The distribution of phosphorus in the subcellular fractions of a uniformly labeled (isotopic equilibrium) marine cyanobacterium, Synechococcus, reported as percent of total radioactivity, was 51%, 0.4%, 44%, and 3%, respectively, for the acid soluble, lipid, RNA, and DNA fractions. The pattern for short-term labeling was 80%, 0%, 19%, and 0%, and 66%, 0.2%, 32%, and 0.8% for a 2h and 6.5 h labeling period, respectively, for acid soluble, lipid, RNA, and DNA. The pattern observed for an oceanic sample also indicated the importance of the length of labeling to the pattern observed. The pattern observed for the 48 h labeling (assumed to be uniformly labeled) average about 41%, 9%, 38%, and 10% for the acid soluble, lipid, RNA, and DNA, respectively.

The microbial community of the Sargasso Sea was in a more balanced growth state than the continental slope community as indicated by the nearly identical rates at which phosphorus was incorporated into the subcellular fractions for the Sargasso microbiota. Cuhel et al. also stress the utility of inorganic nutrient assimilation studies in extending our understanding of microbial ecology.

The majority of the phosphorus studies to date emphasize algae and in some instances algal-bacterial interactions. Phosphorus uptake kinetic studies indicate both Michaelis-Menten type kinetics (Chen, 1974; Burmaster and Chisholm, 1979) and a deviation from Michaelis-Menten relationship (Brown et al., 1978).

Brown and Harris (1978) showed that phosphorus uptake rate (V) was dependent upon both the external phosphorus concentration

and the cell quota (phosphorus content of the cell, Q). V increases with decreasing Q for each external concentration examined. They also demonstrated that the growth rate (U) increased to the maximum growth rate (U_{max}) as Q increased from K_Q (minimum cell nutrient content constant) to 20×10^{-8} μg phosphorus cell^{-1} . They suggest the cell quota concept is useful in examining microbial growth rate relationships to changes in nutrient levels which are growth rate limiting (moderate to high level).

Phosphorus competition studies between a Pseudomonas sp. and a Scenedesmus sp. indicate that the bacterium can suppress algal growth. The suppressed algal growth was attributed to the rapid growth rate of the bacterium which limited the phosphorus level available to the algae (Rhee, 1972). Currier and Kalff (1984) reported that bacteria dominate orthophosphate utilization in lentic systems, accounting for greater than 97% of the total community uptake. They also suggest that algae acquire phosphorus from excreted organic phosphorus compounds as opposed to orthophosphate.

Phosphorus not only affects growth rate of microorganisms (Brown and Harris, 1978; Rhee, 1972; Fuhs, 1969), but it has also been implicated as a controlling factor of cell division in Chlyamydomonas reinhardtii (Lieu and Knutson, 1973). Phosphate concentration affects the rate of glucose uptake and respiration rate of a bacterium isolated in the Plussee (Overbeck and Toth, 1978). Deficiency in bacterial cell wall teichoic acids in response to phosphorus limitation has been observed (Lang et al., 1982).

In summary, the microbial community associated with leaf litter has several roles: 1) nutrient retention; 2) litter decomposition; 3) nutrient regeneration; and 4) food source for higher organisms. The cycling of nutrients in lotic ecosystems can be best understood relative to the nutrient spiraling concept which couples cycling and downstream translocation of the nutrient. Spiraling length is an index of the efficiency with which a nutrient is utilized relative to the downstream transport. The shorter the spiraling length, the greater the number of times a given nutrient is utilized within a given reach of stream. Phosphorus spiraling length varies seasonally, being shortest in the autumn after leaf fall, and is associated with the microbiota. Grazing of the periphyton increases phosphorus spiraling length as a result of decreasing biomass. Evidence points to the hypothesis that the microbial community plays an important role in regulating phosphorus spiraling in stream ecosystems. This hypothesis, however, requires supporting evidence from a detailed analysis of the roles of microbial community biomass and activity associated with CPOM in regulating phosphorus spiraling.

II. OBJECTIVES

The goal of this investigation was to elucidate the phosphorus dynamics of microbiota associated with leaf CPOM in a lotic system.

The specific objectives were:

1. to determine the temporal pattern of microbial colonization and activity on different species of leaf CPOM.
2. to determine the relationship between community biomass, phosphorus incorporation, and turnover rates for the microbiota associated with leaf CPOM.
3. to determine microbial community activity and the phosphorus incorporation and turnover rates for the intracellular phosphorus pools (phospholipid, RNA, DNA, metabolite pool).
4. to determine the effect of grazing on the microbial community and phosphorus incorporation and turnover rates.

The results of these studies will contribute to the understanding of the quantitative role microbiota associated with CPOM have in regulating phosphorus spiraling dynamics in lotic ecosystems.

III. EXPERIMENTAL APPROACH

To meet the objectives of this investigation, artificial stream ecosystems containing leaf CPOM were used so that specific variables, such as grazing and colonization time, could be studied under controlled conditions. The artificial streams were set up to simulate a section of a heterotrophic woodland stream.

Scanning electron microscopy was used to observe the temporal pattern of microbial colonization of different leaf species. The temporal pattern of heterotrophic activity for different leaf species was determined by examining the metabolism of glucose (^{14}C -labeled) by the developing microbiota. Dogwood, red maple, and white oak were the leaf species used for these temporal studies.

Phosphorus (P) dynamics of the microbial community associated with decomposing leaves (red maple or white oak) was studied using radioactive tracers (^{33}P and ^{32}P). Phosphorus turnover rate constants for synthesis for the microbial community associated with decomposing leaves and the intracellular phosphorus pools were determined by a double-labeling procedure. Briefly, $^{33}\text{PO}_4$ was released into the streams until it achieved isotopic equilibrium within the microbial community; $^{32}\text{PO}_4$ was then added and the ratio of ^{32}P to ^{33}P in the microbial community and intracellular phosphorus pools was followed over time. Phosphorus incorporation rates for the community and intracellular phosphorus pools were determined by following ^{33}P or ^{32}P accumulation; whereas, the phosphorus turnover rates for

degradation were determined by following the loss of both ^{33}P and ^{32}P after the addition of the tracers was stopped.

The phosphorus dynamics of the intracellular phosphorus pools (metabolite pool, phospholipid, RNA, DNA) was determined after the microbiota were labeled with the tracer (described above) and each phosphorus containing pool was fractionated, and the radioactivity in each was quantified.

The biomass of the microbiota associated with leaf CPOM was used for comparative purposes (colonization time and grazing effects) and for the generation of biomass-specific rates of P incorporation and turnover.

The effect of snail grazing on the microbial biomass and the phosphorus dynamics of the microbiota associated with leaves was studied by using two artificial streams, one of which contained snails and the other did not.

IV. MATERIALS AND METHODS

Miscellaneous Materials

The following materials were obtained from Sigma Chemical Company (St. Louis, MO): DNA (sodium salt, Type III, salmon testes); RNA (yeast, Type III); protein (albumin bovine, Fraction V powder); m-cresol; diethyl pyrocarbonate; 8-hydroxyquinoline; and carbonyl-cyanide m-chlorophenyl hydrazone. Trichloroacetic acid as a 5% solution or crystalline; Gelman glass fiber filters, Type A/E (25 and 47 mm); sodium dodecyl sulfate (SDS); and sodium naphthalene 1,5-disulfonate were obtained from Fisher Scientific Company (Norcross, GA). Filtration apparatus (glass microanalysis holders, 25 and 47 mm) used were obtained from Micro Filtration Systems (Dublin, CA). All chemical solvents used were reagent/analytical grade. All glassware was soaked in 20% hydrochloric acid (HCl), minimum time 12 h and rinsed repeatedly with deionized distilled water prior to use.

Radionuclides

The following radionuclides were obtained from New England Nuclear (NEN) (Boston, MA): phosphatidyl ethanolamine, L- α -dipalmitoyl-(dipalmitoyl-1- ^{14}C), specific activity (S. A.) 110 mCi mmol^{-1} ; adenine-(2- ^3H), S. A. 21.6 mCi mmol^{-1} ; carrier-free orthophosphoric acid- ^{32}P , 1 mCi, glucose-D-(^{14}C -U), S. A. 329 and 360 mCi mmol^{-1} ; deoxycytidine 5'-triphosphate, tetra-(triethylammonium) salt (α - ^{32}P), S. A. 3000 Ci mmol^{-1} . Carrier-free orthophosphoric acid- ^{33}P was obtained from

Oak Ridge National Laboratory, Nuclear Division, Oak Ridge, TN.

Palmitic acid- ^3H (4×10^6 cpm ml $^{-1}$, S. A. unknown) was kindly provided by Dr. Leaf Huang of the Biochemistry Department at the University of Tennessee.

Preliminary Studies

Preliminary studies were performed to develop and define the limits of the procedures to be used and to test the effectiveness of the organophosphorus fractionation procedure and the method used to dislodge bacteria from the leaf CPOM. In addition, the temporal patterns of microbial activity and microbial colonization of decomposing leaf CPOM was investigated.

Closed-system phosphorus uptake. Closed-system phosphorus uptake experiments were done to become familiar with working with leaf CPOM and ^{32}P and to examine phosphorus uptake kinetics during short uptake times (relative to the times to be used for the double-label study). Determining the importance of abiotic adsorption of phosphorus to CPOM was also a point of interest investigated.

Phosphorus uptake studies were done using glass crystallization dishes (50 x 100 mm) with a stainless steel basket system to hold leaf disks in place while stirring. Filtered (0.2 μ Nuclepore filters) Walker Branch stream water was used for phosphate uptake studies; total volume of 200 ml was used. Tracer amounts of ^{32}P -orthophosphoric acid were added. Abiotic adsorption of phosphate to leaf disks was determined by adding carbonyl-cyanide *m*-chlorophenyl hydrazone (CCCP) (final concentration 0.1 mM) 20 min prior to ^{32}P addition.

CCCP is an uncoupler of oxidative phosphorylation, thus causing a depletion of both the proton gradient and ATP which are required for orthophosphate transport. Uptake studies were done in temperature controlled environmental chambers at in situ temperatures of Walker Branch.

Homogenization time course study. A time course determination for the maximal removal of microbes from leaf CPOM was conducted. Bacteria dislodged from the surface of the CPOM were used to determine the relative population density on the CPOM. Disks were homogenized in a Stomacher Model 80 lab blender (Tekmar, Cincinnati, OH) for various lengths of time. Aliquots of the homogenate were diluted and spread plated on YEPG agar plates (Sayler et al., 1979).

Bacterial removal efficiency. Removal efficiency of bacteria from CPOM was determined by monitoring and comparing dehydrogenase activity of CPOM to that in CPOM extracts. Twenty disks (1.4 cm dia.) were placed in 40 ml of well water and 4 ml of 0.2% 2-p-iodophenyl-3-p-nitrophenyl-5-phenyl tetrazolium chloride (INT) (Sigma Chemical Co., St. Louis, MO) was added, and incubated at 20°C for 30 min. The disks were divided into two equal groups. To one group, 10 ml of acetone and 5 ml of well water was added and shaken for 10 min. The second group was homogenized as in the acridine orange direct counts procedure (see page 37), and 5 ml of homogenate was extracted with 10 ml acetone. The acetone extract was filtered (glass fiber, Type A/E). The absorbance of the extract was read at 490 nm using a Bausch and Lomb Spectronic 21 spectrophotometer.

Background absorbance (leaves only) was subtracted. Removal efficiency of bacteria (based on the percent INT-formazan recovered) was determined using the following equation:

$$\frac{(\text{Abs. homogenate} - \text{Abs. background}) \times t}{\text{Abs. leaves} - \text{Abs. background}} \times 100$$

where $t = 10$ because only 1/10 of the total homogenate volume was extracted.

Analytical recovery of cellular components. The analytical recovery study was done to determine the effectiveness of the procedures used to recover specific organophosphorus compounds. The recovery efficiencies were used to correct values to 100% recovered.

Analytical recoveries were determined by using a radiolabeled tracer of each component and the extraction procedures described in the section on analysis of tracer labeled cellular pools (see below). Lipid phosphate analytical recovery was determined using ^3H -palmitic acid or ^{14}C -phosphatidyl ethanolamine. Metabolite pool analytical recovery was determined using ^{14}C -glucose as a representative acid soluble, small molecular weight compound.

^{32}P -DNA used to determine analytical recovery was synthesized by nick translation of salmon testes DNA with ^{32}P -dCTP according to manufacturer's protocol (Bethesda Research Laboratory, Gaithersburg, MD). The separation of the ^{32}P -labeled oligonucleotides from nucleotides was done using a 2 cc G-50 sephadex column prepared in a 3 cc syringe. Approximately 0.5 ml fractions were collected and the

radioactive peaks were monitored using a hand-held geiger counter. The collected fractions comprising the first peak (oligonucleotides) were pooled together.

$^{3\text{H}}$ -RNA used to determine analytical recovery was prepared by growing E. coli v517 in the presence of $^{3\text{H}}$ -adenine as follows: 1 ml of a 24 h culture of E. coli v517 was added to 50 ml basal salts (Sayler et al., 1979) containing 0.4% glucose and 5 mCi of $^{3\text{H}}$ -adenine. Approximately 22 h later, 0.2 ml of 1% yeast extract was added to the culture due to slow growth, and the culture was incubated for an additional 16 h. The culture was centrifuged at 6000 rpm for 10 min at 4°C in a Sorvall RC2-B centrifuge and washed once with distilled water. RNA was extracted as described by Johnson (1981).

Microbial Biomass and Cell Density

Adenosine triphosphate (ATP). ATP quantitation was performed by the luciferin-luciferase assay using a Lumac Biocounter M1020 photometer (Lumac, Medical Products Division, 3M, St. Paul, MN). Instrument settings were as follows: integration time, 10 seconds; temperature, off position. Leaf disks, cut with a #7 cork borer (1.4 cm diameter) were quick frozen by placing a disk into a 2.0 ml cryotube (Vanguard International, Neptune, NJ) with 200 μl of phosphate buffer (50 mM, pH 7.75) and freezing in a dry ice-acetone bath (for the maple CPOM study) or by placing a leaf disk in a cryotube

and pouring liquid nitrogen into the freezing tube (for the oak CPOM study). Samples were kept at -20°C for no longer than 3 weeks before analysis was done.

The ATP extraction procedure was as follows: 200 μ l of nucleotide releasing reagent (NRB) (Lumac) was added to the cryotube containing phosphate buffer or 200 μ l of NRB and 200 μ l of Tris buffer (25 mM, pH 7.75) were added to the tube containing only a leaf disk. The extraction time was 60 sec. Subsamples, generally 10 μ l, were analyzed for ATP content. Internal standardization procedure was used to quantitate ATP in order to correct for quenching due to color or other interferences. Blank values were subtracted from experimental values (blank = NRB + buffer). If a subsample exceeded the photometer limits, the ATP extract was diluted using Lumit Buffer (Lumac). ATP standards were diluted in glycine buffer (1 mM, pH 10). The values reported are means of five replicate leaf disks.

Acridine orange direct counts (AODC). Direct bacterial cell counts were determined essentially by the method of Daley and Hobbie (1975). Ten leaf disks (1.4 cm dia.) were added to 50 ml sterile well water and homogenized for 5 minutes in a Stomacher Model 80 blender. One ml of homogenate was added to 10 ml sterile well water plus 2 ml of 0.1% or 1% acridine orange, stained for 5 min, filtered through a 0.2 μ m pore size, Irgalan stained, 47 mm Nuclepore membrane with a vacuum of 5 in. of mercury, and then washed with 5 ml of sterile distilled water. Ten fields (eyepiece grid) per membrane were counted. A Nikon optiphot microscope with a mercury lamp HBO-50,

and excitation cassette B (excitation wavelength was 495 nm, excitation filter IF-410, dichroic mirror DM 505, and eyepiece side absorption filter 515 W) was used. For each sample two subsamples were counted and the mean value reported.

Colonization Study

Temporal patterns of heterotrophic activity and microbial succession on dogwood (*Cornus florida*), red maple (*Acer rubrum*) and white oak (*Quercus alba*) leaves were examined for a period of 56 days. Leaves were collected prior to abscission and air-dried before being placed into laboratory streams. The streams were covered with black plastic to prevent algal growth and to establish a heterotrophic microbial community. Decomposing leaf litter, collected from Walker Branch, was placed upstream from the leaf CPOM to serve as a natural inoculum. Leaf disks (1.4 cm dia.) were periodically collected, with the aid of a cork borer, and used to determine the heterotrophic activity of the microbiota and for scanning electron microscopic observations.

Heterotrophic activity determination. The heterotrophic activity of the microbiota was based upon the procedures of Parson and Strickland (1962), Wright and Hobbie (1965), and Hobbie and Crawford (1969). The uptake of ^{14}C -labeled glucose by the microbiota was determined as follows: one leaf disk was placed in a reaction vial (Figure 3) containing 5 ml of filter-sterilized (0.2 μm pore size) stream water. The reaction vial was equipped with a centerwell

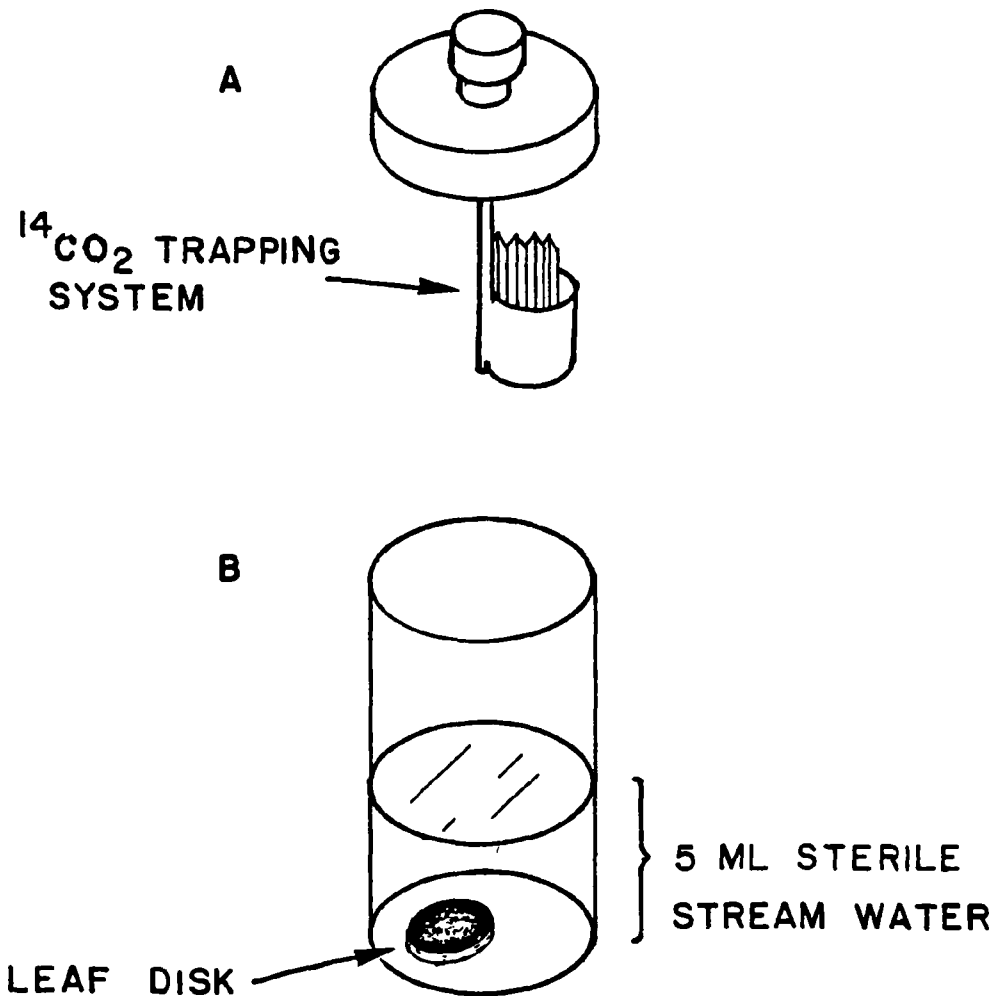


Figure 3. Glucose uptake system.

- A) CO₂ trapping system: polyethylene centerwell with a fluted 1.4 x 5.2 cm piece of Whatman #1 paper saturated with 0.4 ml of 2N KOH.
- B) 20 ml polyethylene scintillation vial containing 5 ml of filter-sterilized (0.2 µ Nuclepore filter) stream water and 1 leaf disk (1.4 cm dia.).

(Kontes, Vineland, NJ) containing a fluted piece of Whatman #1 filter paper (1.4 x 5.2 cm) saturated with 0.4 ml of 2N KOH which served as a CO₂ trap. ¹⁴C-labeled glucose was added (final concentration 50 µg L⁻¹) and after 1 h, 1 ml of 2N H₂SO₄ was added to stop metabolic activity and to drive the CO₂ out of solution (final pH 1.5). The reaction vial was then shaken for 1 h to allow for ¹⁴CO₂ adsorption by the KOH. The centerwell was removed and placed in a scintillation vial containing 10 ml of hydrofluor (National Diagnostics, Somerville, NJ) to determine the amount of ¹⁴C-labeled glucose mineralized.

The leaf disk was washed several times with sterile stream water, dried, and wrapped in ashless filter paper. The wrapped leaf disk was combusted in a Model 306 Packard Tri-Carb sample oxidizer to quantitate the amount of ¹⁴C-labeled glucose assimilated by the microbiota. Total glucose uptake was determined as glucose mineralized + glucose assimilated. Sterile controls used to correct for abiotic absorption were done under identical conditions with the exception that the acid was added prior to the addition of the ¹⁴C-labeled glucose.

The mean ¹⁴CO₂ trapping efficiency of the reaction vial, as determined by ¹⁴C-sodium bicarbonate standard spikes, was 72% with a standard deviation of 3%. This value was used to correct samples to 100%. The mean sample oxidizer efficiency was 68% with a standard deviation of 12% as determined by standard ¹⁴C-glucose addition to identical leaf samples. The samples were corrected to 100% using this value.

DPM data were obtained from a Packard Tri-Carb 460 liquid scintillation spectrophotometer using the DPM mode which uses a stored quench curve to calculate DPM. The DPMs were converted to amounts of glucose based upon the specific activity of the ¹⁴C-labeled glucose.

Fixation method for scanning electron microscopy observation.

Fixation of leaf disks was done by immersing a disk in a 2% (v/v) glutaraldehyde solution buffered with 0.1M sodium cacodylate (final concentration) for 1 h at 4°C. After fixation, leaf disks were dehydrated by transferring through a series of increasing concentrations of ethyl alcohol (10%, 25%, 50%, 75%, and 100%) for a period of 20 min in each.

Critical point drying of the disks was carried out using an Omar SPL-900/EX critical point drying machine. The procedure is as follows: the temperature and pressure were increased to 42°C and 1300 psig, respectively, then the pressure was reduced at a rate of 200 psig per minute until ambient. The critical point dried samples were then coated with gold or palladium/gold using a Denton Vacuum DV-515 Automatic Evaporator. Samples were observed using an ETEC autoscan Scanning Electron microscope.

Analysis of Phosphorus Tracer Labeled Cellular Pools

Whole cell radioactivity. Individual leaf disks were placed in glass scintillation vials containing a piece of ashless filter paper, and combusted at 450°C overnight. Ten ml of Aquasol (NEN,

Boston, MA) and 5 ml of distilled water were added to the residue and the vial was shaken to form a gel and counted.

Phospholipid extraction procedure. The phospholipid extraction procedure used was that of White et al. (1977). Five disks (1.4 cm dia.) were placed into a 30 ml separatory funnel containing 10 ml absolute methanol, 5 ml chloroform, 4 ml distilled water and 0.8 ml concentrated HCl. The mixture was shaken vigorously and let stand for 2 h. Five ml each of chloroform and methanol were then added and the separatory funnel was shaken for 10 min and let stand overnight. The chloroform phase was collected in a glass scintillation vial and evaporated to dryness by an air stream. Ten ml of Aquasol was added to the vial and the radioactivity was determined.

Fractionation of intracellular phosphorus components. Leaf disks were collected and immediately frozen with either dry ice-acetone or liquid nitrogen until fractionation of intracellular components (RNA, DNA, metabolite pool) could be done. The basic extraction procedure for metabolite pool, RNA, and DNA was described by Hanson and Phillips (1981) (Figure 4).

1) Five disks suspended in 3 ml of 5% ice cold trichloroacetic acid (TCA) were homogenized (maximum setting) on ice for 1 to 2 min with a teflon tissue homogenizer attached to a T-line laboratory mixer (Talboys Engineering Corp.).

ORNL-DWG 86-9438

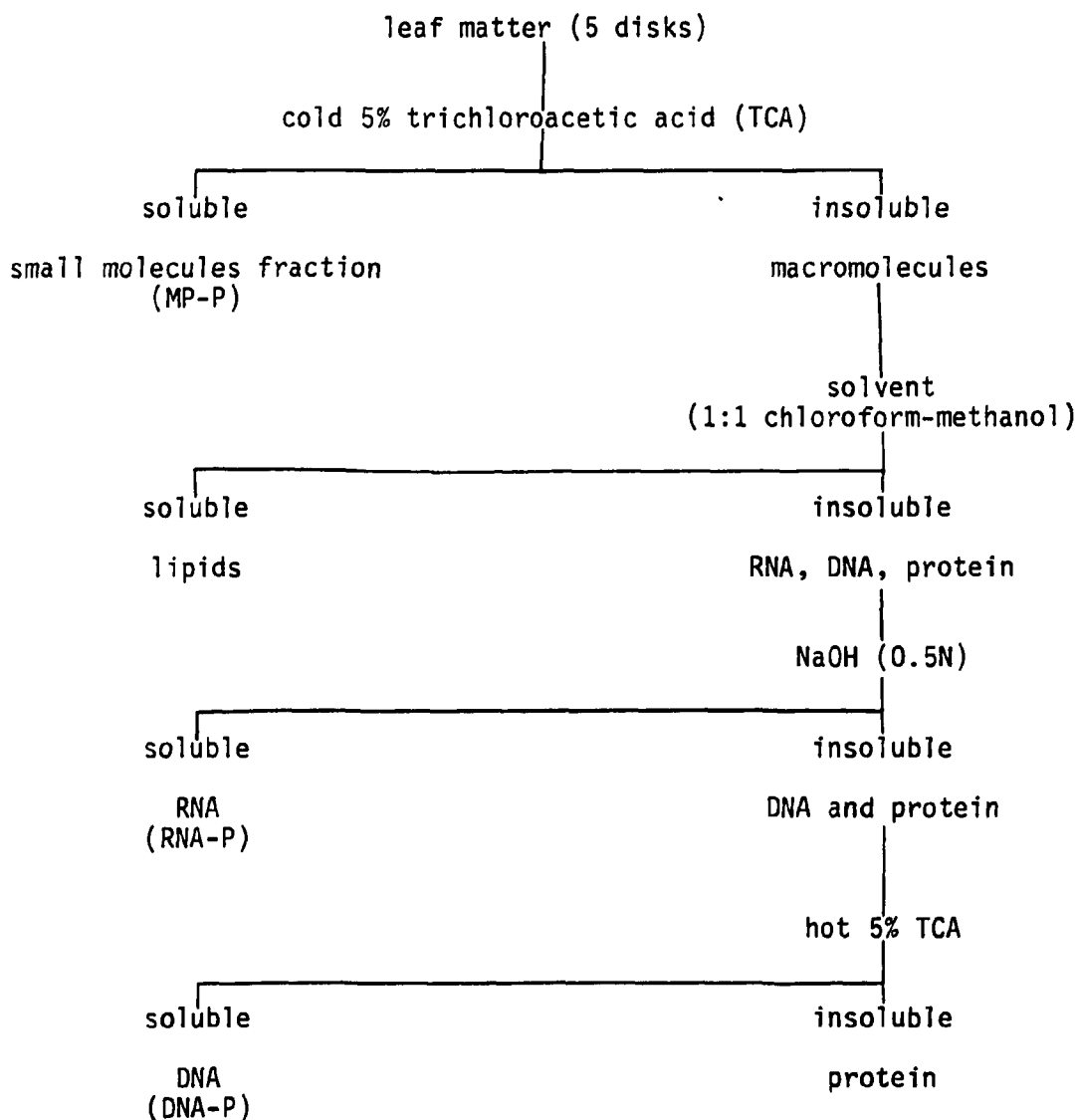


Figure 4. Fractionation scheme for Microbial Phosphorus Pools.

2. The homogenate was transferred to a 10 ml scintillation vial. The homogenation tube and homogenation tip were washed 2 times with 2 ml of ice cold 5% TCA and the rinse was added to the homogenate. Carrier RNA and DNA (200 μ g each) was added to the homogenate. The homogenate was placed on ice for 1 h.

3. The homogenate was filtered (Gelman glass fiber, Type A/E filter). The extraction vial was washed 2 times with 2 ml ice cold 5% TCA and filtered. The filter was washed 2 times with 2 ml ice cold 5% TCA. The collected filtrate was designated as metabolite pool phosphate (MP-P).

4. The filter with precipitate was washed with 5 ml of ice cold 70% ethanol to remove residual TCA. The filtration apparatus and filter containing the precipitate were placed in a drying oven at 45°C for approximately 10 min to warm up. The filter containing the precipitate was sequentially washed, slowly (10 min), with 5 ml 70% ethanol (45°C) and 10 ml of 1:1 mixture of methanol-chloroform to remove lipids from the precipitate which would contaminate the RNA-P and DNA-P fractions.

5. The filter containing the precipitate was air-dried and placed in a 20 ml scintillation vial. The 10 ml of 0.5N NaOH (37°C) was added and the vial was placed in a 37°C water bath for 90 min. with occasional shaking. The sample was rapidly cooled by placing on ice, 3 ml of ice cold 50% TCA was added, and then the sample was left on ice for 30 min.

6. The filter of the filtration apparatus was presoaked with cold 5% TCA and the homogenate was filtered. The extraction vial containing the original filter was washed 2 times with 3 ml ice cold 5% TCA and the wash was filtered. The filter containing the precipitate was washed 2 times with 2 ml of ice cold 5% TCA. The filtrate was collected and designated RNA-phosphate (RNA-P).

7. The filter containing the precipitate was placed back into the extraction vial containing the filter from the RNA digestion and 10 ml of hot (>90°C) 5% TCA was added. The extraction vial was placed in a >90°C water bath for 30 min. Bovine serum albumin (BSA) (200 µg) was added and the extraction vial was placed on ice for 30 min. The hot TCA extract was filtered and the extraction vial was washed 2 times with 2 ml ice cold 5% TCA. The filter was washed 2 times with 1 ml ice cold 5% TCA. The filtrate was collected and designated DNA-phosphate (DNA-P).

The extracts were collected in tared vials (A) and subsequently weighed to get total weight (vial plus extract = B). A subsample (5 ml) was removed to quantitate the radioactivity (³³P and ³²P), and the vial was reweighed to get the weight after the subsample was removed (total weight - subsample weight = C). The fraction of the subsample weight to the total extract weight was used to correct for total radioactivity in the extract.

$$\begin{aligned} (B - A) &= \text{sample extract weight} & \frac{(B - C)}{(B - A)} &= D, \text{ correction factor} \\ (B - C) &= \text{subsample weight} \end{aligned}$$

Radioactivity Quantitation

Radioactivity measurements were made with a Packard Tri-Carb 4640 liquid scintillation spectrometer (Packard Instrument Co., Downers Grove, IL). The parameters were as follows: counting termination time, 10 or 20 min; statistical precision was set at 1%; external standard and automatic efficiency control options were used. Ten ml of Aquasol was used as the scintillation cocktail. Quench curves for ^{32}P and ^{33}P were prepared by adding a known amount of radioactivity to 10 ml Aquasol and varying amounts of the quenching agent, chloroform.

The difference in the beta particle energy spectrum of the two radionuclides permitted good spectral separation. Setting the lower limits of the higher energy region of ^{32}P at or above the endpoint of the ^{33}P spectrum reduced the counting efficiency of the ^{33}P in the higher energy portion to zero. This procedure can be used if the maximum beta particle energy of the two radionuclides differs by at least three-fold, as in the case of ^{33}P (248 KeV) and ^{32}P (1700 KeV).

The double-label mode was used when ^{33}P and ^{32}P were simultaneously being counted, which automatically subtracted the "spill-over" for each isotope. Counts per minute (CPM) were converted to disintegrations per minute (DPM) directly by the scintillation counter based upon stored counting efficiencies of quenched standards. All DPMs were corrected for physical decay. ^{33}P and ^{32}P have physical half-lives of 25.2 days and 14.3 days, respectively.

Phosphorus Dynamics of a Detrital Microbial Community

The experimental design of this phosphorus dynamics study is shown in Figure 5. The basic procedure is that of Berman and Skyring (1979). This procedure allows the determination of phosphorus turnover rates by a phased double isotopic labeling procedure using $^{33}\text{P}_4$ and $^{32}\text{P}_4$.

The microbial community associated with leaf CPOM was initially labeled with ^{33}P until isotopic equilibrium was achieved in the phosphorus pools. ^{32}P in conjunction with ^{33}P was then added (referred to hereafter as time zero). Samples were subsequently taken at various times to determine the ratio of ^{32}P to ^{33}P in the microbial community (unfractionated) and in the intracellular phosphorus pools.

The advantages of this double-labeling procedure are:

- 1) There is no need to determine the specific activity of the phosphorus pools, thus it is not necessary to quantitate the phosphorus pools (e.g., phospholipid).
- 2) The system does not need to be in steady-state.
- 3) Quantitative extraction of the phosphorus pool is not required since the ratio of ^{32}P to ^{33}P is being determined for each phosphorus pool.

The distribution of phosphorus in the various phosphorus pools can, also, be determined by monitoring ^{33}P in the pools when isotopic equilibrium is attained since ^{33}P will be distributed exactly as stable ^{31}P at this time. The gross phosphorus uptake (influx only) can also be determined by measuring ^{33}P or ^{32}P increase in the cellular phosphorus pools with time.

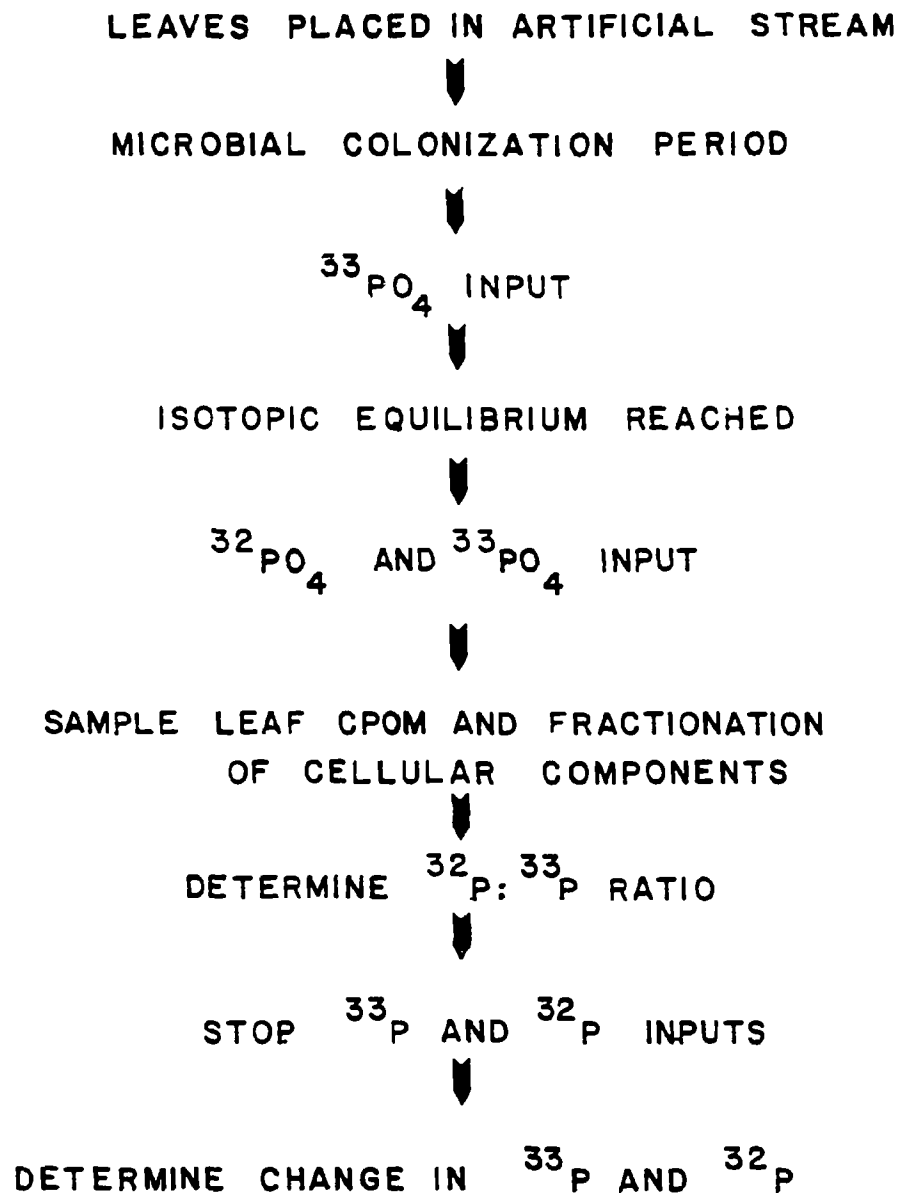
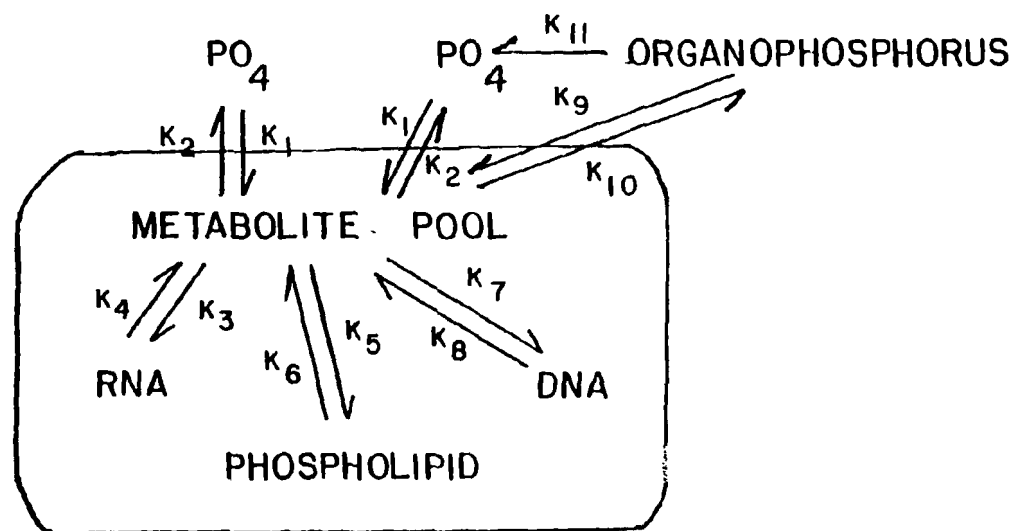
EXPERIMENTAL DESIGN

Figure 5. Experimental protocol used for phosphorus dynamics studies.

The ratio of ^{32}P to ^{33}P in the phosphorus pool (e.g., RNA-P) was compared to the ratio expected at isotopic steady-state (i.e., the ratio of ^{32}P to ^{33}P in the stream water). The ratios were expressed as a fraction of the steady-state isotopic ratio (i.e., the ratio of ^{32}P to ^{33}P in the stream water). The fraction of the steady-state ratio was plotted versus time and the slope was taken to be the turnover rate constant for synthesis. The turnover rate was also determined by monitoring the decrease in radioactivity associated with the phosphorus pool, after the input of tracers was ceased.

A schematic representation of the phosphorus dynamics associated with the microbial community is shown in Figure 6. As orthophosphate enters the cell (rate k_1), it becomes part of the metabolite pool (inorganic phosphate and organic phosphate precursor molecules). From this precursor pool, phosphorus is made available for the incorporation into RNA, phospholipid, and DNA at rates k_3 , k_5 , and k_7 , respectively. Phosphorus from organophosphorus molecules (extracellular) is also available for microbial use via extracellular enzymatic hydrolysis (k_{11}) to orthophosphate or direct uptake (k_9). Cellular phosphorus components of microbes are in a dynamic state (continuous synthesis and breakdown), thus the cellular phosphorus pools are turned over (degraded) and the phosphorus reenters the metabolite pool at a certain rate (turnover rate) for RNA (k_4), phospholipid (k_6), and DNA (k_8). Phosphorus turnover for the intact cell can occur via PO_4 (k_2) and organophosphorus (k_{10}) release back to the environment.

EXTRACELLULAR PHOSPHORUS POOLS



CELLULAR PHOSPHORUS POOLS

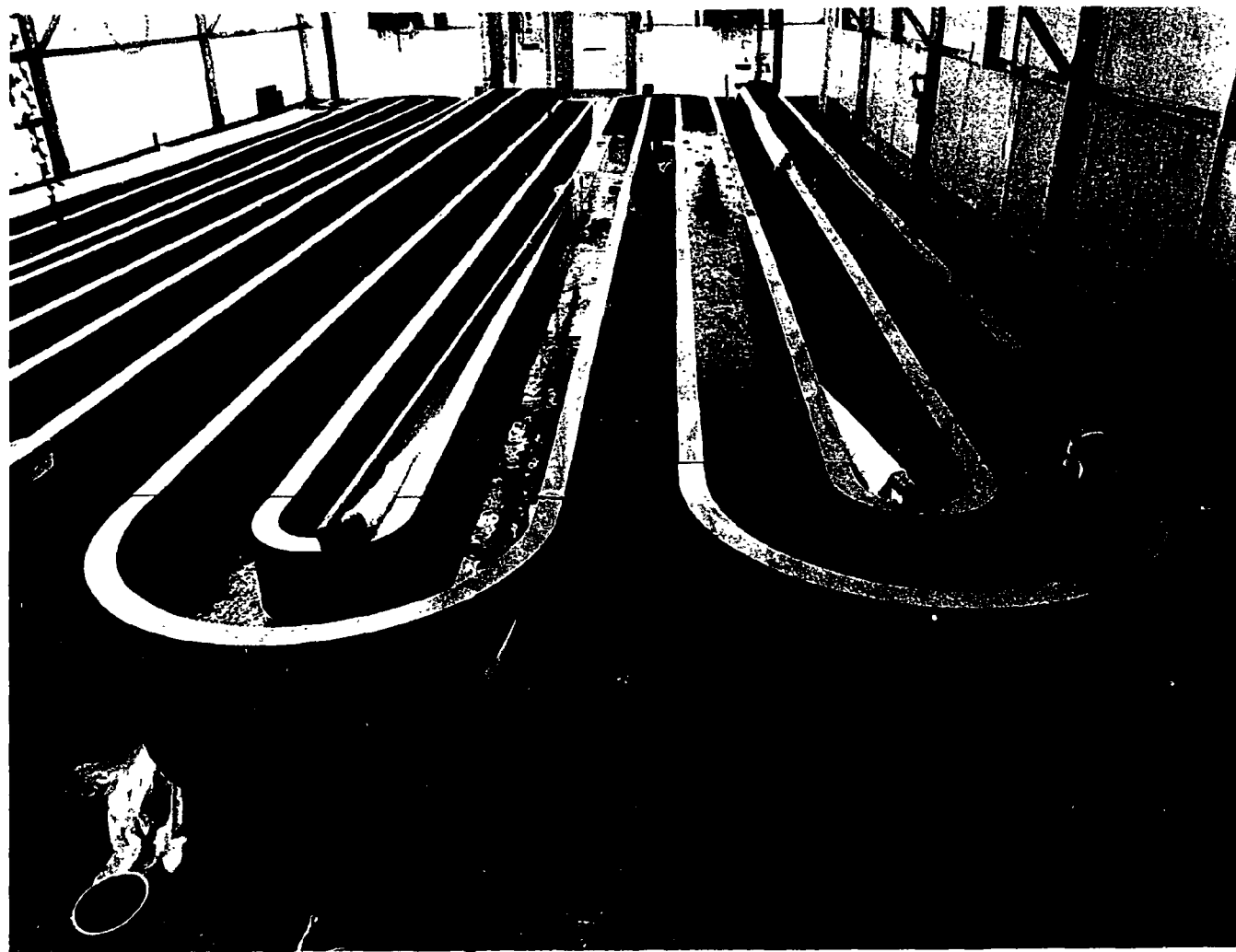
Figure 6. Schematic representation of the phosphorus dynamics associated with a microbial community.

The research of this study was centered on the orthophosphate portion of the extracellular phosphorus pool. The movement of phosphorus through the microbial community and intracellular phosphorus pool was determined (see below). Two studies were carried out. The first study used ungrazed red maple leaves. The second study used white oak leaves in two streams, one contained snails (shredder/grazer) and the other did not, to examine the effect of grazing on phosphorus flux through the microbial community.

Laboratory streams description. Laboratory streams used for these studies were housed in greenhouses at Oak Ridge National Laboratory-Environmental Sciences Division (ORNL-ESD). The streams consisted of fiberglass channels, 0.3 m wide and 45 m long, containing gravel and cobble substratum, obtained from a nearby stream (Walker Branch) (Figure 7). Each channel received a continuous input of groundwater. The streams were covered with black plastic to prevent algal growth and to establish a heterotrophic stream system. The groundwater flow was 0.38 L s^{-1} and 0.50 L s^{-1} for maple study and oak study, respectively. The maple study utilized about the last 5 meter section of the artificial stream, whereas the oak study used about a 10 meter section of the stream.

Snails, Goniobasis clavaeformes, were collected from Walker Branch and used for the oak study to examine the effect of grazing on the phosphorus flux. The snail density was approximately 430 snails m^{-2} .

ORNL-PHOTO 3245-81



52

Figure 7. Artificial streams at Oak Ridge National Laboratory, Environmental Sciences Division. (See text for description.)

Red maple leaves, Acer rubrum, were collected just prior to abscission in the Fall of 1982, air dried, and stored until needed. Dried white oak leaves, Quercus alba, were collected in the Fall of 1983. Leaves were placed in streams and allowed to colonize from an inoculum (decomposing leaves) from Walker Branch which was placed upstream. The colonization period was 21 days and 112 days prior to the start of tracer addition (³³P) for the maple study and the oak study, respectively.

Radiolabeled phosphate release. The addition of radiolabeled orthophosphoric acid into laboratory streams was done using a peristaltic pump (Pharmacia Fine Chemicals, Model P-3). The input rates were approximately 960 ml day⁻¹ and 400 ml day⁻¹ for the maple CPOM study and the oak CPOM study, respectively. A polyethylene carboy (Nalgene) containing 0.01N HCl, to diminish side wall adsorption, was used as the tracer feed reservoir. For the maple study, 4.7 mCi of ³³P-orthophosphoric acid was diluted into 25 L of HCl, whereas for the oak study, 25.6 mCi of ³³P-orthophosphoric acid was diluted into 50 L of HCl. When ³³P reached isotopic equilibrium within the cellular phosphorus pools, 4 mCi and 3.8 mCi of ³²P-orthophosphoric acid was added to the remaining input solution for the maple CPOM study and oak CPOM study, respectively. The input was continued until the time at which the feed solution would not last another day.

³³P and ³²P orthophosphate were uniformly distributed, at tracer concentrations, throughout the water of the streams. The

in situ phosphate concentration (as soluble reactive phosphate (SRP)) for the red maple study was $5.0 \mu\text{g P L}^{-1}$; the ^{33}P and ^{32}P phosphate additions were $9.3 \times 10^{-8} \mu\text{g P L}^{-1}$ and $2.6 \times 10^{-7} \mu\text{g P L}^{-1}$, respectively. The combined addition of ^{33}P and ^{32}P ($3.53 \times 10^{-7} \mu\text{g P L}^{-1}$) resulted in a calculated increase in the in situ SRP concentration in the water of $7.1 \times 10^{-6}\%$. The mean in situ SRP concentration for the white oak study was $2.3 \mu\text{g P L}^{-1}$; the ^{33}P and ^{32}P additions were $5.7 \times 10^{-8} \mu\text{g P L}^{-1}$ and $2.1 \times 10^{-8} \mu\text{g P L}^{-1}$, respectively. The combined ^{33}P and ^{32}P addition ($7.8 \times 10^{-8} \mu\text{g P L}^{-1}$) resulted in a $3.4 \times 10^{-6}\%$ increase in the in situ phosphorus concentration in the water for the oak CPOM study.

Stream sampling for fractionation of CPOM. CPOM samples were collected by cutting disks from leaves using a #7 or #10 cork borer. One leaf disk was cut per leaf and placed in a glass dish containing approximately one liter of non-radioactive well water, the same as in the streams, until enough disks were collected (less than 30 min). This was done for two reasons: first, to rinse off any tracer in solution on the disks; and secondly, to maintain the environment of the microbial community. Leaf disks were randomly selected and dispensed for whichever phosphorus pool was to be examined (see specific extraction procedure).

Phosphate analysis. SRP was determined by a modified method of Murphy and Riley (1965) as outlined by Wetzel's and Liken's (1979) alternative B procedure. A Varian Series 634 spectrophotometer

with slit setting of 2 nm, absorbance setting of 885 nm, and a 1 cm cell was used. Dissolved phosphate was also determined by the Murphy and Riley (1962) procedure using a Perkin-Elmer Hitachi Model 200 spectrophotometer using a 10 cm cell, with a 2 nm slit and absorbance setting of 885 nm. Phosphate concentration was determined from a standard curve of phosphate concentration versus absorbance unit at 885 nm. The modified procedure was used by me to determine the SRP level, whereas the technical staff of ESD used the Murphy and Riley method.

Leaf mass. Dry weight (DW) was determined by drying leaf disks at 105°C overnight. Ash weight (AW) of leaves was determined by combusting leaf matter in precombusted and tared aluminum pans at 450°C overnight. Ash-free dry weight (AFDW) was obtained by subtracting ash weight from the dry weight.

Data analysis. Data were analyzed using the Statistical Analysis System (Helwig and Council, 1982), a statistical package, using a DEC 10, IBM 360/5-370/148 computer system at the University of Tennessee, Knoxville. Linear regression and analysis of variance (ANOVA) were performed using the General Linear Model (GLM) subprogram. The temporal data for the isotope ratios and concentrations were subjected to a linear regression analysis to determine the slope of the curve. Biomass data was subjected to ANOVA to determine whether there was significant grazing effect on the microbial community. Duncan's Multiple Range Analysis was used to test for

significant difference among mean biomass for the ungrazed and grazed streams and temporal differences with the ungrazed and grazed streams. All statistical tests for significance were done at $P \geq 0.95$. The 95% confidence level for the regression coefficient, the slope, was calculated according to Sokal and Rohlf (1969) ($\alpha = 0.05$).

V. RESULTS

Preliminary Studies

In order to determine the bacterial cell density associated with leaf CPOM, the cells had to be removed from the CPOM surface. As indicated in Table 3, a 5 minute homogenation time was found optimum for the maximal recovery of bacterial cells from the surface of leaf CPOM. This procedure, however, does not quantitatively remove bacteria from the leaf surface. It was found that only 54% of the cells were removed by this procedure (see Methods--recovery of bacteria). A homogenation time of 15 minutes significantly elevated the homogenate temperature which might have reduced the relative recovery of viable bacteria. Subsequently the bacterial densities reported are relative values and were used for comparative purposes.

Closed system studies were done to become skilled in working with a CPOM associated microbial community and to evaluate variability of parameters under study. Initial phosphorus incorporation rates, phosphorus uptake, incorporation into phospholipid, and distribution of ^{32}P -tracer in the intracellular pools were monitored using red maple CPOM.

Phosphorus uptake by a red maple CPOM microbial community which was allowed to develop for 19 days prior to the tracer addition is shown in Figure 8. The initial phosphorus incorporation rate, defined as the slope of the linear portion of the uptake curve, was $0.56 \text{ ng PO}_4\text{-P cm}^{-2} \text{ min}^{-1}$. The rate constant of 0.021 h^{-1} was

Table 3. Comparison of stomacher homogenation times for the removal of bacteria from the leaf surface.

Homogenation Time (Minutes)	Cells Per ml of Homogenate ^a ($\times 10^4$)
1	115 \pm 14
3	149 \pm 8
5	246 \pm 61
10	235 \pm 11
15	197 \pm 50

^aAs determined by plate counts after four days' incubation at 25°C; reported values are means \pm 1 S.D.

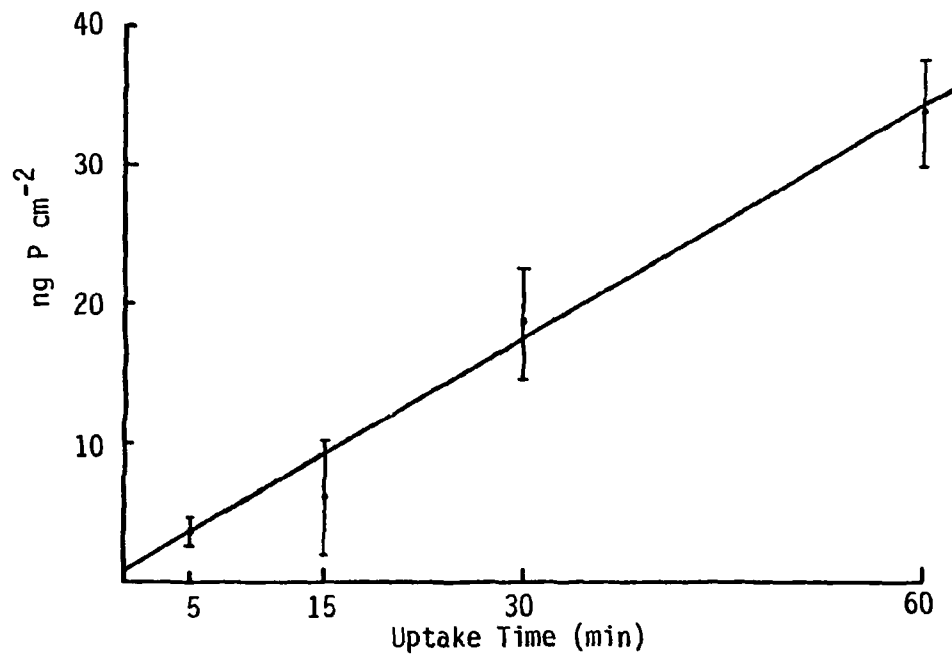


Figure 8. Phosphate uptake by microbiota associated with decomposing red maple CPOM established for 19 days. The curve is a linear best fit using all data. Shown are the means ± 1 S.D. $y = 0.56x + 0.65$; $r = 0.97$.

determined by the method described by Lean and White (1983) in which the log of the percent radioactivity remaining in solution is plotted versus time (Figure 9). The phosphate turnover time for the phosphate in the water was calculated to be 48 h (surface area to solution ratio was 0.123). The bacterial cell density and the organic content of the maple CPOM was 6.82×10^6 cells cm^{-2} of leaf surface and 16.8 mg ash-free dry weight (AFDW) cm^{-2} , respectively. The water had a phosphorus concentration of 2.5 $\mu\text{g PO}_4\text{-P L}^{-1}$ as soluble reactive phosphate (SRP) and a temperature of 14°C.

Phosphorus uptake was also examined using red maple CPOM colonized for 31 days (Figure 10). The initial incorporation rate was 0.169 ng $\text{PO}_4\text{-P cm}^{-2} \text{min}^{-1}$. Microbial biomass, as ATP, and the bacterial cell density were 4197 pg ATP cm^{-2} of leaf surface and 3.27×10^7 cells cm^{-2} of leaf surface, respectively. The calculated ATP content per cell was 1.28×10^{-4} pg ATP. The organic content of the CPOM was 0.78 mg AFDW cm^{-2} . The phosphorus concentration of the water was 3.3 $\mu\text{g PO}_4\text{-P L}^{-1}$ as SRP; the water temperature was 17.5°C.

Comparing the above closed system studies, it is interesting that the phosphorus uptake rate for the younger microbial community (19 days) was approximately three times greater than the 31 day community, even though the concentration of available Pi was less and the cell density and water temperature were lower. The organic content, however, of the 19 day CPOM was about twenty times greater than the 31 day CPOM suggesting the older microbial community might

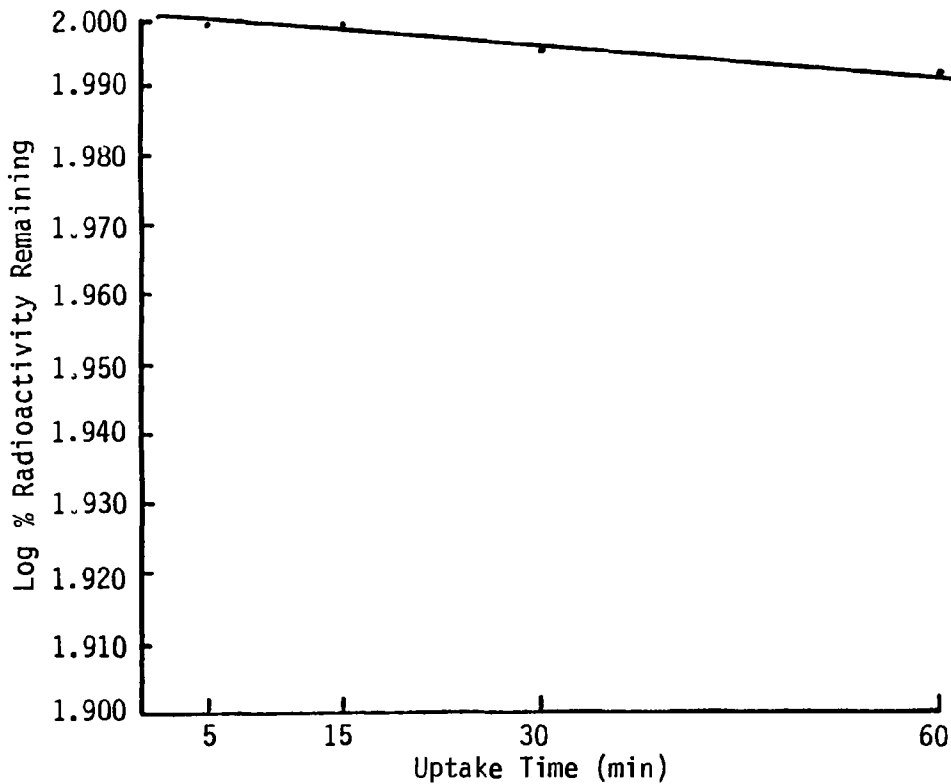


Figure 9. Kinetics of phosphate removal by microbiota associated with red maple CPOM established for 19 days. One ml of water was filtered and assayed for radioactivity for each point. $y = (1.506 \times 10^{-4})x + 1.999$; $r = 0.99$.

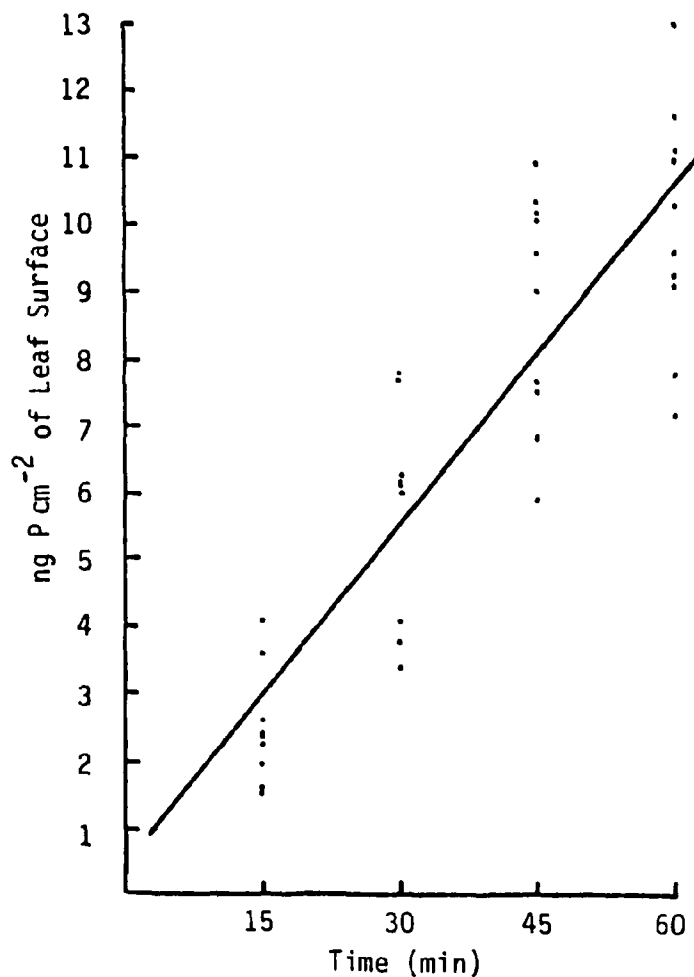


Figure 10. Phosphorus uptake by microbiota associated with red maple CPOM established for 31 days. Each datum is a single leaf disk. The curve is a linear best fit to the points. $y = 0.169x + 0.447$; $r = 0.87$.

have been carbon limited or metabolically less active. This comparison, also, indicates greater phosphorus cycling by the younger microbial community compared to the older microbial community.

Phosphorus uptake rates were determined based on single time point uptake (sample taken at one time point only, 1 h or 20 h). An uptake rate of $3.30 \text{ ng P cm}^{-2} \text{ h}^{-1}$ and $0.74 \text{ ng P cm}^{-2} \text{ h}^{-1}$ was determined for 1 h and 20 h uptake times, respectively. The red maple CPOM was colonized for 15 days and had a microbial biomass of $12,877 \text{ pg ATP cm}^{-2}$ and a bacterial cell density of $2.90 \times 10^7 \text{ cells cm}^{-2}$. The calculated ATP content per cell was $4.44 \times 10^{-4} \text{ pg ATP}$ and the CPOM organic content was $1.09 \text{ mg AFDW cm}^{-2}$ of leaf surface. The phosphate concentration of the water was $3.3 \mu\text{g PO}_4\text{-P L}^{-1}$ as SRP; the water temperature was 14°C .

Comparing the calculated uptake rates for the 1 h and 20 h time points indicated that a linear uptake did not occur over the 20 h period. Uptake kinetics appear to be biphasic with an initial rapid uptake period followed by a period of slower uptake. One reason for this occurrence may be that the concentration of available Pi might have become limited by the 20 h sampling. Another possible explanation is that by the 20 h sample sufficient efflux had occurred thus decreasing the amount of phosphorus initially accumulated (1 h sample) resulting in a lower calculated uptake rate.

The incorporation of ^{32}P into lipid-P (phospholipid) was also determined using maple CPOM colonized for 15 days. The incorporation of phosphorus into lipid-P was linear for the 20 h period

examined with a calculated incorporation rate of $0.148 \text{ ng P cm}^{-2} \text{ h}^{-1}$ (Figure 11). Assuming one phosphate atom per phospholipid molecule, the calculated synthesis of phospholipid was $1.53 \text{ pmol cm}^{-2} \text{ h}^{-1}$, and $5.46 \times 10^{-9} \text{ pmol cell}^{-1} \text{ h}^{-1}$ of phospholipid was synthesized by the microbial community present ($2.9 \times 10^7 \text{ cells cm}^{-2}$).

The contribution of abiotic absorption to the total uptake of phosphorus by CPOM microbial community is shown in Table 4. Abiotic adsorption of phosphorus ranged between 4% to 11% of the total phosphorus accumulated. Abiotic adsorption accounted for a greater percentage of the total phosphorus uptake for short uptake times ($\leq 15 \text{ min}$) indicating that the abiotic uptake rate was slower than the biotic uptake rate. It is concluded that abiotic adsorption of phosphorus onto CPOM is relatively insignificant compared to the biotic absorption.

A preliminary cellular fractionation study was done using the red maple CPOM which had been colonized for 15 days. The microbial community was labeled with $^{32}\text{P}_04\text{-P}$ for 20 h and the intracellular phosphorus pools were fractionated. The distribution of ^{32}P -tracer in the intracellular pools, as percent of whole cell-P (WC-P), was as follows: metabolite pool-P (MP-P), 20.1%; lipid-P (L-P), 19.9%; RNA-P, 51.9%; DNA-P, 13.9%; and total recovered in all fractions, 105.8%.

Analytical Recovery Efficiencies for Intracellular Phosphorus Pools

The analytical recovery of phosphorus in intracellular pools was determined with the use of radioactive standard compounds

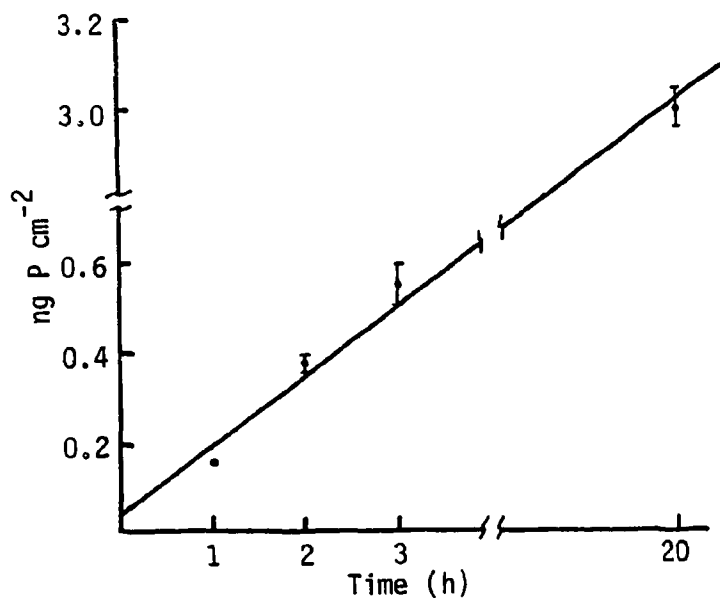


Figure 11. Incorporation of phosphate into phospholipid. The curve is a linear best fit to the individual datum; $n = 2$. Shown are the mean ± 1 S.D. $y = 0.148x + 0.047$; $r = 0.99$.

Table 4. Abiotic adsorption of phosphate to maple leaf CPOM in closed systems.^a

Phosphate Uptake Time (Min)	CCCP Conc. (mM)	Exposure ^b to CCCP (Min)	Leaf ^c Age (Days)	CCCP Treatment (DPM/Disk) ^d	Water Only (DPM/Disk) ^e	Abiotic PO ₄ Uptake (% of Total) ^f
5	0.10	15	19	2065 ± 978	18,080 ± 4,256	11.42
15	0.10	15	19	3420 ± 530	35,203 ± 9,003	9.72
30	0.10	15	19	3469 ± 1152	87,252 ± 17,621	3.98
60	0.10	15	19	5353 ± 2513	150,212 ± 16,094	3.56
60	0.10	30	15	989 ± 296	10,521 ± 941	9.40
120	0.10	30	10	2744 ± 833	51,372 ± 9,336	5.34
60	0.25	30	31	3917 ± 2060	56,080 ± 10,737	6.99

99

^aCarbonyl-cyanide m-chlorophenyl hydrazone (CCCP) was used to inhibit microbial uptake.

^bThe time leaf disks were exposed to CCCP prior to the addition of ³²P tracer.

^cDays leaves were in stream before use in experiments.

^dMean ± 1 S.D.; DPM associated with CCCP treated leaf disks.

^eMean ± 1 S.D.; DPM associated with untreated leaf disks.

^fMean DPM in CCCP treatment/Mean DPM in untreated disks.

(Table 5). The recovery efficiency for L-P was estimated using two amphipathic compounds, palmitic acid and phosphatidyl ethanol-amine. Both compounds were recovered at an efficiency of 92%. Glucose was used as a representative acid soluble low molecular weight compound to estimate the MP-P recovery efficiency. The recovery efficiency for glucose ranged from 101% to 111%, so the recovery efficiency for MP-P was taken to be 100%. Using ^{32}P -labeled nick-translated salmon sperm DNA, a DNA recovery efficiency of 77% was determined, and RNA recovery efficiency, as determined by an *E. coli* total RNA standard, was 84%. The resulting recovery efficiencies were used to correct fractionated pools of phosphorus in microbes associated with CPOM to 100% recovered.

Microbial Colonization of Leaf CPOM

Glucose metabolism and metabolic activity of CPOM associated microbial communities. The rate of glucose metabolism by decomposing dogwood, maple, and oak CPOM are shown in Table 6 and Figures 12, 13, 14, 15. The data are divided into four categories, glucose assimilated (labeled glucose taken up and retained in cellular material), glucose mineralized (glucose taken up and subsequently respiration), total glucose uptake (assimilated plus mineralized), and percent of glucose uptake mineralized. It was assumed that the in situ glucose concentration was negligible compared to the added glucose ($50 \mu\text{g L}^{-1}$), thus the effective glucose concentration was that of the added glucose.

Table 5. Recovery of standards during CPOM fractionation.^a

Phosphorus ^b Pool	Recovery Standard	Determination of Recovery Efficiency			% Recovered ^e
		DPM Added ^c	DPM Recovered ^d	% Recovered	
L-P	palmitic acid phosphatidyl ethanolamine	76,081 ± 2,604* 620,167 ± 3,182*	69,712 ± 5,544* 570,091 ± 7,652*	92 ± 8 92 ± 1	
DNA-P	oligonucleotide Experiment 1 Experiment 2	1,976,700 ± 21,442** 2,392,417 ± 44,548*	1,541,092 ± 69,401* 1,827,255 ± 44,000*	78 ± 4 76 ± 20	
MP-P	glucose Experiment 1 Experiment 2	2,046,772 ± 7,869** 4,168,823 ± 34,892**	2,266,664 ± 11,569* 4,231,278 ± 43,322*	111 ± 1 101 ± 1	88
RNA-P	Total RNA	3,347,472 ± 87,401**	2,791,457 ± 122,859*	84 ± 4	

^aBased upon radiolabel recovery.

^bL-P, lipid phosphate; DNA-P, DNA phosphate; MP-P, metabolite pool phosphate; RNA-P, RNA phosphate.

^cMean ± 1 S.D. DPM added determined by spiking replicate scintillation vial with same amount added to CPOM homogenate; error represents pipeting error.

^dMean ± 1 S.D.; DPM recovered from spiked CPOM homogenate.

^eMean ± 1 S.D.

*n = 3; +n = 2; **n = 4.

Table 6. Glucose metabolism by microbes associated with decomposing dogwood, maple, and oak CPOM.^a

Leaf Species	Days in Stream	Uptake ^b	Assimilated ^b	Mineralized ^b	% Mineralized
Dogwood	1	--	--	0.06 ± 0.02	--
	3	11.31 ± 3.81	9.16 ± 2.65	2.15 ± 1.64	17.8 ± 10.9
	7	9.45 ± 5.03	5.17 ± 2.70	4.26 ± 2.39	44.6 ± 4.3
	10	9.96 ± 3.58	6.06 ± 1.93	3.90 ± 1.72	38.1 ± 4.9
	15	8.22 ± 4.75	5.77 ± 3.50	2.45 ± 1.30	31.6 ± 5.2
	22	10.03 ± 2.16 ^c	7.15 ± 1.56 ^c	2.88 ± 0.66 ^c	28.7 ± 2.9 ^c
	29	18.12 ± 9.54	12.13 ± 5.81	5.99 ± 4.38	31.4 ± 14.3
	36	16.04 ± 6.86	10.12 ± 4.54	5.88 ± 2.49	36.7 ± 5.1
Oak	1	--	--	0.03 ± 0.03 ^c	--
	3	1.42 ± 0.32	0.22 ± 0.12	1.08 ± 0.41	83.2 ± 11.4
	7	3.75 ± 2.61	1.93 ± 1.17	1.83 ± 1.49	43.9 ± 12.4
	10	4.82 ± 1.86 ^d	3.06 ± 0.99 ^c	1.99 ± 0.78 ^d	41.2 ± 0.5 ^d
	15	8.98 ± 5.47 ^c	6.70 ± 3.25 ^c	3.04 ± 2.25	31.0 ± 6.1 ^c
	22	8.48 ± 4.01	5.80 ± 2.76	2.68 ± 1.31	31.9 ± 5.8
	29	10.36 ± 2.07	6.69 ± 3.28	2.21 ± 1.21	20.6 ± 8.9
	36	9.41 ± 4.96	5.13 ± 1.61	4.28 ± 3.53	40.6 ± 11.9
Maple	1	--	--	0.01 ± 0.10	--
	3	6.39 ± 2.53	5.39 ± 2.25	1.00 ± 0.63	16.3 ± 6.9
	7	4.86 ± 1.86	2.97 ± 1.03	1.90 ± 1.09	37.7 ± 10.8
	10	13.56 ± 3.06	7.78 ± 2.43	5.78 ± 0.94	43.3 ± 6.0
	15	6.80 ± 6.62	3.46 ± 3.97	3.34 ± 2.73	54.9 ± 13.8
	22	8.61 ± 1.95	5.52 ± 2.12	3.09 ± 1.04	37.5 ± 17.8
	29	8.17 ± 2.87	6.07 ± 2.23	2.10 ± 1.03	26.4 ± 10.1
	36	14.26 ± 8.99	8.15 ± 4.60	6.10 ± 4.53	40.0 ± 8.9

^aUnits of measurement are ng glucose h⁻¹ cm⁻² of leaf surface.^bMean ± 1 S.D.; n = 5.^cn = 4.^dn = 3.

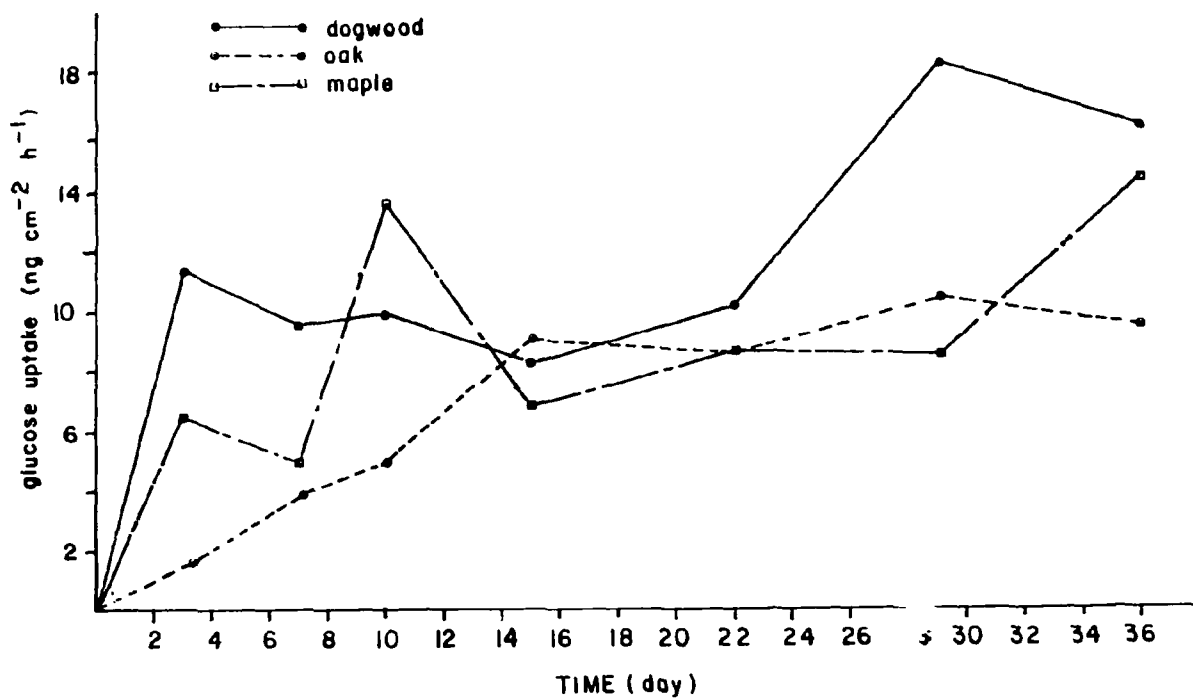


Figure 12. Temporal patterns of glucose uptake (i.e., assimilated plus mineralized) rates by decomposing leaf CPOM. Each point represents the mean of five replicate leaf disks (1.4 cm dia.).

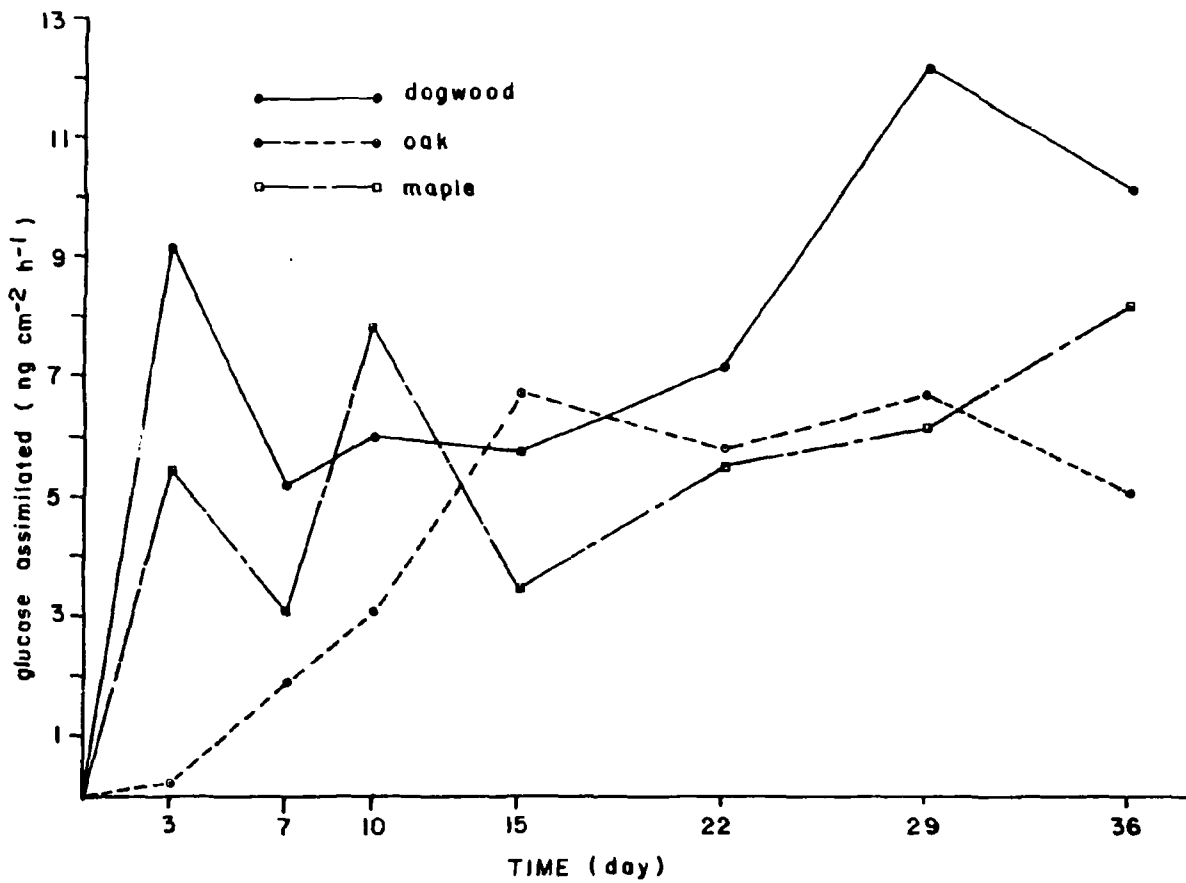


Figure 13. Temporal pattern for glucose assimilation rates by decomposing leaf CPOM. Each point represents the mean of five replicate leaf disks (1.4 cm dia.).

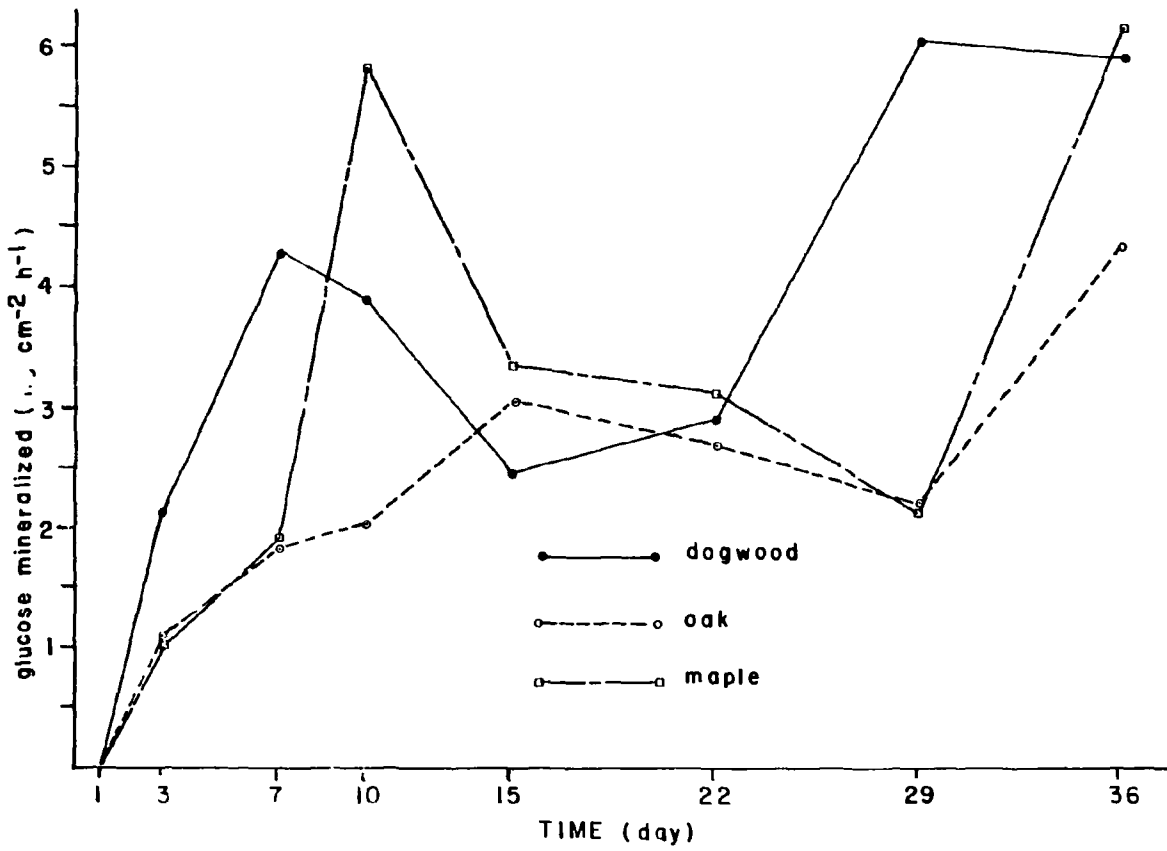


Figure 14. Temporal pattern for glucose mineralization rates for decomposing leaf CPOM. Each point represents the mean of five replicate leaf disks (1.4 cm dia.).

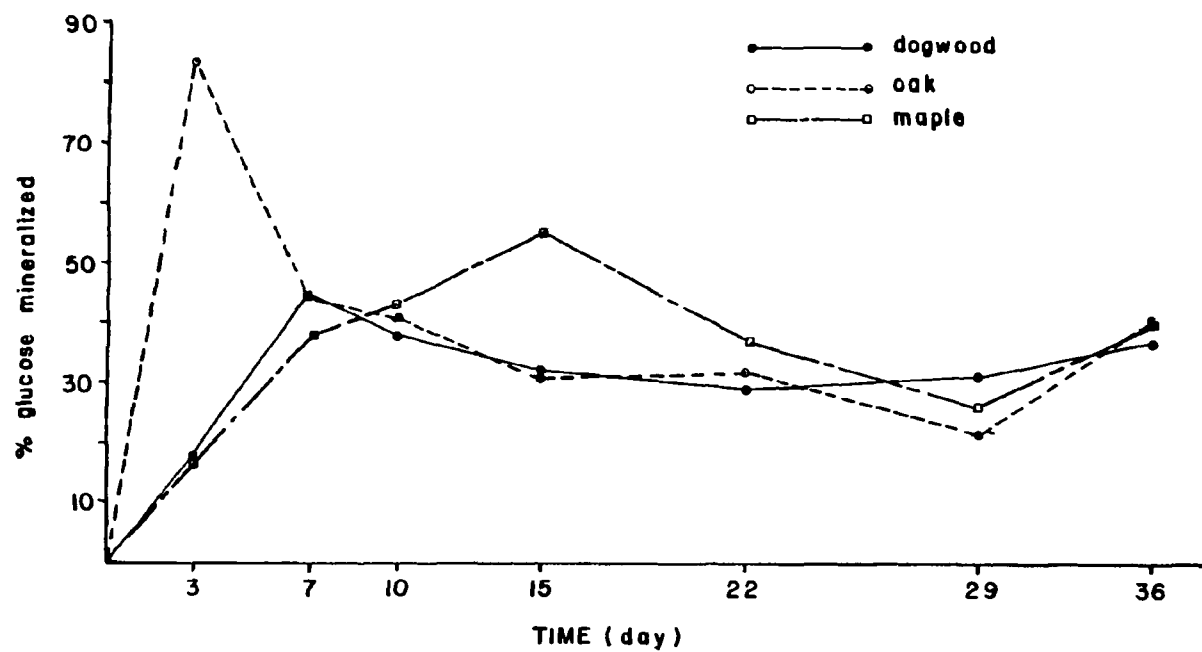


Figure 15. Temporal pattern for CPOM of percentage of glucose uptake which was mineralized.

The glucose uptake rate for dogwood CPOM increased as a function of the time leaves had been in the artificial stream, rapidly at first, remained relatively constant until day 22, and then subsequently increased with a slight decline by day 36 (Figure 12). The maple CPOM showed a fluctuating pattern of increase and decline in the glucose uptake rate until day 22. The rate remained relatively constant until day 29 with a final increase in the rate occurring on day 36. The glucose uptake rate for the oak CPOM showed a different pattern from the dogwood and maple CPOM. A gradual increase in the rate was observed to reach a maximum by day 15 followed by a period of constancy to the end of the study period.

Glucose assimilation rate for dogwood CPOM rapidly increased initially and then declined and remained relatively constant until day 15 and then increased again with a subsequent decline at day 36 (Figure 13). The rate of assimilation for maple CPOM increased rapidly then declined, increased again and declined, and then gradually increased for the remainder of the study period. The assimilation rates for the oak CPOM gradually increased and reached a maximum by day 15 and remained relatively constant for the remainder of the study.

The rate of glucose mineralization for dogwood CPOM exhibited a bimodal trend (Figure 14). Initially, the rate increased rapidly until day 7 and subsequently declined until day 15 and remained constant followed by a subsequent increase until day 29 and remained constant. The mineralization rate for maple CPOM increased at first

to a maximum by day 10 and then declined until day 29 and subsequently increased. The mineralization rate for the oak CPOM gradually increased until day 10 then decreased slightly until day 29 and increased thereafter.

The percent glucose mineralized by decomposing dogwood CPOM increased to a maximum of about 45% by day 7 and then gradually declined and remained relatively constant (30% to 37%) for the rest of the period (Figure 15). The percentage of glucose mineralized by the maple CPOM gradually increased to a maximum of 55% by day 15. A decline in the percentage occurred until day 30 (25%) after which the percentage increased to 40% on day 36. The percentage of glucose mineralized by oak CPOM was greatest on day 3 (83%) and declined for the next 12 days to 31%. The percent mineralized then remained constant until day 22, which was followed by a slight decline until day 30 after which it increased to 40% on day 36.

CPOM mass (organic content). The organic content (ash-free dry weight) of the decomposing leaf CPOM was monitored during colonization (Figure 16). The organic content of dogwood CPOM had an initial rapid decrease (3 days), then remained relatively constant for the next 12 days. A period of decrease was observed again lasting for 14 days which was followed by a slight increase and subsequent decline in the amount of organic content present. A more rapid decrease in organic content occurred within 1 day for maple CPOM and remained constant for the next 2 days. An increase in maple CPOM organic

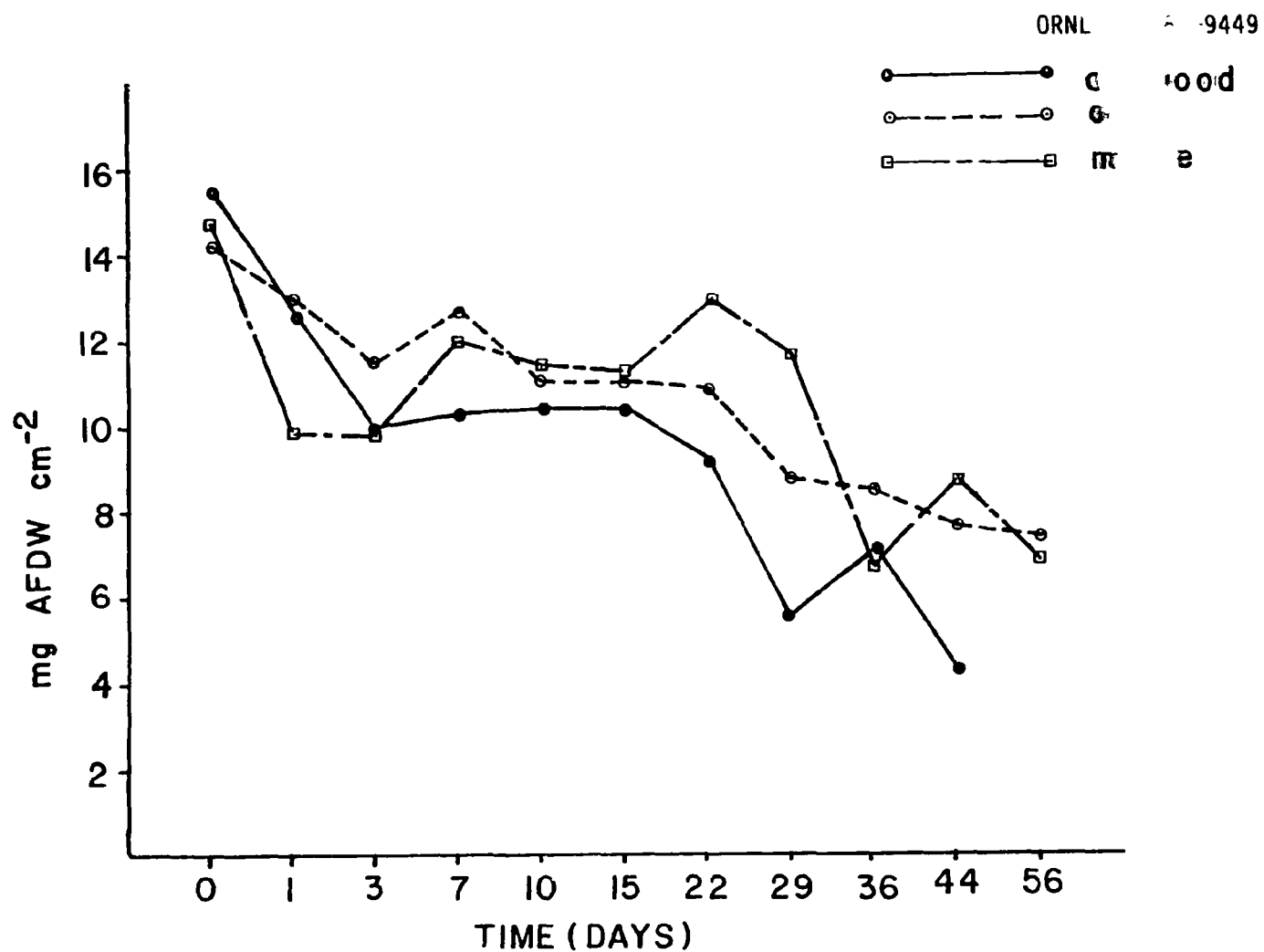


Figure 16. Temporal pattern of leaf CPOM organic content as measured by ash-free dry weight (AFDW). Five disks (1.4 dia.) per species per sampling time.

content occurred on day 4 and remained relatively constant for the next 8 days. After a slight increase, the organic content decreased for a 14 day period (days 22 to 36), as in dogwood CPOM, followed by another increase and subsequent decrease. The organic content of oak CPOM decreased during the first 3 days, but not as rapidly as that of the dogwood and maple CPOM. A slight increase in organic content occurred followed by a period of constant organic content until the twenty-second day. A subsequent decline in organic content was observed for the remainder of the study.

Scanning electron microscopy of CPOM. The scanning electron microscopy (SEM) was done to observe the general temporal pattern of microbial community development on CPOM. This analysis was not intended to be a definitive study, in that observations made might be biased due to the sampling procedure. Only one leaf disk was randomly cut from a leaf and prepared for SEM viewing and replicate samples from different specific areas of leaves (e.g., midrib, veins, ancillary veins, top and bottom surfaces) were not collected.

Dogwood CPOM. Observation of dogwood leaves prior to placement in the stream revealed sparse fungal colonization already present on veins (Figure 17). This fungal population was probably a portion of the phylloplane microbial community present prior to the collection of the dogwood leaves. By the third day in the stream, bacterial colonization was evident and the leaf surface was still relatively free of fungal growth. Spore accumulation near puberulent hairs,

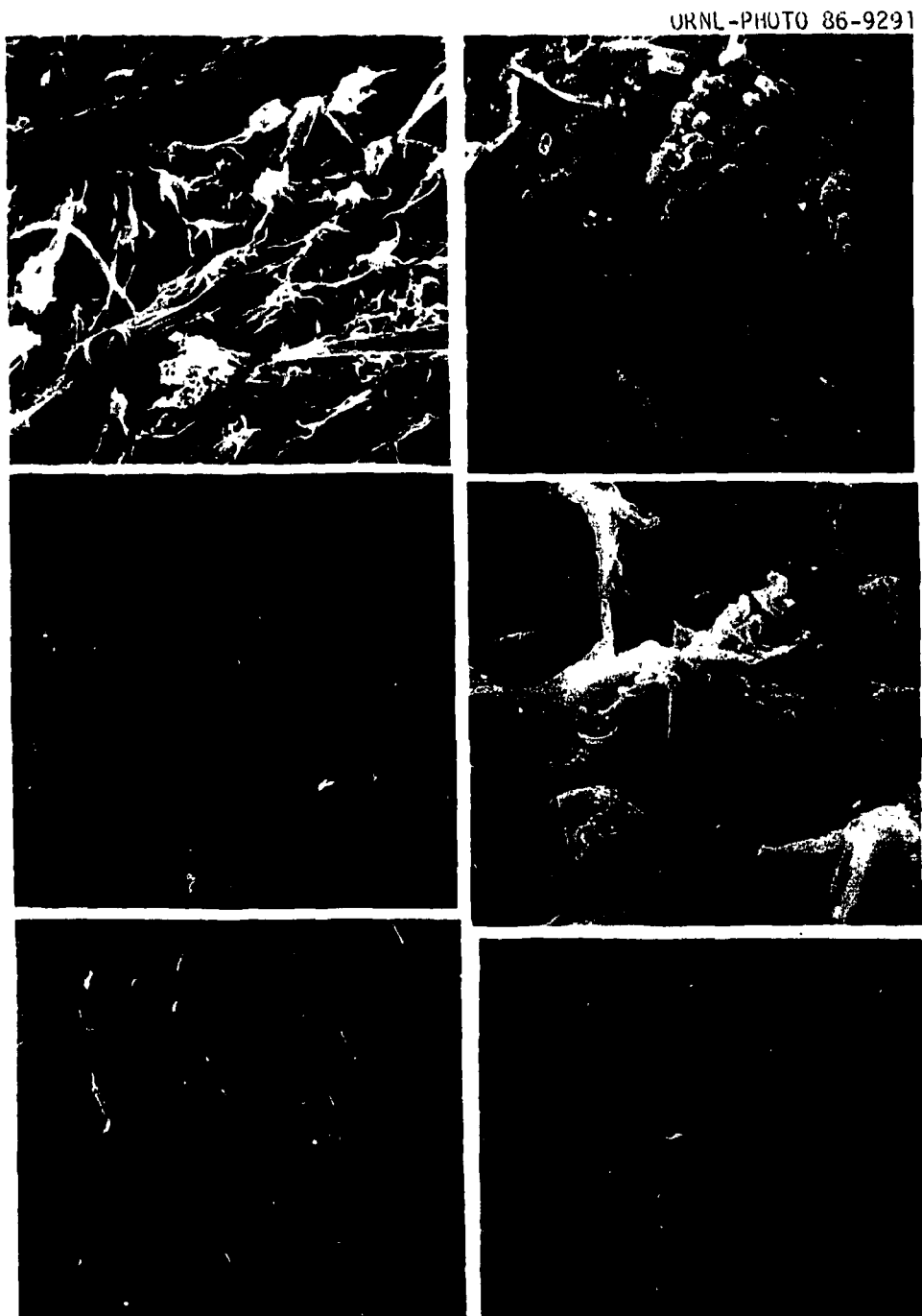


Figure 17. Dogwood leaf CPOM, day 0 to day 3.

Plate A. Day 0, prior to placement in stream; 300x; stomata indicated by arrows.

Plate B. Day 3. 3000x; bacterial colonization.

Plate C. Day 3. 300x; puberulent hairs with accumulated spores indicated by arrow.

Plate D. Day 3. 1500x; bacterial colonization.

Plate E. Day 3. 60x; top surface of leaf showing lack of fungal accumulation. Arrow indicates hairs seen in Plate C.

Plate F. Day 0. 30x; fungal colonization of veins.

however, can be seen (Figure 17C). These spores were probably present prior to placement in the stream because of terrestrial morphology (spherical) of the spores.

The development of the fungal community in dogwood leaves has begun by the seventh day (Figure 18) and continued to a maximum population density by day 22 (Figures 18 and 19). During this period, a build-up of organic matter on the surface was occurring (Figure 18B). Germinating spores were observed on CPOM in the stream for 10 days. After 22 days in the stream, the dogwood CPOM had a dense population of bacteria and fungi (Figure 19). A variety of morphological types of bacteria were observed on 22 day CPOM (Figure 19), and *amoeba*-like protozoa were also seen. Heavy accumulation of organic debris and leaf tissue deterioration was associated with the dense microbial community (bacteria and fungi) on 29 day old CPOM (Figure 19). Bacterial microcolonies associated with a fungal septal area were observed on day 29. Observations made after day 29 revealed a dense build-up of organic matter making it difficult to observe fungi on the surface or perhaps the fungal population had decreased substantially (Figure 20). Bacteria can be seen, however, associated with the organic debris (Figure 20).

Maple CPOM. The development of the microbial community on maple CPOM began by the third day in the stream. Bacterial colonization and initial development of the fungal community (germinating spores and early hyphal growth) was observed for the period between

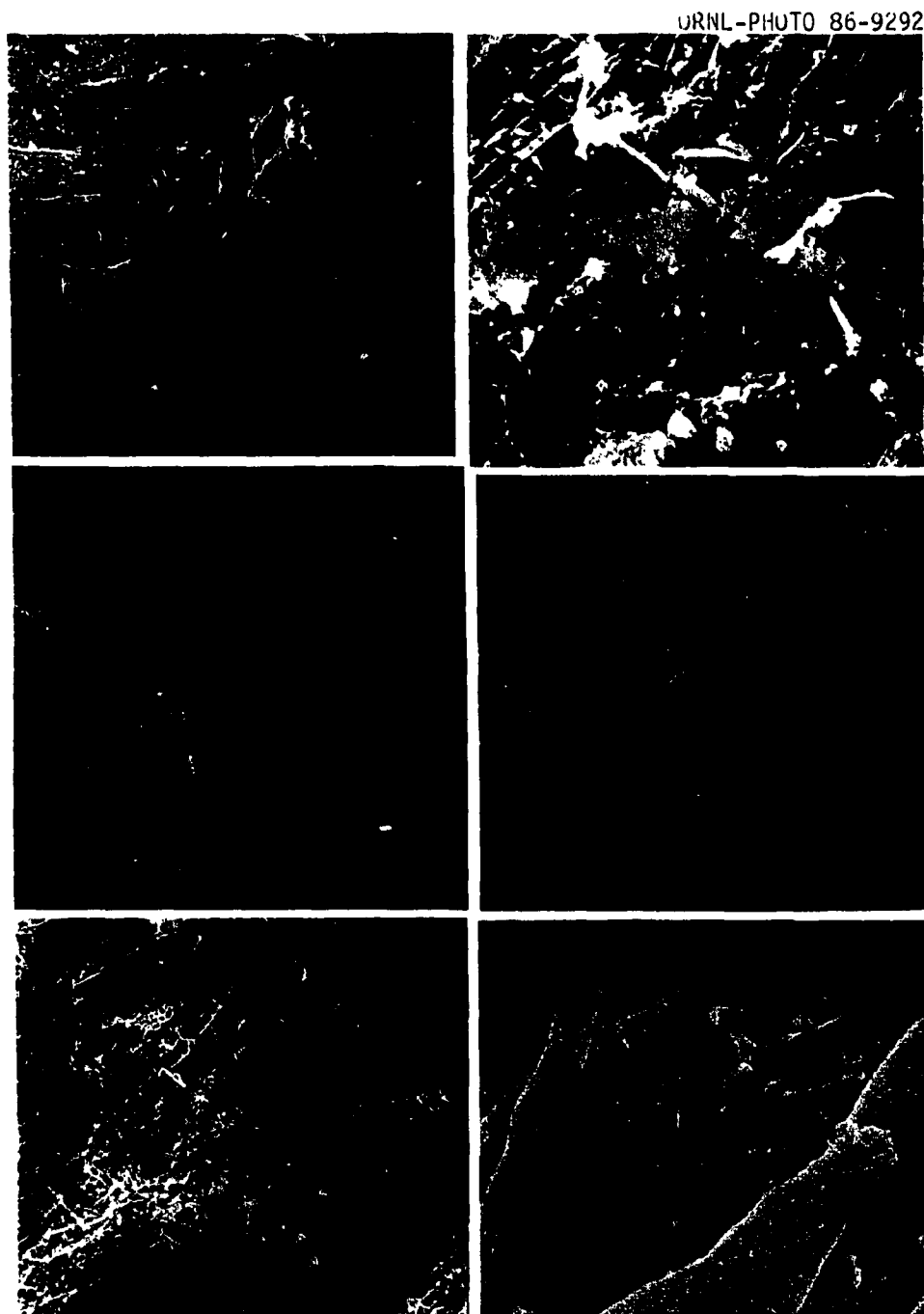


Figure 18. Dogwood leaf CPOM, days 7 to 22.

Plate A. Day 10. 60x; fungal growth starting to develop.

Plate B. Day 15. 1500x; fungal growth (arrow) and debris accumulating.

Plate C. Day 7. 600x; fungal growth and debris accumulation evident.

Plate D. Day 10. 3000x; germinating spore.

Plate E. Day 22. 60x; dense accumulation of fungal community.

Plate F. Day 22. 3100x; bacteria evident amongst fungi.

ORNL-PHOTO 86-9293

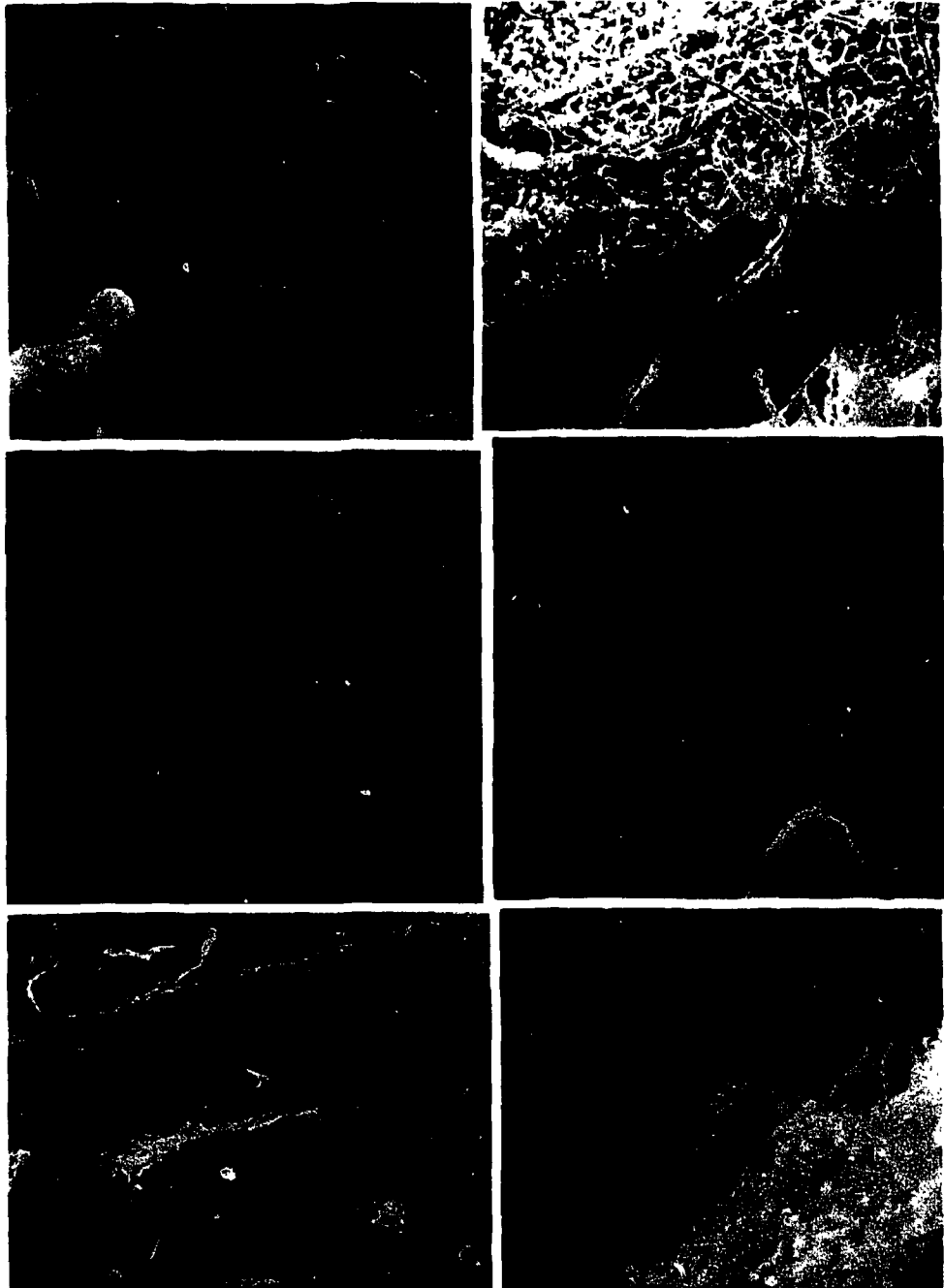


Figure 19. Dogwood leaf CPOM, days 22 to 29.

Plate A. Day 22. 3100x; bacteria located in a clear zone on the leaf surface; note colonies covered with polymer (arrow).

Plate B. Day 29. 140x; fungal mat with polymer.

Plate C. Day 29. 3000x; bacterial microcolony associated with fungal hyphae.

Plate D. Day 22. 3000x; vase-like protozoa; arrow indicates bacteria and polysaccharide.

Plate E. Day 29. 5600x; various morphological types of bacteria present; note cell with fuzzy polymer.

Plate F. Day 20. 5600x; bacteria associated with surface.

URNL-PHOTO 86-9294

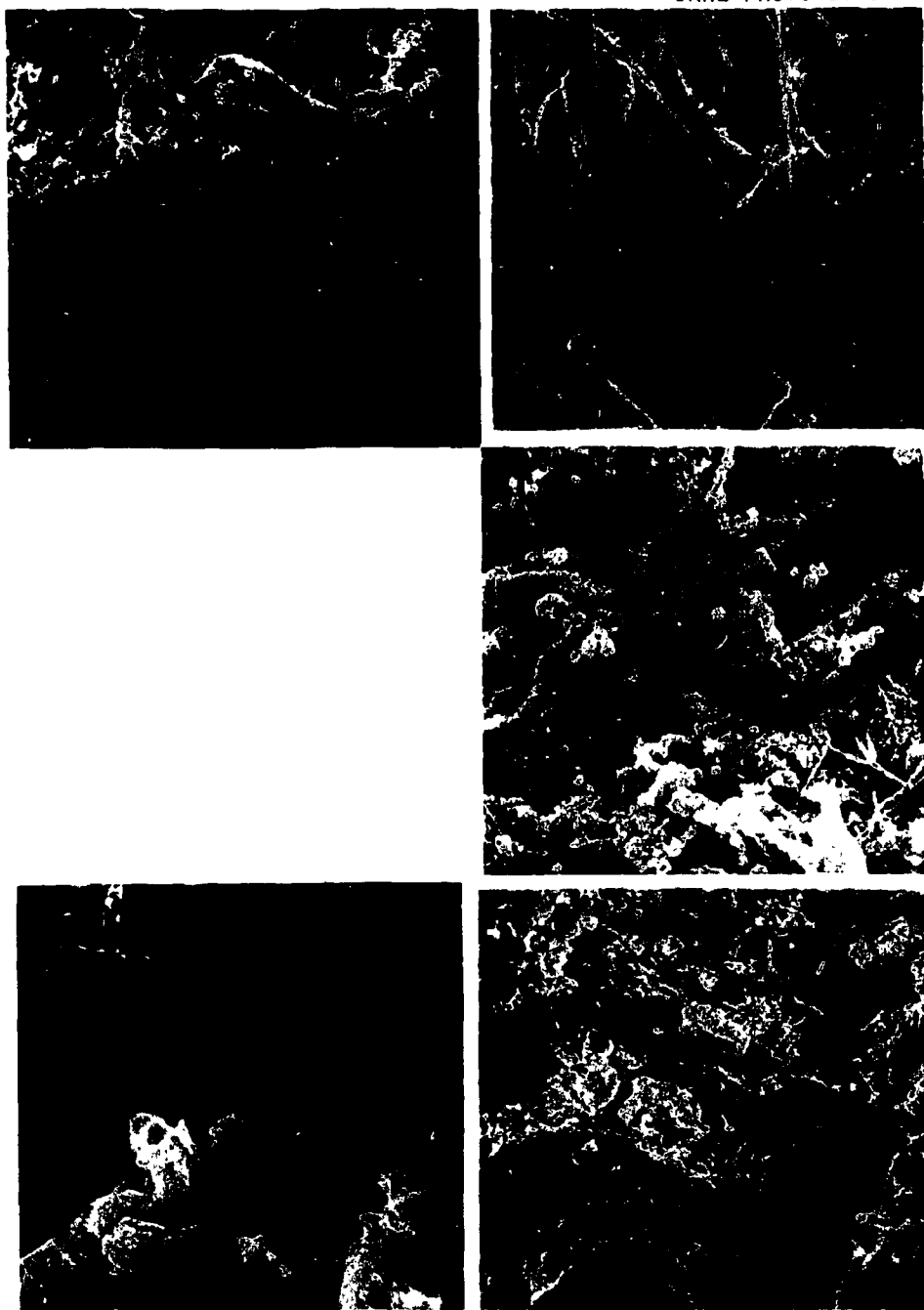


Figure 20. Dogwood leaf CPOM, days 22 to 44.

Plate A. Day 36. 300x; surface polymer; note decrease in fungal population.

Plate B. Day 22. 300x; fungal community.

Plate C. Day 44. 540x; surface polymer and associated spores and diatoms (arrow).

Plate D. Day 44. 3200x; close-up of polymer and associated bacteria.

Plate E. Day 36. 150x; surface free of fungi, polymer build-up continues.

the third and seventh day in the stream (Figure 21). The fungal community was patchy (Figure 22) and areas of dense bacterial colonization were seen (Figure 22). Diatoms were also observed occasionally (Figure 24). By day 15, organic debris was increasing on the surface of the maple CPOM (Figure 23). Between the twenty-second and thirty-sixth day in the stream, organic debris increased, leaf tissue was breaking down, fungal growth was sparse, and bacterial microcolonies were observed (Figures 23, 24). A microcolony of about five generations of growth and perhaps spiny bacteria were also seen (Figure 23). The fungal population was increasing but only in patches (Figure 23). The colonization period from days 44 to 56 shows an increase in organic debris, leaf tissue breakdown, and limited fungal population (Figure 24). A fungal-free vein and bacterial association with the organic debris was observed.

Oak CPOM. Prior to placing it in the stream, oak CPOM appears as if it were coated with a polymer and had surface debris present (Figure 25). By the third day in the stream, bacteria are present on the surface, debris was patchy and spores were observed (Figure 25). The colonization period from 10 to 22 days revealed the fungal population and debris on the oak CPOM increasing, however it never achieved the density seen on dogwood (Figures 25, 26). Fungi seem to play a role in the debris entrapment (Figure 26), however, this may be an artifact of sample preparation. Bacteria and fungi associated with veins were observed by day 22 (Figure 26). The fungal

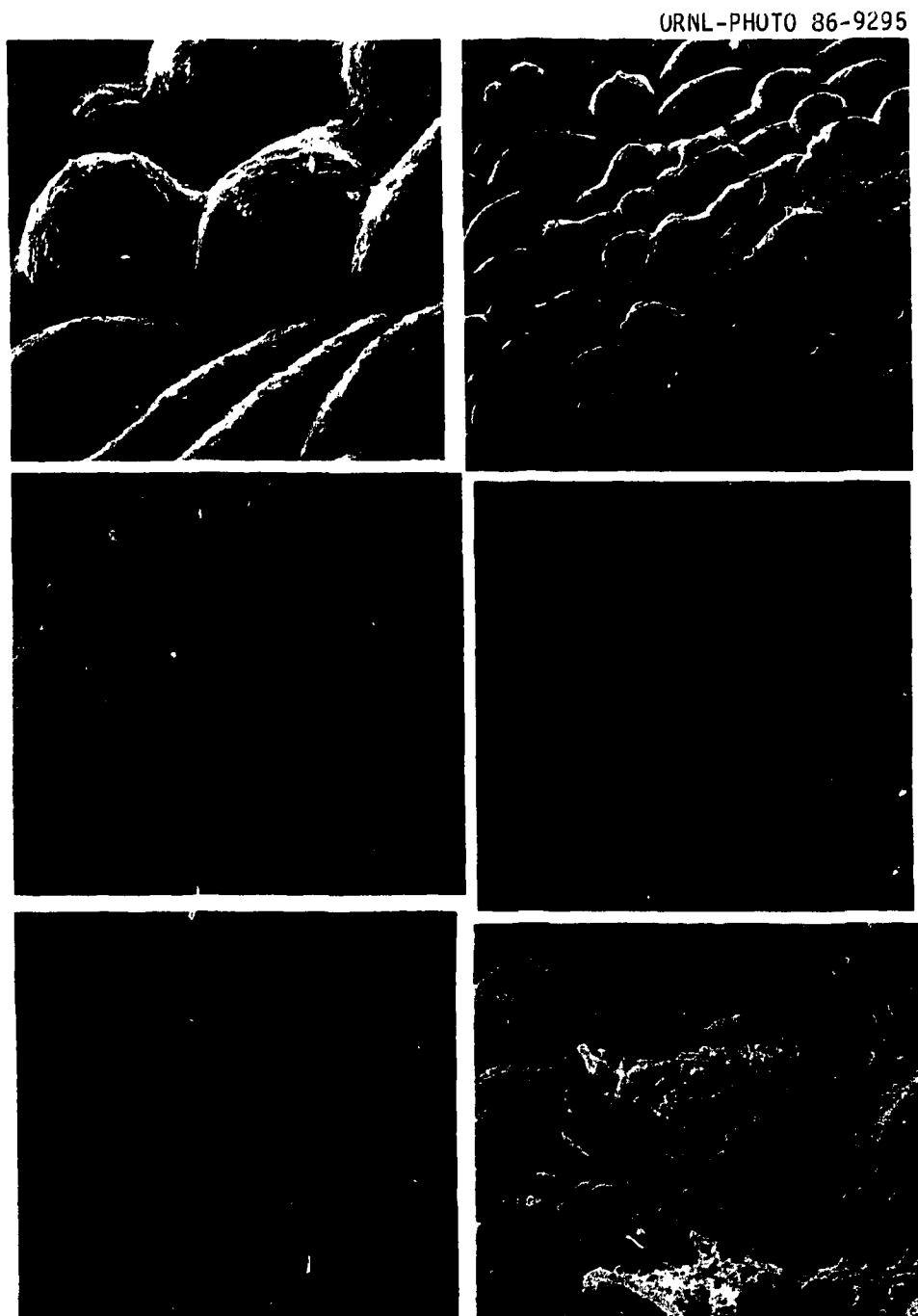


Figure 21. Maple leaf CPOM, days 0 to 7.

Plate A. Day 0. 1500x; polymer coating appearance on leaf surface prior to placement in stream.

Plate B. Day 0. 600x; overview of leaf surface.

Plate C. Day 7. 60x; fungal population development starts.

Plate D. Day 7. 30x; fungal population on veins.

Plate E. Day 3. 3000x; germinating spore.

Plate F. Day 3. 1500x; bacteria evident on surface.

ORNL-PHOTO 86-9296

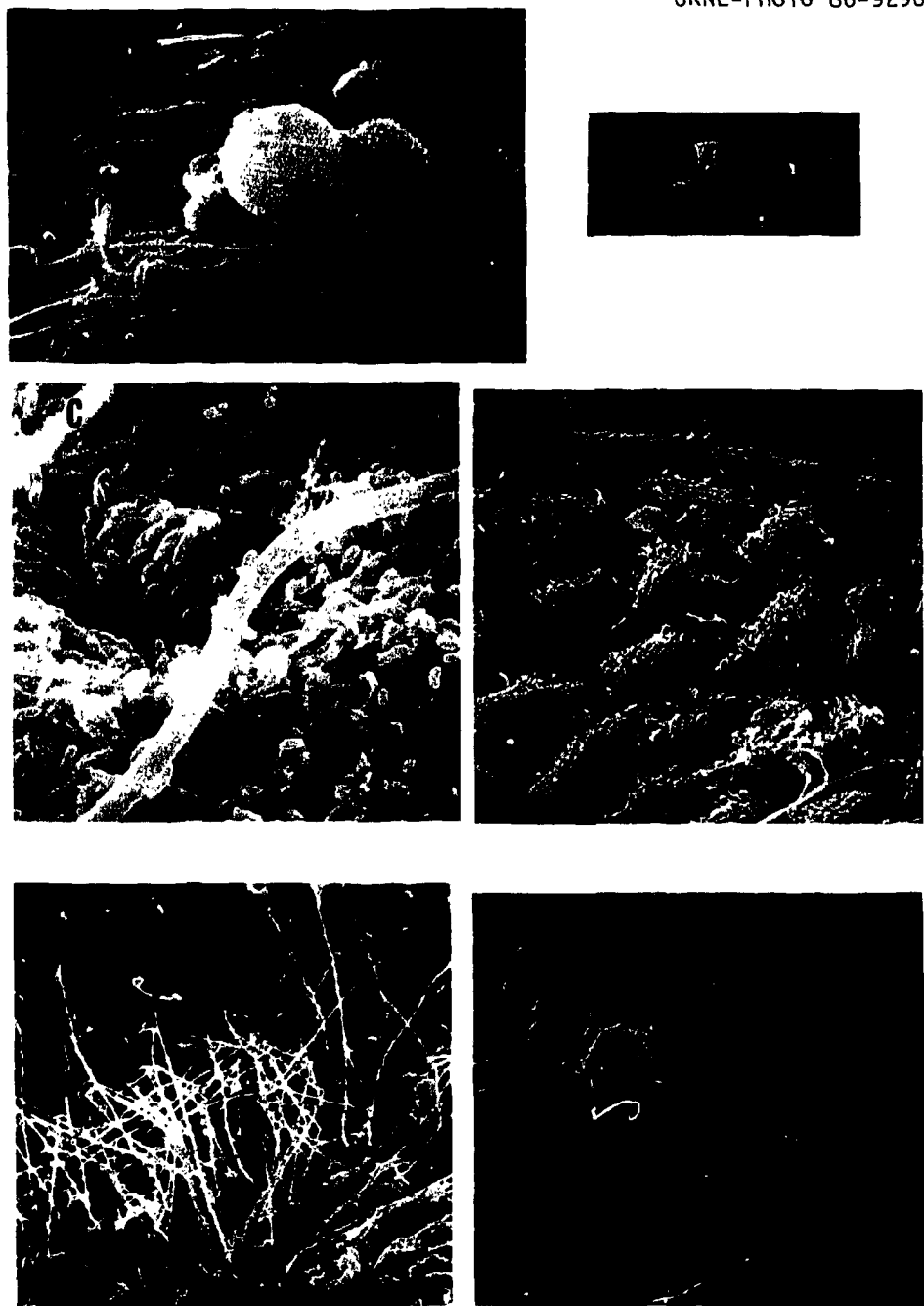


Figure 22. Maple leaf CPOM, days 3 to 10.

Plate A. Day 3. 3000x; top surface of leaf disk; bacteria and spore or pollen grain evident.

Plate B. Day 3. 3000x; bacterial microcolony.

Plate C. Day 3. 3000x; large bacterial microcolony.

Plate D. Day 7. 600x; fungal population increasing.

Plate E. Day 10. 270x; fungal patch on surface.

Plate F. Day 7. 3200x; germinating spore.

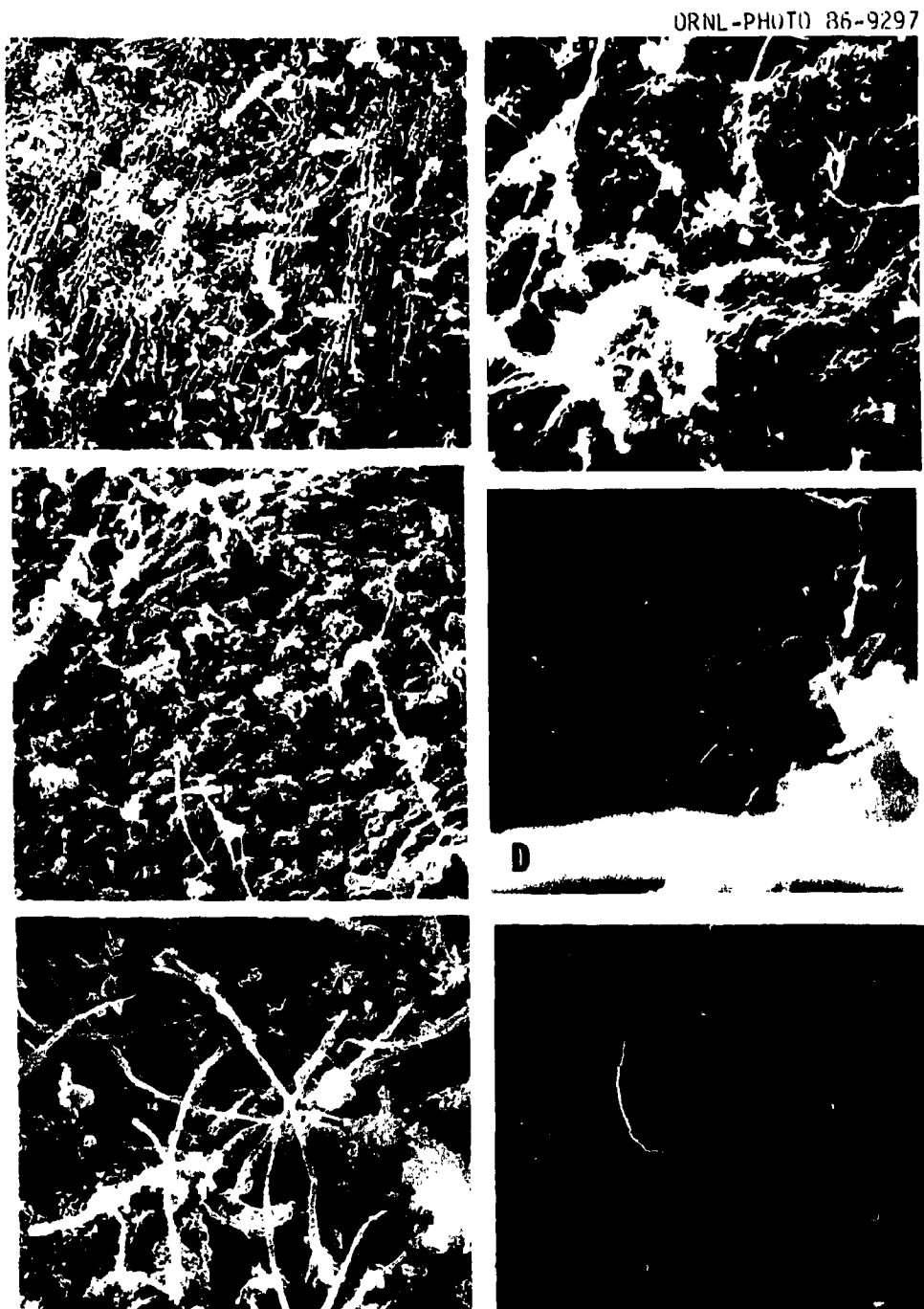


Figure 23. Maple leaf CPOM, days 15 to 29.

Plate A. Day 15. 600x; debris accumulation and increasing fungal population.

Plate B. Day 15. 600x; close-up of polymer.

Plate C. Day 22. 300x; fungi and polymer.

Plate D. Day 22. 5600x; bacterial microcolony; note bacteria pinching off and almost complete division; spiny bacteria (arrow).

Plate E. Day 22. 560x; low density of fungal population (compare Dogwood).

Plate F. Day 29. 120x; fungal population (compare with Fig. 18, Plate E).

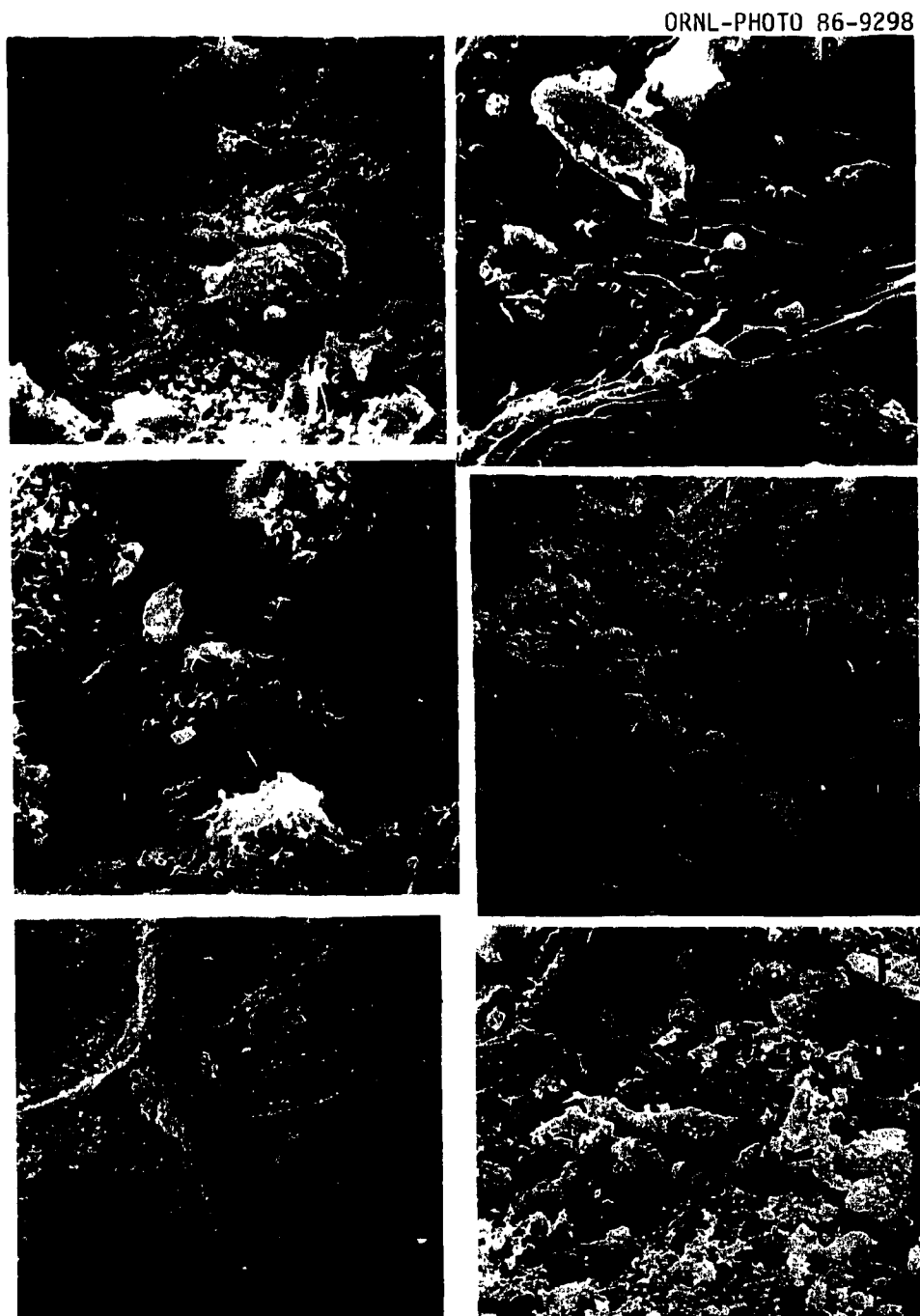


Figure 24. Maple leaf CPOM, days 36 to 56.

- Plate A. Day 44. 300x; polymer build-up.
- Plate B. Day 36. 1500x; diatom and bacteria.
- Plate C. Day 36. 3000x; bacteria associated with polymer on surface.
- Plate D. Day 36. 1500x; aggregated organic matter (polymer).
- Plate E. Day 56. 30x; vein free of fungal growth.
- Plate F. Day 56. 600x; surface polymer.

ORNL-PHOTO 86-9299

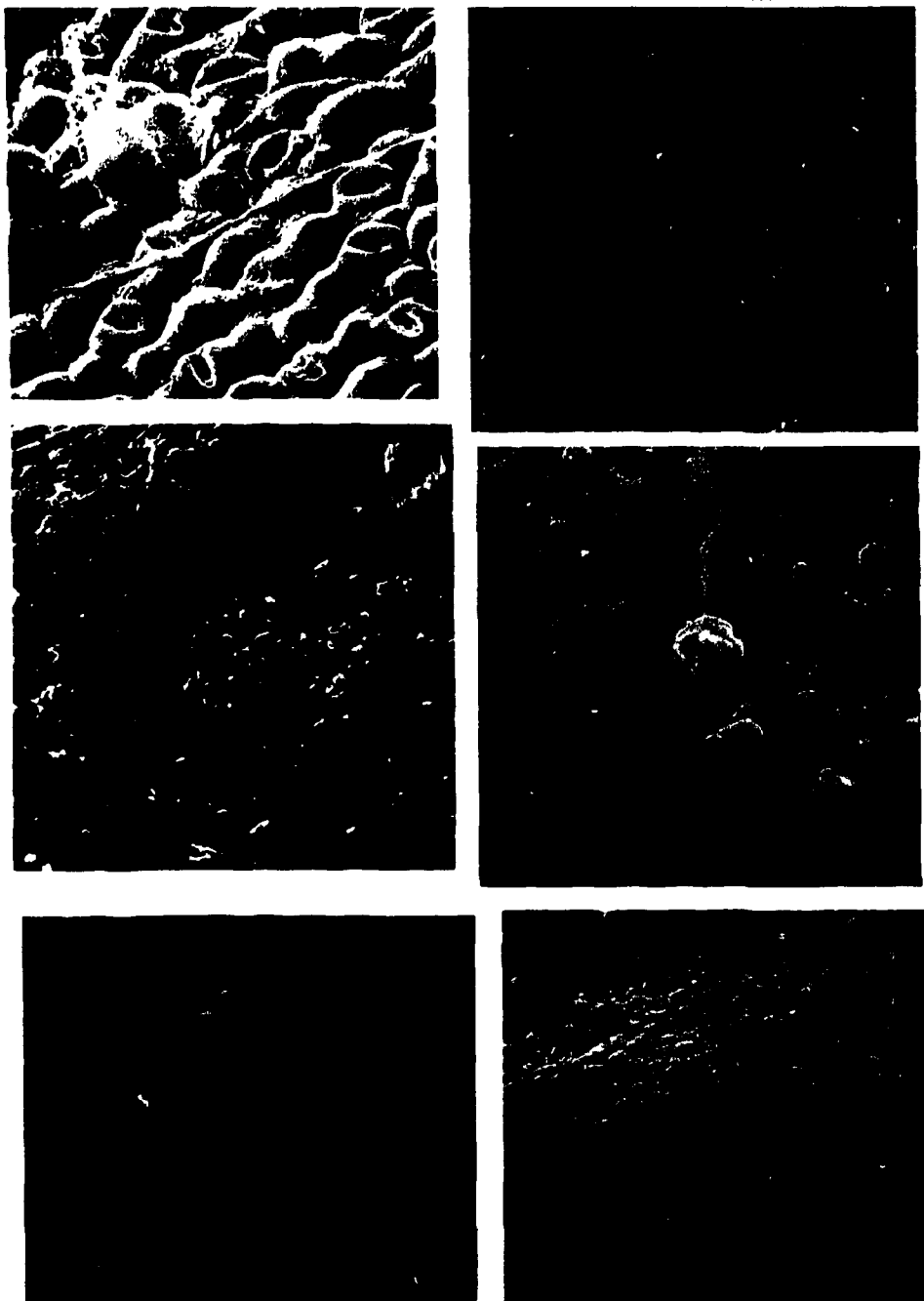


Figure 25. Oak leaf CPOM, days 0 to 10.

Plate A. Day 0. 600x; leaf surface.

Plate B. Day 0. 60x; leaf surface with some associated debris.

Plate C. Day 3. 200x; surface with debris build-up.

Plate D. Day 3. 1500x; spores and bacteria.

Plate E. Day 10. 600x; fungal patch.

Plate F. Day 10. 120x; sparse fungal growth on surface.

ORNL-PHOTO 86-9300

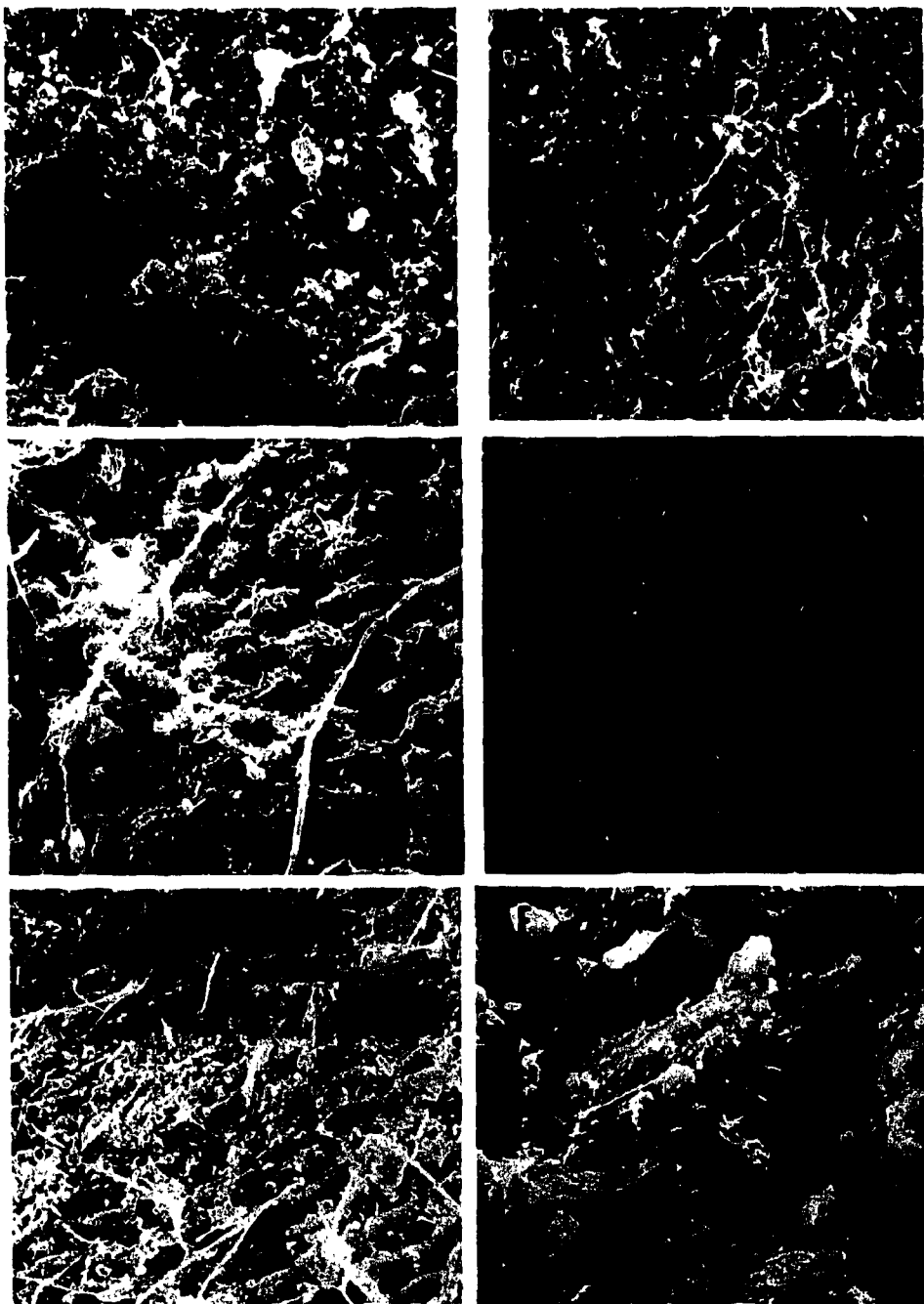


Figure 26. Oak leaf CPOM, days 15 to 22.

Plate A. Day 15. 300x; fungal development and surface break-up evident.

Plate B. Day 15. 150x; fungal development and organic matter accumulating.

Plate C. Day 22. 600x; top surface of leaf disk; polymer associated with fungi.

Plate D. Day 22. 60x; sparse fungal community (compare to Figure 18, Plate E).

Plate E. Day 22. 280x; fungal development, increasing debris.

Plate F. Day 22. 1500x; top surface of leaf disk, note stalked bacteria (arrow).

population and debris continued to increase to day 29 with bacteria being associated with the debris (Figure 27). Leaf tissue deterioration and decreasing surface colonization by fungi began by day 36 (Figure 27) and continued until day 56 (Figure 28). Fungal fruiting bodies and bacteria were observed on the leaf surface during this time (Figure 28). Bacteria were still associated with the debris on the leaf surface on the forty-fourth day in the stream.

The general observation of increasing microbial biomass and organic matter with time was observed for all leaf species used. The dogwood CPOM had a more rapid and denser fungal community development than did either the maple or oak CPOM. Dogwood is also a rapidly decomposing leaf species. The oak CPOM microbial community was the least developed for the period examined during the study.

Phosphorus Dynamics of CPOM Associated Microbial Communities

Following these preliminary experiments, studies were undertaken to elucidate the roles of microbial biomass and activity in phosphorus dynamics of CPOM. The first of these studies was conducted to determine the phosphorus flux through an ungrazed microbial community associated with red maple CPOM. The second study was conducted as a comparative evaluation of snail grazing effects on phosphorus flux through a microbial community associated with white oak CPOM.

The phosphorus dynamics for both studies were analyzed in three components: Phase 1-- ^{33}P release (pre-equilibrium period); Phase 2-- ^{33}P and ^{32}P release (equilibrium period); Phase 3--no tracer

ORNL-PHOTO 86-9301

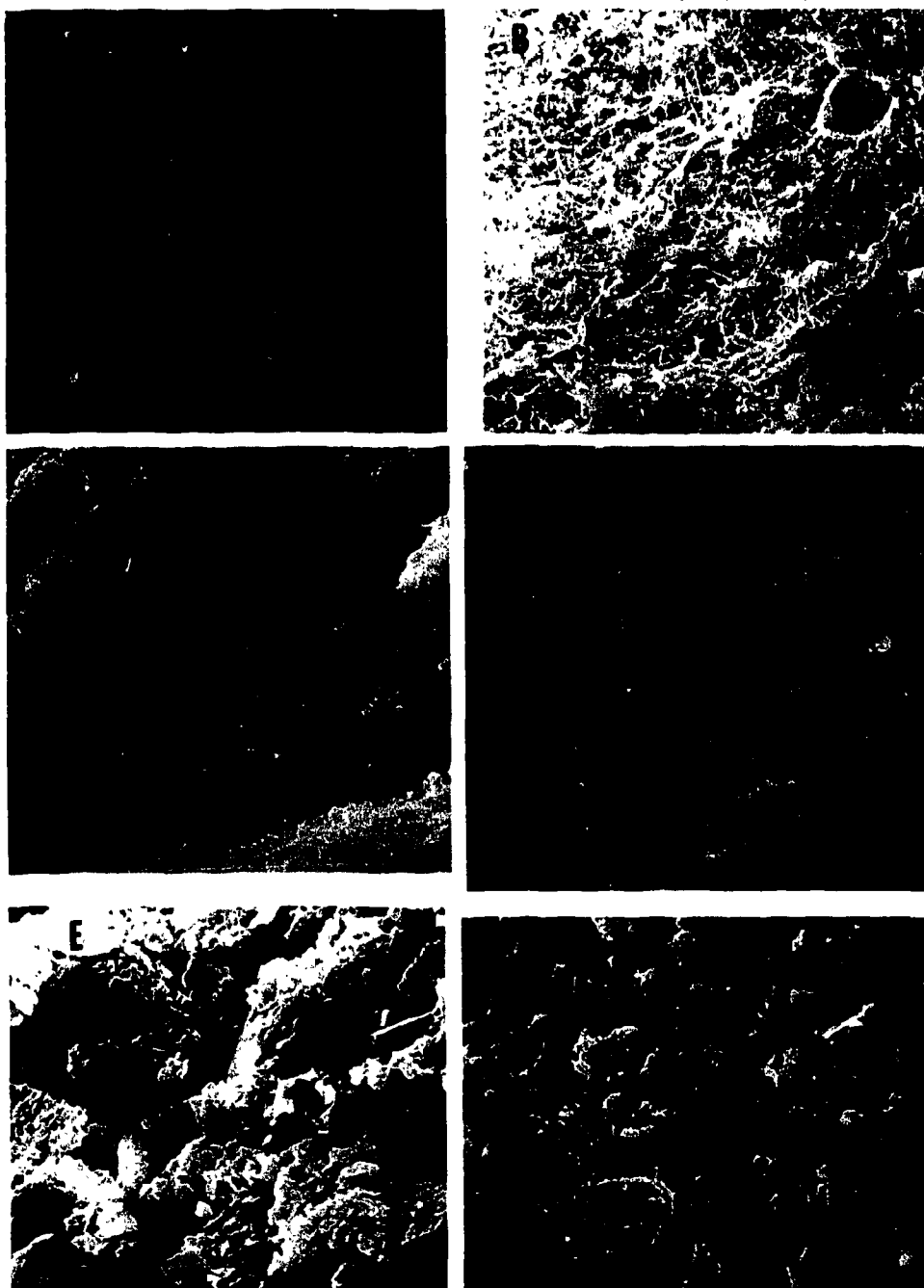


Figure 27. Oak leaf CPOM, days 29 to 36.

Plate A. Day 29. 60x; top surface, development of fungi.

Plate B. Day 29. 120x; development of fungi and organic matter debris.

Plate C. Day 29. 3000x; bacteria associated with debris.

Plate D. Day 29. 3000x; top surface, bacteria associated with debris.

Plate E. Day 36. 1500x; deterioration of leaf surface.

Plate F. Day 36. 300x; sparse fungi; organic matter increasing.

ORNL-PHOTO 86-9302

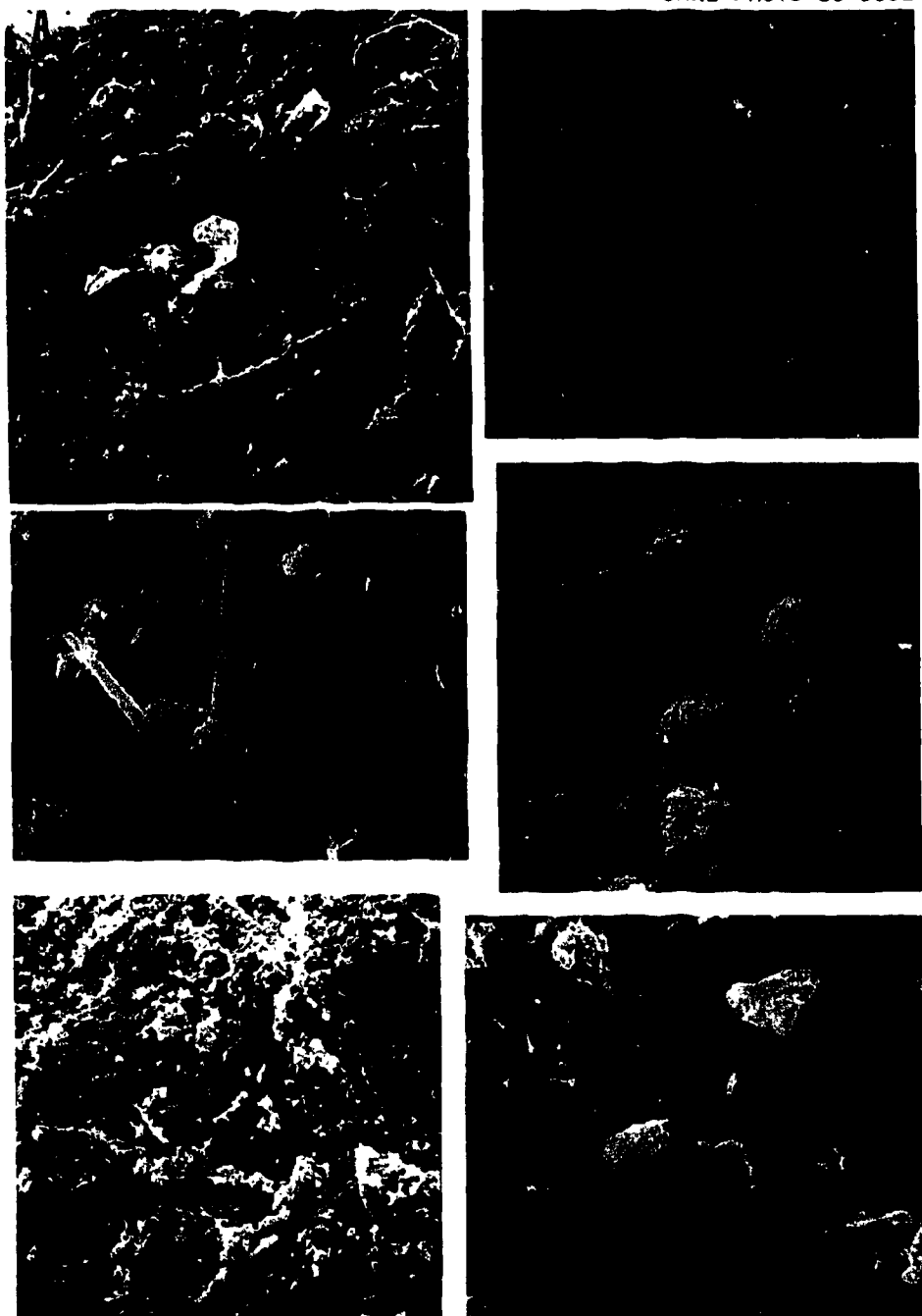


Figure 28. Oak leaf CPOM, days 36 to 56.

Plate A. Day 44. 300x; decrease in fungi evident; organic matter accumulating.

Plate B. Day 44. 60x; surface free of fungal population.

Plate C. Day 36. 1200x; top surface, spore entrapped.

Plate D. Day 44. 1500x; vase-like protozoa; polymer coated filament.

Plate E. Day 56. 150x; organic matter accumulating.

Plate F. Day 56. 3000x; close-up of surface organic matter and associated bacteria (arrow).

release (see Figure 5, page 48). Phase 1 data were used to determine the initial phosphorus incorporation rates. Phase 2 data were used to determine phosphorus turnover rate constants for synthesis; the ^{32}P portion of Phase 2 was also used to determine the initial phosphorus incorporation rates. Phase 3 data were used to calculate phosphorus turnover rates for degradation.

Turnover rate constant for synthesis is used in the sense as expressed by Swick et al. (1956) and Koch (1962). Briefly, the phosphorus turnover rate is defined as the fraction of the phosphorus pool which is either synthesized or degraded per unit time. The smaller rate is generally chosen to represent the turnover rate (Reiner, 1953); however, turnover connotes a degradative process more than a synthetic process. The use of turnover rate for synthesis, therefore, was invoked to avoid any confusion. As pointed out by Koch (1962), results of kinetic studies in which increases in specific activities are determined yield turnover rate constants for synthesis and not the turnover rate constant for degradation.

The initial incorporation rate is defined as the slope of the best fit curve to the linear portion of Phase 1, and to the ^{32}P portion of Phase 2 data. Phosphorus turnover rate constants for synthesis were determined as the slope of the line obtained by plotting the ratio of $(^{32}\text{P}/^{33}\text{P})$ pool to $(^{32}\text{P}/^{33}\text{P})$ water versus time of phosphorus incorporation. Pool refers to the phosphorus containing component of interest, e.g., RNA. Phosphorus turnover time of the water is defined as the time required for the phosphorus

pool to exchange an equivalent amount of phosphorus as in the stream water. The phosphorus turnover rates for degradation were determined by a linear best fit model to the Phase 3 data; the loss of both ^{33}P and ^{32}P were monitored.

In addition to phosphorus flux, microbial biomass was monitored as a function of colonization time. This measurement was used to develop biomass specific rates and community activity estimates.

Phosphorus Dynamics of a Red Maple CPOM Microbial Community

For this study the microbial biomass and the flux of phosphorus were examined in an ungrazed microbial community associated with red maple leaves over a 51 day interval. The phosphate concentration of the stream water was $5.0 \text{ } \mu\text{g P L}^{-1}$ as SRP, and the water temperature was 20°C .

Microbial Biomass

Microbial biomass associated with maple CPOM was measured as ATP (Figure 29). The biomass estimates at each time had a great deal of variability which probably reflects the non-random distribution of the microbial community on the surface of leaves.

The initial colonization period was missed since the first sample was taken 15 days after leaves were placed in the stream. By the time the first sample was taken, a substantial microbial community had already developed. The biomass remained relatively constant until day 20 then decreased to a low on day 32. After

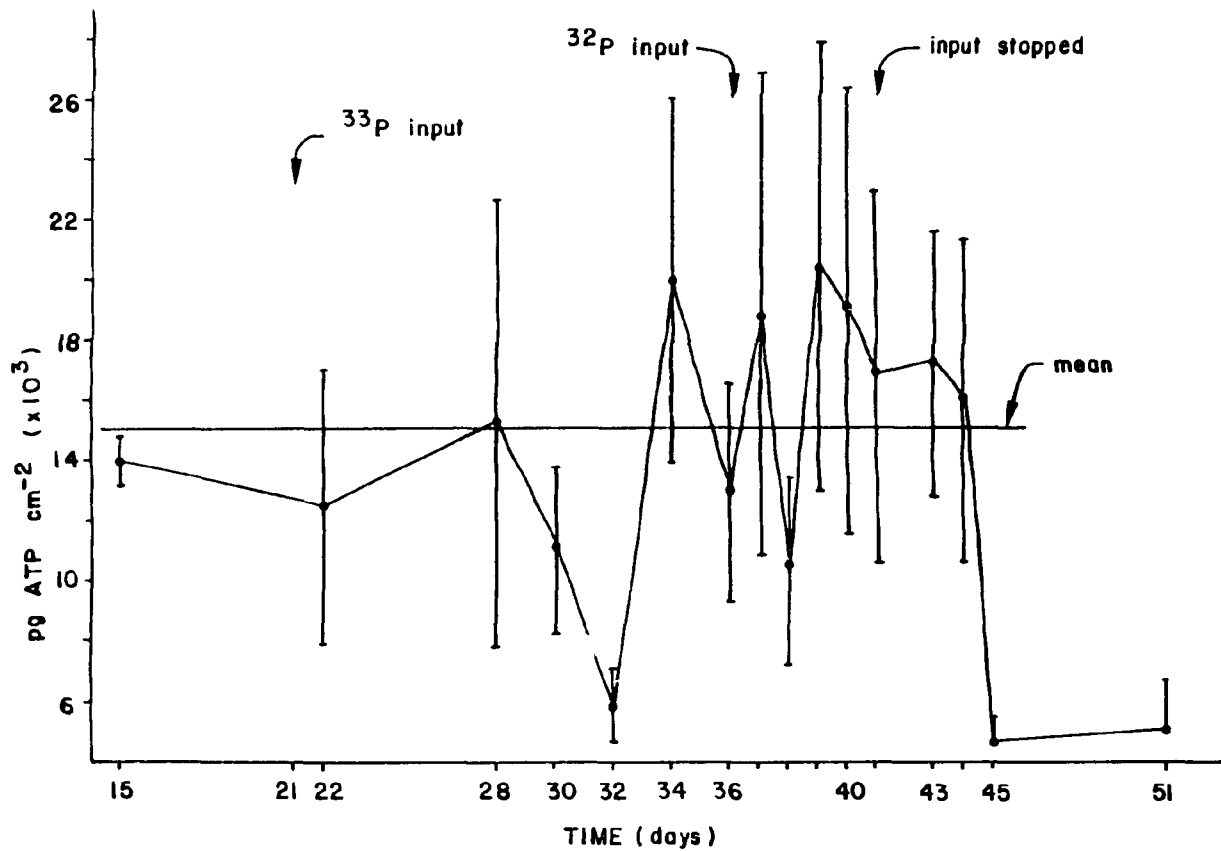


Figure 29. Temporal pattern of ATP biomass for maple leaf CPOM microbial community. Points represent mean of five replicate disks \pm standard deviation. Note: Days 45 and 51 were estimated from a standard curve and might be 30% to 40% low; all other ATP estimates were determined by an internal standard procedure.

an increase, the biomass remained relatively constant until it dropped on day 45.

The reason for this biomass drop after day 44 is an artifact due to procedural error. The ATP concentration prior to day 45 was determined using an internal standard method, whereas the ATP value for days 45 and 51 was determined from an ATP standard curve of ATP concentration versus relative light units since the ATP stock was depleted. The reason for this difference is due to the complexing of the phosphate in the buffer used with magnesium ions which are required for the luciferin-luciferase reaction. Thus, a lower ATP concentration (30% to 40%) resulted compared to what was obtained by the internal standard method which corrected for the quenching by the phosphate buffer. Due to this problem, Tris buffer was substituted for the subsequent phosphorus dynamics study.

Analysis of variance and the Duncan multiple range test was used to test for significance between dates of the ATP values during the double-labeling period (days 36 to 41). It was found that the mean ATP concentration for days 39, 40, 37, 41, and 36 (ranked high to low) were not significantly different from each other, and days 40, 37, 41, 36, and 38 were not significantly different from each other. Only the ATP content for days 38 and 39 were found to be significantly different from each other.

The grand mean ATP concentration for the entire time period (days 15 to 41) was 14,904 pg ATP cm⁻² of leaf surface.

Phosphorus Incorporation Rates

Area-specific rates. The Phase 2 WC-P (whole cell) phosphorus incorporation rate was approximately two-fold greater than the RNA-P rate, four-fold greater than the MP-P and DNA-P incorporation rates, and six-fold greater than the L-P rate (Table 7 and Figures 30-32). Based upon the 95% confidence limit ($P=0.05$), the phosphorus incorporation rate of RNA-P was significantly greater than L-P (2.5x), and MP-P and DNA-P (approx. 2x). The phosphorus incorporation rates of MP-P and DNA-P were significantly greater than the L-P rate (1.5x). As phosphorus enters the metabolite pool (MP-P) (Figure 17, page 78) RNA-P is the major pool which utilizes the MP-P. The incorporation of phosphorus into DNA is in equilibrium with the addition of phosphorus into the MP-P pool and the amount of phosphorus entering the L-P pool is the least.

Phase 1 phosphorus incorporation rates, independently derived, were only determined for the WC-P and LP-P pools. The Phase 1 ^{33}P and Phase 2 ^{32}P (incorporation rates for both WC-P and L-P were in close agreement (Table 7 and Figures 33-35). The Phase 1 rates had greater variability than did the Phase 2 rates (compare 95% confidence limits) due to the limited number of time point analyses (4 time points) for the Phase 1 study compared to 12 time points for the WC-P and L-P and 10 time points for the RNA-P, MP-P, and DNA-P for the Phase 2 rate determination study.

ATP-specific phosphorus incorporation rates. The Phase 2 phosphorus incorporation rate for WC-P was approximately six-fold

Table 7. Comparison of initial phosphorus incorporation rates for a maple leaf detrital microbial community.^a

<u>Radionuclide^b</u>	<u>Fraction</u>	<u>Phosphorus Incorporation Rates</u>			
		<u>Area-Specific</u> <u>ng P cm⁻² h⁻¹</u>	<u>r^{2c}</u>	<u>ATP-Specific</u> <u>ng P pg ATP⁻¹ h⁻¹</u> ($\times 10^{-4}$)	<u>r^{2c}</u>
³³ P (Phase 1)*	WC-P	1.49 \pm 0.86	0.66	1.23 \pm 0.74	0.65
	L-P	0.23 \pm 0.25	0.72	0.18 \pm 0.25	0.63
³² P (Phase 2) [†]	WC-P	1.67 \pm 0.28	0.71	0.94 \pm 0.19	0.63
	L-P	0.28 \pm 0.02	0.98	0.16 \pm 0.02	0.92
	MP-P	0.40 \pm 0.06	0.93	0.22 \pm 0.06	0.77
	RNA-P	0.74 \pm 0.08	0.96	0.42 \pm 0.07	0.88
	DNA-P	0.40 \pm 0.06	0.94	0.23 \pm 0.06	0.78

^aRate \pm 95% confidence limits; P = 0.05.

^bRadionuclide used to determine incorporation rate; ³³P incorporation during Phase 1 and ³²P incorporation during Phase 2.

^cCoefficient of determination.

*Time points = 4.

[†]Time points = 12 (WC-P) and L-P); 10 (MP-P, RNA-P, DNA-P).

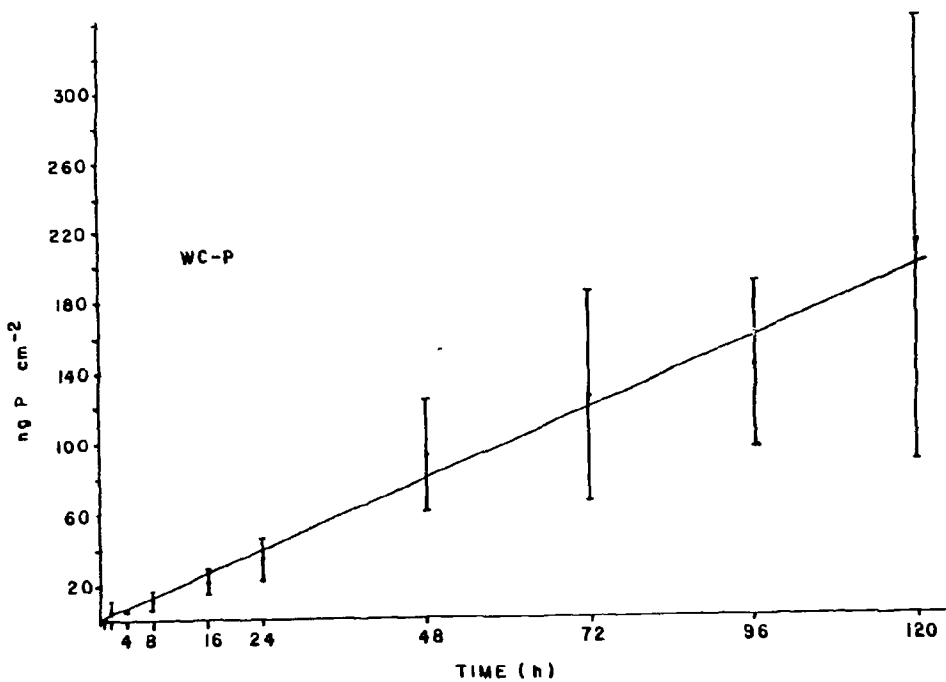


Figure 30. Area-specific incorporation of phosphorus into whole cell phosphorus (WC-P) pool of an ungrazed microbial community associated with maple CPOM. Points represent mean \pm 1 S.D. The line is the best fit to all data points.

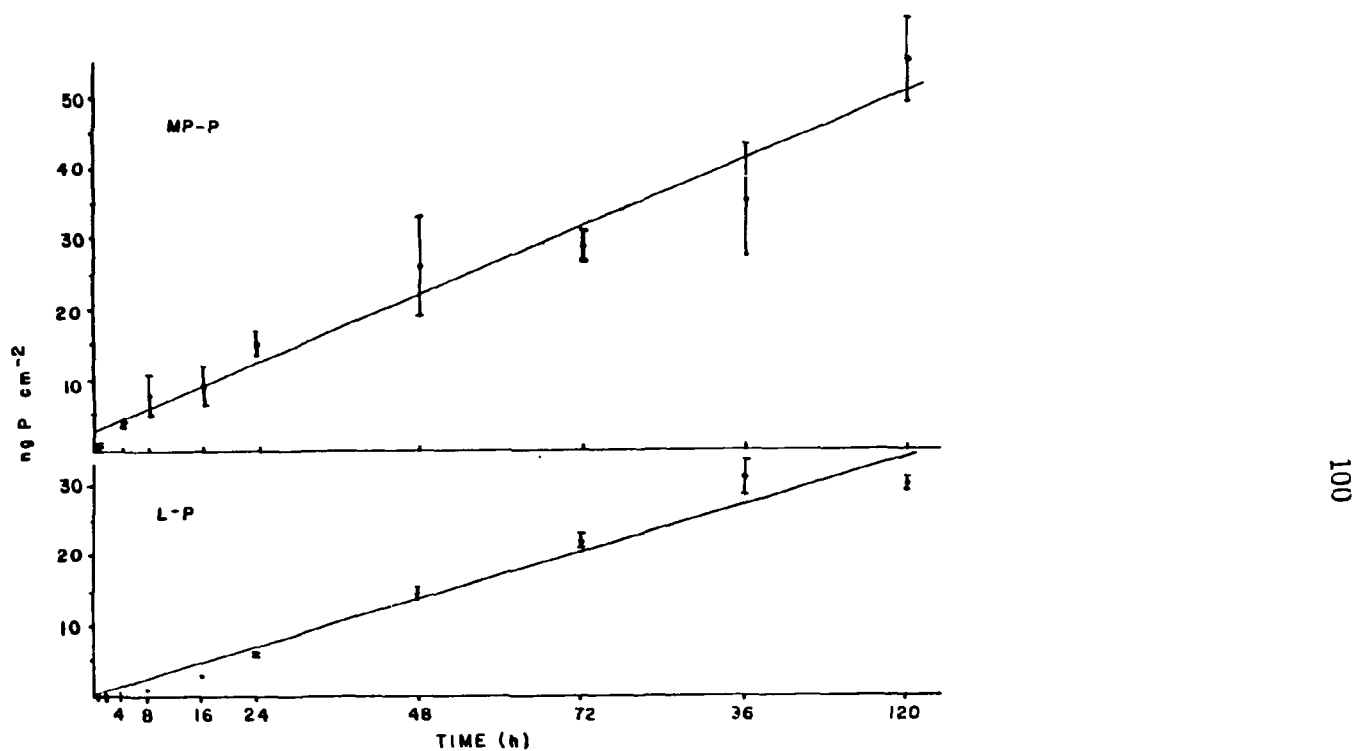


Figure 31. Area-specific incorporation of phosphorus into metabolite pool phosphorus (MP-P) and lipid phosphorus (L-P) pools of an ungrazed microbial community associated with maple CPOM. Points are means \pm S.D. of duplicate samples. The line is the best fit to the individual data points. Points without error bars have error bars less than the size of the data points.

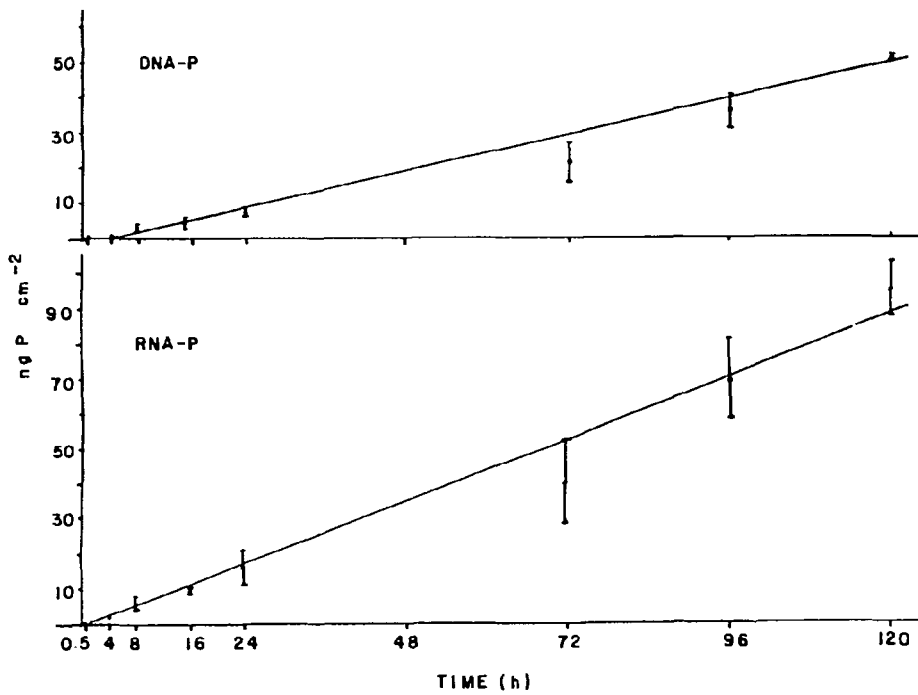


Figure 32. Area-specific incorporation of phosphorus into the deoxyribonucleic acid phosphorus (DNA-P) and ribonucleic acid phosphorus (RNA-P) pools of an ungrazed microbial community associated with maple CPOM. Points represent mean \pm S.D.; $n = 2$ except at 48 h wherein $n = 1$. The line is the best fit to all individual data points and not to the mean values. Points without error bars have errors less than the size of the data points.

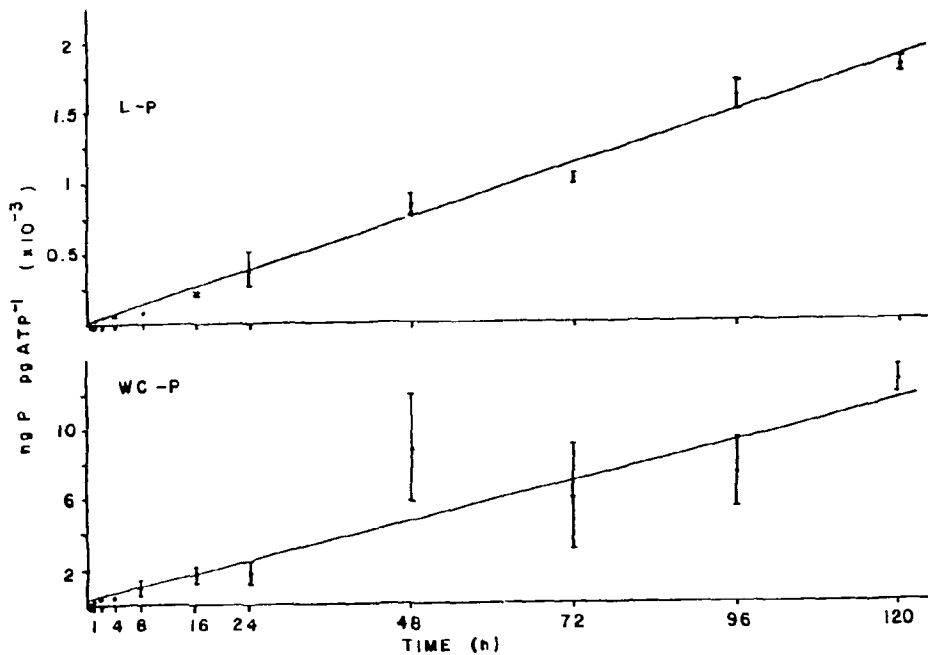


Figure 33. ATP-specific phosphorus incorporation into lipid phosphorus (L-P) and whole cell phosphorus (WC-P) pools of an ungrazed microbial community associated with maple CPOM. Each point represents the mean \pm S.D. The line is the best fit to the individual data points. Points without error bars have errors less than the size of the data points.

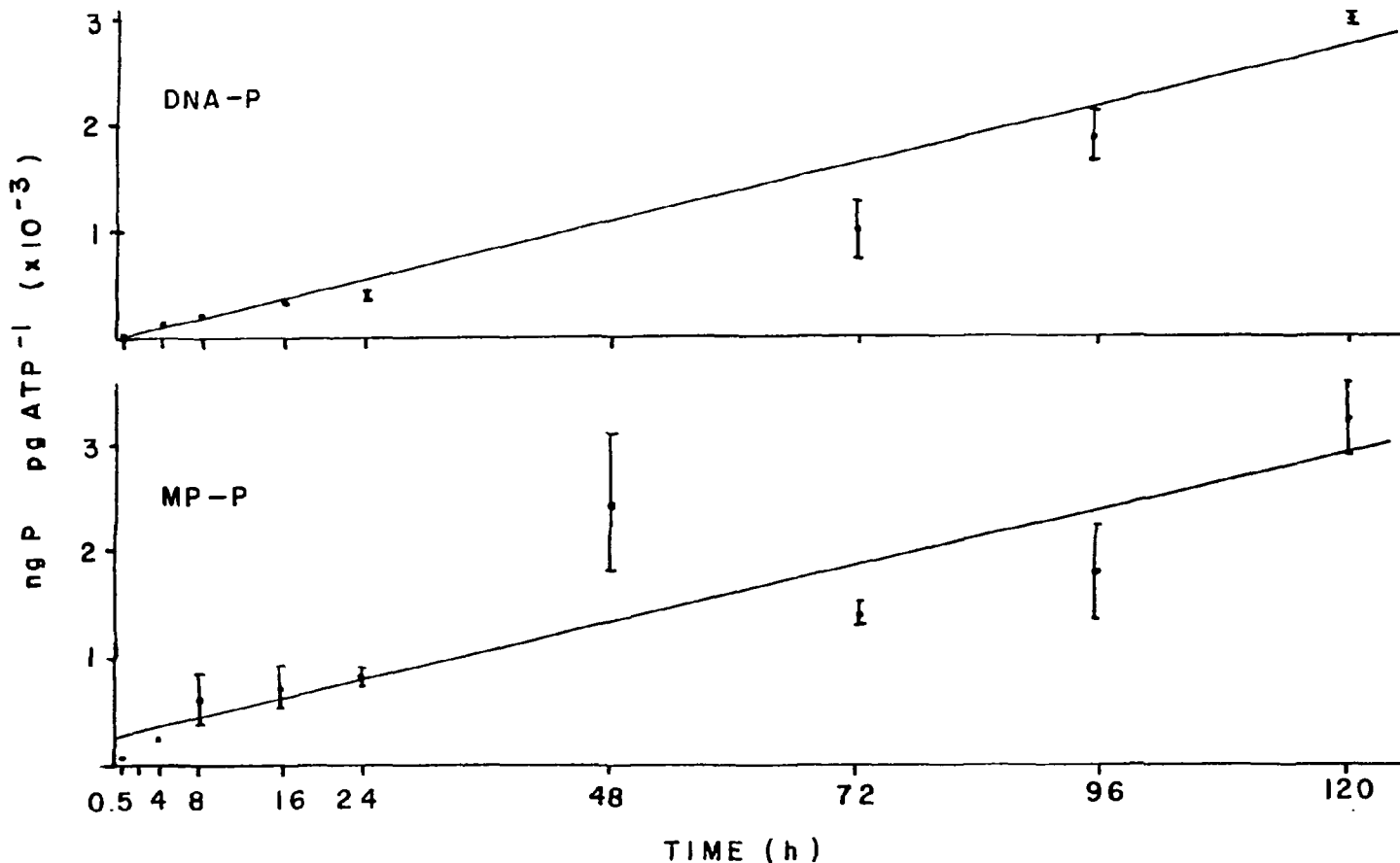


Figure 34. ATP-specific incorporation of phosphorus into deoxyribonucleic acid phosphorus (DNA-P) and metabolite pool phosphorus (MP-P) pools of an ungrazed microbial community associated with maple CPOM. Each point represents the mean \pm S.D. The line is the best fit to the individual data points. Points without error bars have errors less than the size of the data points.

ORNL-DWG 86-9456

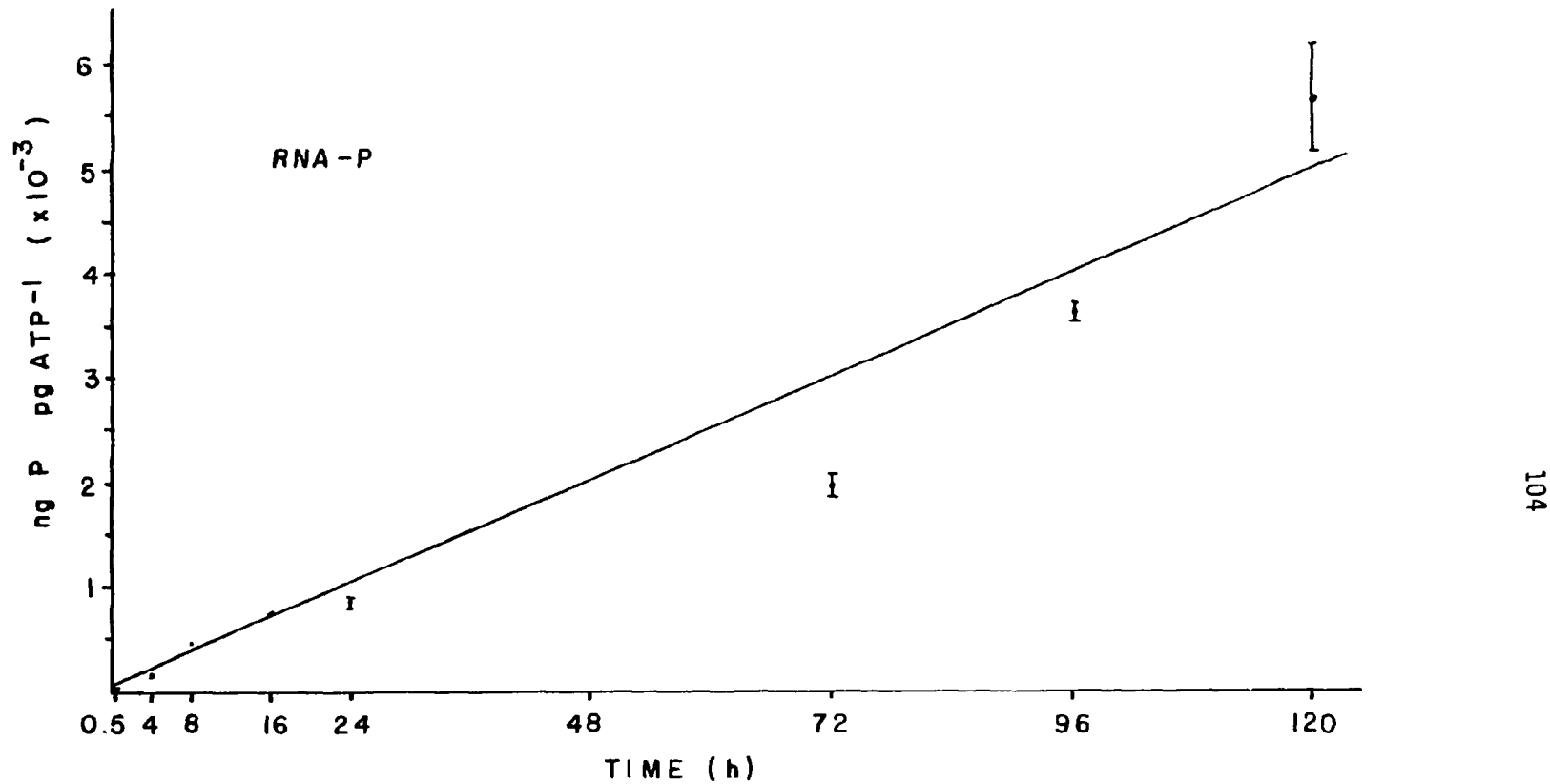


Figure 35. ATP-specific incorporation of phosphorus into ribonucleic acid phosphorus (RNA-P) pool by an ungrazed microbial community associated with maple CPOM. Each point represents the mean \pm S.D. The line represents the best fit to the individual data points. Points without error bars have errors less than the size of the data points.

greater than the L-P rate, four-fold greater than the rates for MP-P and DNA-P, and two-fold greater than the RNA-P incorporation rate (Table 7). The RNA rate was significantly greater than the MP-P (2x), DNA-P (2x), and L-P (2.5x) rates. The incorporation rates for LP, MP, and DNA were not significantly different from each other.

^{33}P Distribution in the Intracellular Pools

Seven days after the start of the ^{33}P addition into the stream, a CPOM sample was fractionated and the distribution of ^{33}P in the intracellular pools was monitored. The WC-P contained 590 ± 257 DPM cm^{-2} (total DPM 1817). The percent of WC-P for the intracellular pools was as follows: L-P, $18 \pm 6\%$; MP-P, $20 \pm 4\%$; RNA-P, $32 \pm 0\%$; and DNA-P, $15 \pm 3\%$. The total recovery (calculated from means) of the intracellular pools accounted for 85% of the radioactivity associated with the WC-P. The calculated percentages were based on the mean ($n = 2$) DPM cm^{-2} of the intracellular pool. Total surface area extracted for L-P was 15.4 cm^2 , and for the MP-P, RNA-P, and DNA-P was 83.1 cm^2 .

The distribution of ^{33}P during the period of isotopic equilibrium (days 15 to 20) is shown in Table 8. The microbial community associated with maple leaf CPOM had 18% of the phosphorus associated with the LP-P pool, 21% with the MP-P pool, 43% with the RNA-P pool and 22% with the DNA-P pool. Generally, the LP, DNA and MP pools had approximately the same amount of cellular phosphorus, however,

Table 8. ^{33}P distribution for the period of isotopic equilibrium in the intracellular phosphorus pools (as % of WC-P) for maple CPOM microbial community.^a

Phosphorus Pool	% of WC-P
L-P	18 \pm 4 n = 12 ^b
MP-P	21 \pm 7 n = 10
RNA-P	43 \pm 13 n = 10
DNA-P	22 \pm 6 n = 10
Total	104

^aThe microbial community was at isotopic equilibrium on days 15 to 20.

^bn refers to the number of sampling times at which duplicate samples were taken.

the RNA phosphorus pool was about two-fold greater than the other pools.

Phosphorus Turnover Rate Constants

To determine the turnover rate constants of phosphorus in the various phosphorus pools, a double-labeling procedure was used. For this procedure ^{33}P must be in isotopic equilibrium with ^{31}P , the stable isotope of phosphorus, in the various phosphorus pools prior to the addition of ^{32}P . Figures 36 and 37 show some representative examples of the incorporation of ^{33}P into phosphorus pools. ^{33}P reached isotopic equilibrium in 15 days (360 h). At this point, ^{32}P and ^{33}P were simultaneously released into the stream. The ratio of the two isotopes (^{32}P to ^{33}P) was determined at various times and used to calculate the turnover rate constants for the internal P pools.

The phosphorus turnover rate constants for the phosphorus pools are shown in Table 9. The microbial community (WC-P) had a phosphorus turnover rate constant of $0.319\% \text{ h}^{-1}$ and a turnover time of 313 h. Turnover time can be defined as the time required for a complete exchange of phosphorus in the community equivalent to that of the water.

The comparison of the phosphorus turnover rate constants (confidence limits) for the intracellular phosphorus pools indicated that the turnover rate constants for the MP-P, RNA-P, and DNA-P were not significantly different from each other, however they were

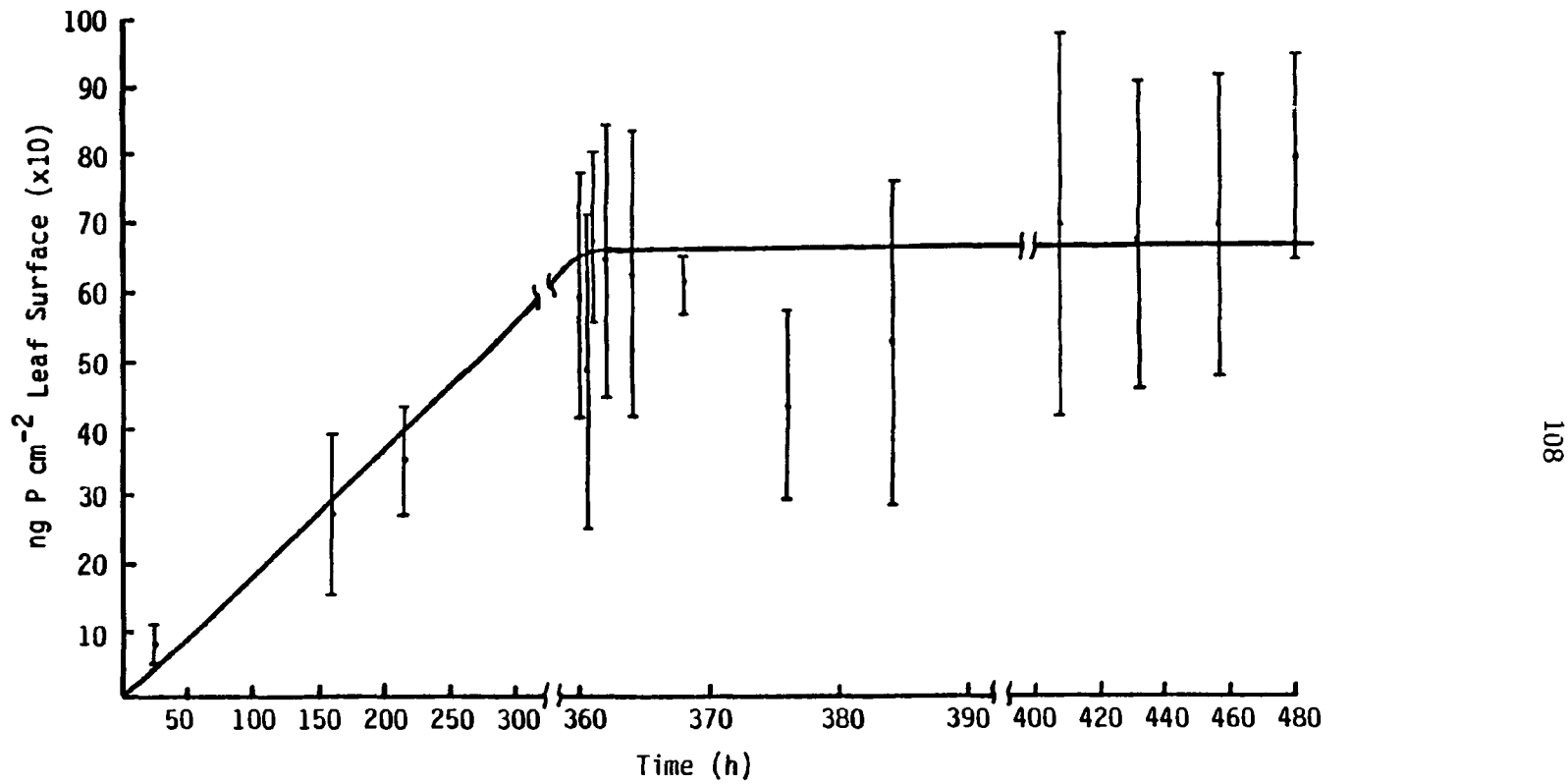


Figure 36. Incorporation of ^{33}P (as ng P cm^{-2}) into the whole cell phosphorus (WC-P) pool of an ungrazed maple CPOM microbial community before and after isotopic equilibrium was achieved. Isotopic equilibrium was achieved in the WC-P pool by 360 h.

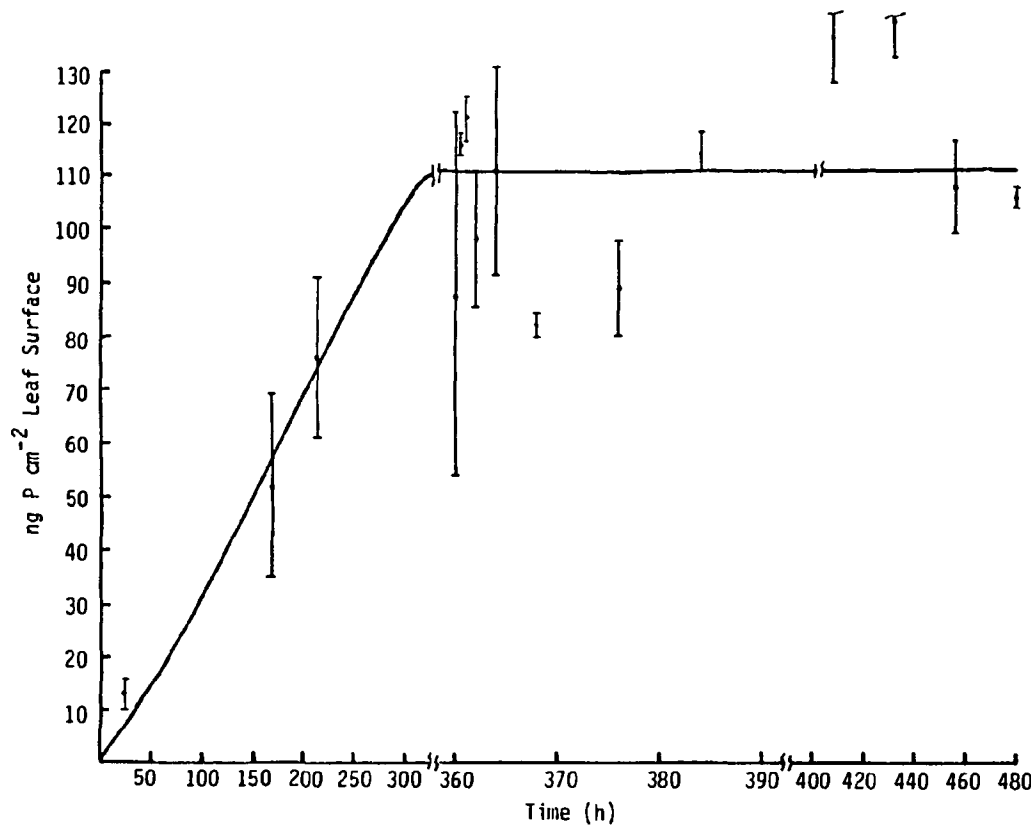


Figure 37. Incorporation of ^{33}P (as ng P cm^{-2}) into the lipid phosphorus (L-P) pool of an ungrazed microbial community associated with maple CPOM before and after isotopic equilibrium was achieved. Isotopic equilibrium was achieved in the L-P pool by 360 h.

Table 9. Comparison of phosphorus turnover rate constants for synthesis for a maple detrital microbial community.^a

Pool	Phosphorus Turnover Rate Constants ^b							
	h ⁻¹ (x10 ⁻³)	r ^{2c}	% h ⁻¹	Turnover Time (h)	Area-Specific cm ⁻² h ⁻¹ (x10 ⁻³)	r ²	ATP-Specific pg ATP ⁻¹ h ⁻¹ (x10 ⁻⁷)	r ²
WC-P	3.19 ± 0.43	0.79	0.319	313	1.04 ± 0.14	0.79	1.26 ± 0.17	0.86
L-P	3.79 ± 0.26	0.98	0.379	264	0.24 ± 0.02	0.98	0.14 ± 0.02	0.95
MP-P	5.77 ± 0.36	0.99	0.577	173	0.25 ± 0.02	0.99	0.14 ± 0.03	0.85
RNA-P	5.35 ± 0.84	0.92	0.535	187	0.24 ± 0.04	0.93	0.13 ± 0.03	0.86
DNA-P	4.78 ± 0.64	0.95	0.478	209	0.21 ± 0.03	0.95	0.12 ± 0.03	0.83

^aAs determined by (DPM ³²P/DPM ³³P)_{pool} / (DPM ³²P/DPM ³³P)_{water}.

^bRate ± 95% confidence limit; $\alpha = 0.05$.

^cCoefficient of determination.

significantly greater than that of L-P. The turnover rate constants can be generally ranked as follows: MP-P>RNA-P>DNA-P>L-P. The intracellular phosphorus pools had the following ranking for turnover times: MP-P<RNA-P<DNA-P<L-P (Table 9). The phosphorus in the MP, RNA, DNA, and L-P pools were completely replaced in 173 h, 187 h, 209 h, and 264 h, respectively.

ATP-specific phosphorus turnover rate constants. ATP-specific phosphorus turnover rate constants are shown in Table 9. The WC-P (community) turnover rate constant was significantly greater than the intracellular rate constants. The phosphorus turnover rate constants for the intracellular phosphorus pools were not significantly different from each other which suggests a balanced metabolic state, in which all of the cellular components increase at the same rate.

Area-specific phosphorus turnover rate constants. Area-specific turnover rate constants are shown in Table 9. The WC-P (community) turnover rate constant was significantly greater (4x) than the intracellular rate constant. The intracellular phosphorus turnover rate constants were not significantly different from each other, suggesting a balanced growth state (all cellular components increase at the same rate) for the microbial community.

Phosphorus Turnover Rate

The following turnover rates were determined by following the decrease in radioactivity (loss of phosphorus) associated with

the phosphorus pool (Figures 38 and 39). WC-P and L-P turnover rates were the only rates determined using this procedure. ATP-specific rates were not determined because of the problem associated with two of the four ATP estimates (see Biomass section for explanation). Area-specific phosphorus turnover rates for degradation are shown in Table 10. The ^{33}P -derived rate for the WC-P was approximately three and one-half times greater than the ^{32}P derived rates, whereas these same rates derived for the L-P had a two-fold difference. The ^{33}P - and ^{32}P derived rates, however, were not significantly different from each other.

The percent of ^{33}P loss from the WC-P for the sampling times at 48 h, 96 h, and 240 h was 11%, 25%, and 57%, respectively, while those for the ^{32}P percent loss as were 2%, 15%, and 55%, respectively, for the same time. The percent ^{33}P loss from the L-P pool for the sampling times as the WC-P were 5%, 0%, and 31%, while the percent ^{32}P loss was 16%, 16%, and 42%.

The loss of ^{33}P and ^{32}P from the L-P indicated that following an initial loss, a period of relatively constant phosphorus, then a rapid decrease in the phosphorus associated with the L-P pool occurs (see Figure 39). Due to the kinetics of phosphorus loss for the L-P pool, the turnover rate was calculated for the period from 0 h to 48 h and 96 h to 240 h. The turnover rates for the 0 h to 48 h period derived from both ^{33}P and ^{32}P were identical, $0.07 \text{ ng P cm}^{-2} \text{ h}^{-1}$. The turnover rate estimated for the 96 h to 240 h period for ^{33}P was $0.14 \text{ ng P cm}^{-2} \text{ h}^{-1}$, and for ^{32}P was $0.04 \text{ ng P cm}^{-2} \text{ h}^{-1}$.

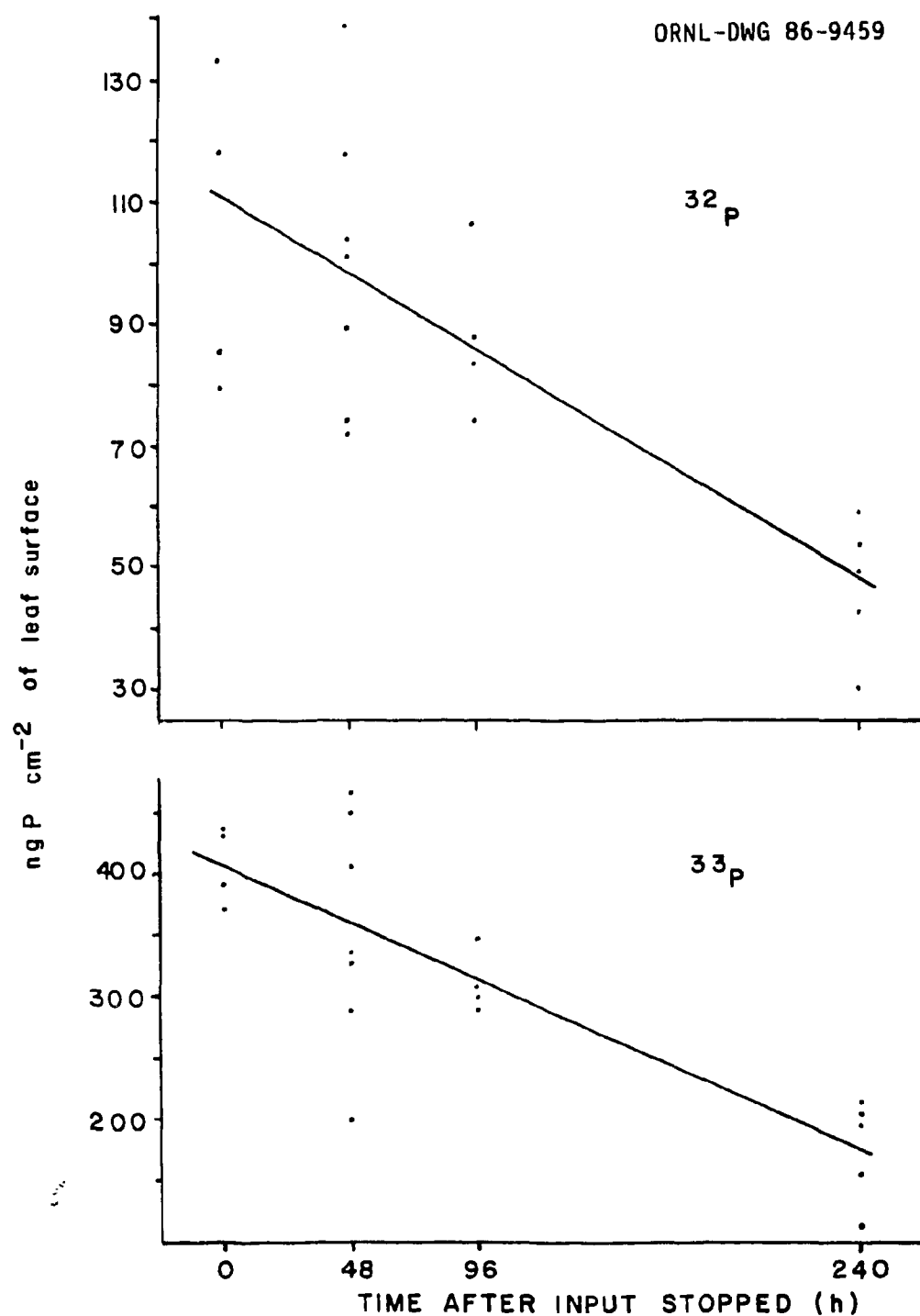


Figure 38. Phosphorus turnover kinetics for WC-P pool for ^{33}P and ^{32}P of an ungrazed maple CPOM microbial community. Each point represents a single leaf disk (1.4 cm dia.). The line is a linear best fit to the data points.

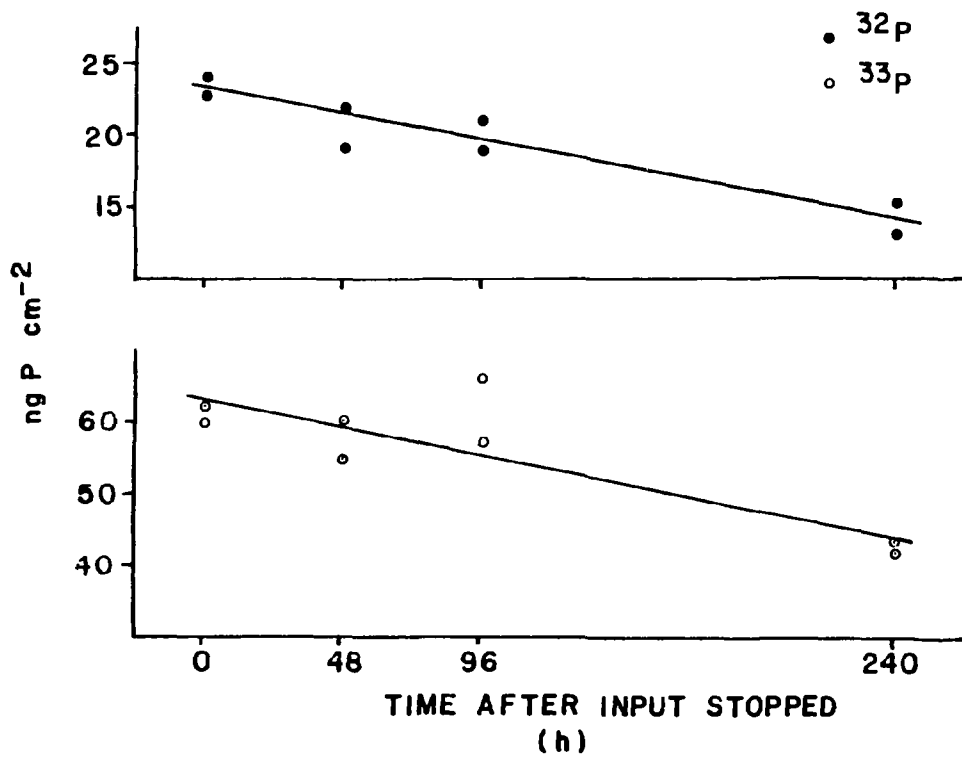


Figure 39. Phosphorus turnover kinetics of the L-P pool for ³³P and ³²P (as ng P cm⁻²) for an ungrazed maple CPOM microbial community. The line fitted to the points was determined by regressing ³³P or ³²P versus time after tracer input was stopped.

Table 10. Comparison of phosphorus turnover rates for degradation for a maple leaf detrital microbial community.

Radionuclide ^b	Area-Specific Phosphorus Turnover Rates ^a		
	Pool	ng P cm ⁻² h ⁻¹	r ^{2c}
33P	WC-P	0.96 ± 0.67	0.67
	L-P	0.08 ± 0.09	0.73
32P	WC-P	0.26 ± 0.21	0.59
	L-P	0.04 ± 0.02	0.91

^aRate ± 95% confidence limits; $\alpha = 0.05$.

^bRadionuclide used to determine loss rates.

^cCoefficient of determination.

Phosphorus turnover times were calculated as the reciprocal of the turnover rate which was determined as the slope of the plot of the log of the percent initial activity per cm^2 versus time. The P turnover time for the microbial community (WC-P) was 690 h and 625 h, respectively, for the ^{33}P and ^{32}P data. The phosphorus turnover time for L-P was 1241 h and 1064 h, respectively, for ^{33}P and ^{32}P .

Phosphorus Dynamics in an Ungrazed and Grazed Oak CPOM Microbial Community

Microbial community biomass, activity and phosphorus flux were examined in an ungrazed and a grazed (snails present) artificial stream containing white oak CPOM. The oak CPOM, a slow decomposing species, was colonized for 112 days prior to the start of the ^{33}P input. The leaves in the grazed channel were also exposed to the grazers for the same period of time (i.e., 112 days). The purpose of this study was to determine what influence grazing has on the phosphorus dynamics of the microbiota as well as on the microbial community.

CPOM Organic Content

The organic content per unit surface area for both the ungrazed and grazed oak CPOM remained relatively constant throughout the course of this study (Table 11). No difference in the organic content of the ungrazed and grazed oak CPOM was observed (nonstatistical).

Table 11. Comparison of the organic content of oak CPOM for an ungrazed and a grazed stream.^a

Date ^b	Organic Content (mg AFDW ^c cm ⁻²)	
	Ungrazed	Grazed
4/13/84	1.83 ± 0.22	1.88 ± 0.29
4/18/84	1.85 ± 0.20	1.77 ± 0.16
4/24/84	1.84 ± 0.18	1.80 ± 0.20
5/01/84	1.74 ± 0.12	1.76 ± 0.10
5/08/84	1.84 ± 0.20	1.81 ± 0.14
6/07/84	1.76 ± 0.25	1.59 ± 0.28
6/20/84	1.83 ± 0.20	1.93 ± 0.28

^aReported values are mean ± S.D.; 5 or 10 leaf disks per pan; n = 2.

^bDate CPOM sampled.

^cAFDW = ash-free dry weight.

statement). The consistency of the organic content between the ungrazed and grazed CPOM suggests that (1) the higher density microbial community associated with the ungrazed CPOM (see page 133) was counterbalanced by less organic material associated with the leaf, or (2) the grazed community, although lower in density, has more organic matter per organism to compensate for lower community density.

Stream Orthophosphate Concentration

The mean soluble reactive phosphate (SRP) for the ungrazed stream was $2.2 \pm 0.8 \mu\text{g SRP-P L}^{-1}$ and ranged from 0.9 to $4.2 \mu\text{g SRP-P L}^{-1}$ (Table 12). The grazed stream had a mean SRP of $2.3 \pm 0.9 \mu\text{g SRP-P L}^{-1}$ and ranged from 1.1 to $4.8 \mu\text{g SRP-P L}^{-1}$. Samples for SRP analysis were not collected at each time period during the double-labeling period. The mean SRP concentration, therefore, was used to calculate the specific activity which was then used to convert the DPM data to quantities of P uptake.

Stream Water Temperature

The water temperature for both the ungrazed and grazed streams were identical. The water temperature ranged from 13°C to 16°C during the pre-equilibrium period, 14.5°C to 16°C during the isotopic equilibrium period, and 15°C to 18°C during the period after label input ceased.

Microbial Biomass and Bacterial Cell Density

Microbial biomass and cell density associated with oak leaf CPOM of the grazed and ungrazed streams was determined by measuring

Table 12. Comparison of SRP concentration in water in the ungrazed and grazed stream.

Sampling Date	SRP Concentration ($\mu\text{g P L}^{-1}$)			
	Ungrazed		Grazed	
12/22/83	1.9	2.9	2.6	3.8
12/29/83	2.6	0.9	1.5	1.9
1/05/84	4.0	4.2	4.0	4.8
1/12/84	1.3	0.9	2.0	1.3
1/19/84	3.8	3.0	3.2	3.0
1/31/84	2.2	2.1	2.2	2.3
2/09/84	1.9	1.7	2.5	1.8
2/21/84	2.0	2.0	2.2	2.2
3/01/84	2.4	2.2	2.1	2.0
3/13/84	1.9	2.0	2.0	1.9
4/13/84	1.4	1.5	1.1	1.5
4/18/84	2.2	2.6	1.7	1.7
5/01/84	2.4	2.2	2.2	2.6
Mean \pm S.D.	2.2 ± 0.8		2.3 ± 0.9	

the ATP concentration and direct bacterial counts (Table 13; Figures 40 and 41). The first samples collected occurred after the CPOM had been in the streams for 112 days. The CPOM in the grazed channel were exposed to grazing for the same 112 day period. The ATP content and the bacterial cell density for both the ungrazed and grazed CPOM was relatively constant through the study period, with significantly higher ATP content and cell densities associated with the ungrazed CPOM microbial community (Table 13).

The ungrazed streams had a mean biomass of 4164 pg ATP cm⁻² and a cell density of 2.35x10⁷ cells cm⁻², whereas the grazed stream biomass was 3345 pg ATP cm⁻² and with a cell density of 1.40x10⁷ cells cm⁻². Although there was a statistically significant biomass and cell density difference between the streams, some significant within stream variability did occur between the sampling times for ATP and cell density (Table 13). The biomass as ATP ranged from 1299 to 5892 pg ATP cm⁻² for the ungrazed stream CPOM and 1152 to 5415 pg ATP cm⁻² for the grazed CPOM. Cell densities ranged from 1.63x10⁷ to 3.21x10⁷ cells cm⁻² for the ungrazed CPOM and 0.97x10⁷ to 2.20x10⁷ cells cm⁻² for the grazed leaf CPOM. The general trend for the microbial community associated with both ungrazed and grazed oak CPOM was a steady-state community with respect to the biomass and cell density.

Table 13. Comparison of microbial biomass associated with oak CPOM in an ungrazed and grazed stream channel.^a

Date ^b	pg ATP cm ⁻² of Leaf Surface		Cells cm ⁻² of Leaf Surface (x10 ⁷)	
	Ungrazed	Grazed	Ungrazed	Grazed
4/10/84	5646 ± 1544	3524 ± 1410	1.78 ± 0.54	1.44 ± 0.18
4/12/84	1299 ± 298	3011 ± 472	2.55 ± 0.08	1.52 ± 0.18
4/15/84	5209 ± 1478	2853 ± 605	1.63 ± 0.08	1.15 ± 0.03
4/18/84	4382 ± 525	4153 ± 1436	1.79 ± 0.19	1.22 ± 0.02
4/25/84	4476 ± 585	5416 ± 2230	2.25 ± 0.04	1.88 ± 0.18
5/02/84	5750 ± 730	3697 ± 1282	2.16 ± 0.33	1.07 ± 0.06
5/10/84 ^c	3910 ± 712	4852 ± 1672	2.50 ± 0.04	2.20 ± 0.04
5/11/84 ^c	5251 ± 794	4088 ± 946	3.21 ± 0.03	1.10 ± 0.27
5/12/84 ^c	4161 ± 1431	3482 ± 783	2.61 ± 0.25	1.21 ± 0.13
5/13/84 ^d	4452 ± 1042	2741 ± 813	2.35 ± 0.66	1.45 ± 0.33
5/14/84 ^c	2909 ± 744	2435 ± 1507	2.56 ± 0.03	1.76 ± 0.23
5/15/84 ^c	3373 ± 594	2913 ± 1239	1.92 ± 0.16	0.97 ± 0.14
5/17/84 ^c	5646 ± 1527	3891 ± 1663	2.00 ± 0.50	1.29 ± 0.04
5/21/84	5868 ± 1679	3881 ± 973	2.41 ± 0.19	1.35 ± 0.03
5/30/84	2454 ± 892	1152 ± 461	2.58 ± 0.21	1.10 ± 0.18
5/31/84	3972 ± 808	3960 ± 1023	2.53 ± 0.39	1.44 ± 0.04
6/01/84 ^c	3318 ± 820	2766 ± 989	2.51 ± 0.14	1.95 ± 0.11
6/04/84 ^d	3038 ± 1594	2380 ± 1123	2.12 ± 0.32	1.23 ± 0.04
6/07/84	4794 ± 978	2798 ± 684	2.51 ± 0.12	1.60 ± 0.09
6/28/84 ^c	2680 ± 561	2758 ± 825	3.07 ± 0.23	1.12 ± 0.11
<hr/>				
Grand ^e Mean	4164 ± 1511	3345 ± 1420	2.35 ± 0.44	1.40 ± 0.34

^aMean ± 1 S.D.; n = 5 for ATP and n = 2 for cell densities.

^bSampling date; leaves originally placed in streams 12/20/83.

^cNo significant difference between the streams' ATP biomass.

^dNo significant difference between the streams' cell densities.

^eMean ± S.D. for each stream treatment.

(α = 0.05)

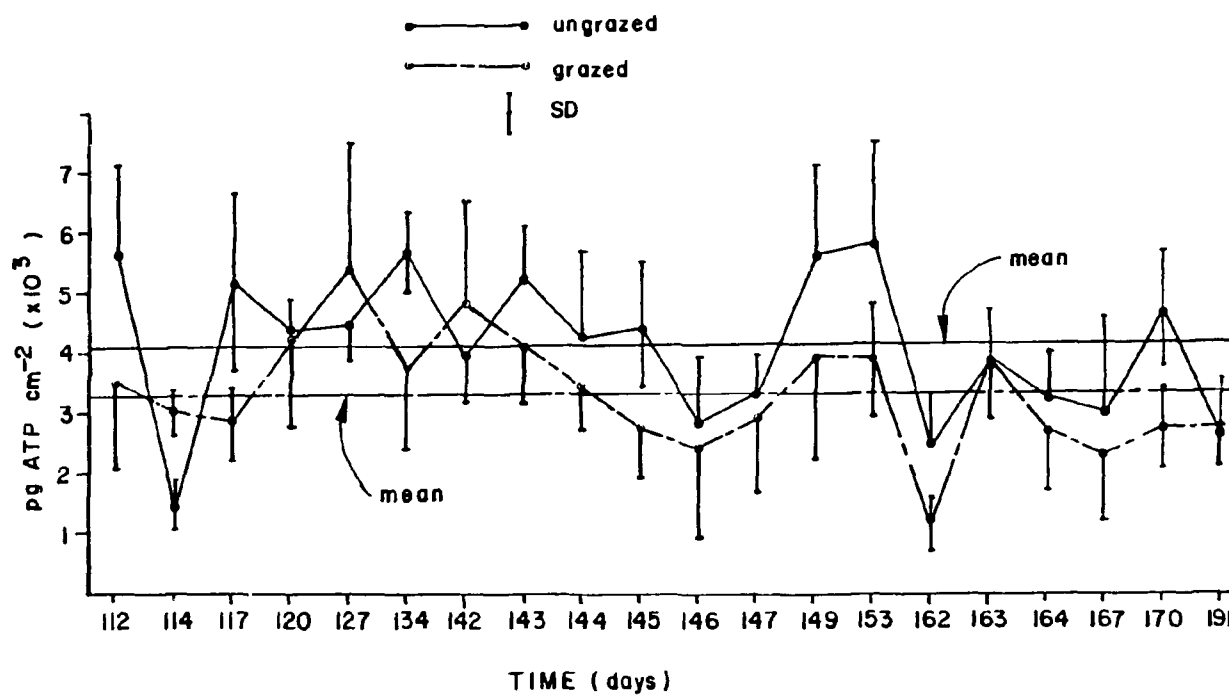


Figure 40. Temporal pattern of ATP biomass for an ungrazed and a grazed oak CPOM microbial community. Points represent means of five replicate disks \pm standard deviation. Leaves placed in streams 12/20/83; first sample collected 4/10/84 (112 days).

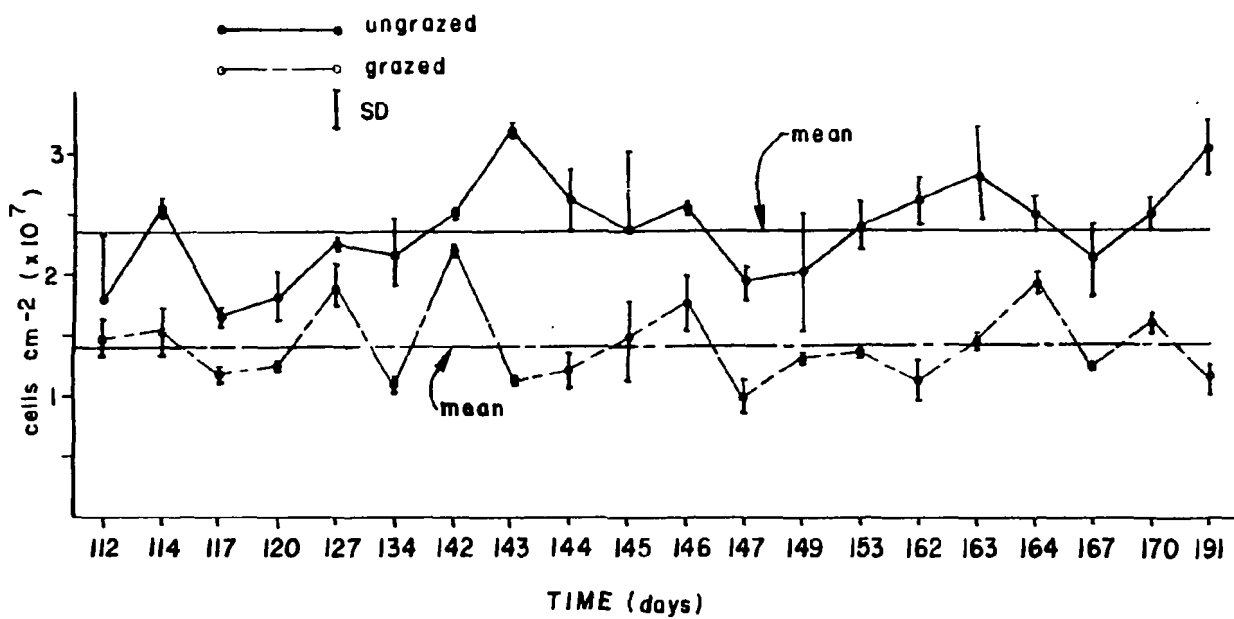


Figure 41. Temporal pattern of bacterial cell density for an ungrazed and a grazed oak CPOM microbial community. Points represent means of duplicate counts \pm standard deviation. Leaves were placed in streams on 12/20/83; first sample collected 4/10/84 (112 days).

Physiological Activity of an Ungrazed and Grazed
Microbial Community

The ATP and cell density data were used to calculate ATP per cell, an index of the physiological activity, during the course of this study (Table 14). The general trend was that the grazed microbial community had a higher ATP content per cell than the ungrazed microbial community; thus, grazing by snails seems to increase microbial activity. The grand mean for the ungrazed CPOM microbial community was 1.89×10^{-4} pg ATP cell $^{-1}$, whereas the grazed microbial community had a ratio of 2.46×10^{-4} pg ATP cell $^{-1}$.

Phosphorus Incorporation Rates

The WC-P incorporation rate on an area-specific, cell-specific, and ATP-specific basis for the ungrazed microbial community was approximately eight-fold greater than the L-P rate, four-fold greater than the MP-P and DNA-P rates and two-fold greater than the RNA-P rate (Table 15). Comparing the incorporation rates on an area-, cell- and ATP-specific basis for the intracellular phosphorus pools for the ungrazed community indicated that the RNA-P rate was approximately two-fold greater than the MP-P and DNA-P rates, and three and one-half-fold greater than the L-P rate. The incorporation rates of MP-P and DNA-P were about the same, and both were two-fold greater than the slowest, L-P rate. The incorporation rates of the intracellular phosphorus pools for the ungrazed community ranked as follows: RNA-P > MP-P = DNA-P > L-P. These rate differences for

Table 14. Comparison of calculated ATP content per cell for an ungrazed and a grazed oak CPOM microbial community.^a

Date ^b	pg ATP Cell ⁻¹ (x10 ⁻⁴)		Date	pg ATP Cell ⁻¹ (x10 ⁻⁴)	
	Ungrazed	Grazed		Ungrazed	Grazed
4/10/84	3.17	2.45	5/15/84	1.76	3.01
4/12/84	1.57	1.98	5/17/84	2.82	3.01
4/15/84	3.20	2.48	5/21/84	2.43	2.87
4/18/84	2.45	3.41	5.30/84	0.95	1.04
4/25/84	1.97	2.88	5/31/84	1.56	2.75
5/02/84	2.66	3.46	5/01/84	1.32	1.42
5/10/84	1.56	2.21	6/04/84	1.43	1.93
5/11/84	1.63	3.72	6/07/84	1.91	1.75
5/12/84	1.59	2.88	6/28/84	0.88	2.46
5/13/85	1.89	2.03	Grand ^c Mean		1.89 ± 0.69 2.46 ± 0.73
5/14/84	1.14	1.38			

^aThe mean ATP and cell numbers for the sampling dates were used to calculate the ATP cell⁻¹ value reported.

^bSampling date.

^cGrand mean is the mean of all sample dates.

Table 15. Comparison of initial phosphorus incorporation rates for an ungrazed and a grazed oak leaf detrital microbial community.^a

Stream	Pool	Initial Incorporation Rates ^b					
		Area-Specific		Cell-Specific		ATP-Specific	
		ngP cm ⁻² h ⁻¹ (x10 ⁻¹)	r ² ^c	ngP cell ⁻¹ h ⁻¹ (x10 ⁻⁹)	r ²	ngP pgATP ⁻¹ h ⁻¹ (x10 ⁻⁵)	r ²
Ungrazed	WC-P	1.59 ± 0.06	0.96	6.36 ± 0.30	0.94	5.64 ± 0.42	0.86
	L-P	0.20 ± 0.02	0.97	0.84 ± 0.10	0.92	0.72 ± 0.11	0.88
	MP-P	0.41 ± 0.04	0.95	1.99 ± 0.22	0.91	1.47 ± 0.23	0.88
	RNA-P	0.73 ± 0.14	0.83	2.91 ± 0.54	0.84	2.79 ± 0.70	0.74
	DNA-P	0.39 ± 0.04	0.95	1.55 ± 0.17	0.94	1.40 ± 0.24	0.86
Grazed	WC-P	1.63 ± 0.10	0.91	14.23 ± 0.70	0.93	11.49 ± 0.81	0.87
	L-P	0.22 ± 0.02	0.95	1.91 ± 0.14	0.97	1.54 ± 0.24	0.88
	MP-P	0.44 ± 0.06	0.89	4.03 ± 0.61	0.89	3.39 ± 0.76	0.79
	RNA-P	0.69 ± 0.14	0.82	6.50 ± 0.99	0.89	5.80 ± 1.35	0.77
	DNA-P	0.44 ± 0.04	0.95	4.10 ± 0.53	0.92	3.60 ± 0.77	0.80

^aAs determined by ³²P incorporation.

^bRate ± 95% confidence limit; $\alpha = 0.05$.

^cCoefficient of determination.

the intracellular pools are statistically significant ($P \leq 0.05$), based on the 95% confidence limits.

The phosphorus incorporation rates on an area-specific, cell-specific, and ATP-specific basis for a grazed microbial community display the same basic trends (Table 15). The following description, therefore, will be representative of each.

The WC-P phosphorus incorporation rate was approximately seven-fold greater than the L-P rate, four-fold greater than the rates for MP-P and DNA-P, and two-fold greater than the phosphorus incorporation rate for the RNA-P pool. The phosphorus incorporation rate of the RNA-P pool was about three-fold greater than the rate for L-P, one and one-half-fold greater than MP-P and DNA-P, each having the same rate of incorporation. The rates of MP-P and DNA-P were two-fold greater than the phosphorus incorporation rate for L-P. The incorporation rates for the intracellular pools are ranked as follows: RNA-P > MP-P = DNA-P > L-P. The difference between the rates are significant based upon 95% confidence limits.

A comparison of the incorporation rates between the ungrazed and grazed microbial community indicates that the rates for each corresponding pool are not significantly different from each other based on the 95% confidence limits. Generally, the phosphorus incorporation rates for the grazed microbial community were greater, although not significantly different, from the corresponding incorporation rates for the ungrazed microbial community. The only exception to this observation is the RNA-P incorporation rate of

the ungrazed community which was greater than the rate for the grazed community.

Comparison of Phosphate Accumulation for an Ungrazed and Grazed Oak CPOM Microbial Community

Phosphate accumulation for the ungrazed and grazed oak CPOM microbial community was compared by analysis of variance and the Duncan multiple range test. The microbial communities were significantly different with respect to the mean phosphate concentration accumulated into the pools (Table 16). On an area-specific basis, the ungrazed microbial community incorporated a significantly greater amount of phosphate in the pools than did the grazed microbial community. This was due to a greater cell density per unit surface area associated with the ungrazed microbial community (Table 15). On a cell-specific basis, however, the grazed microbial community incorporated a significantly greater amount of phosphate in the pools than did the ungrazed microbial community.

Distribution of ^{33}P in the Intracellular Pools

Table 17 shows the distribution of ^{33}P in the intracellular phosphorus pools for the ungrazed and grazed oak CPOM microbial communities during the period of isotopic equilibrium. The distribution of ^{33}P (% of WC-P) in the intracellular phosphorus pools for the ungrazed microbial community was 19% for the L-P, and 24% each for the MP-P, RNA-P, and DNA-P pools. The ^{33}P distribution in the grazed community was 17% for the L-P, and 22% each for the MP-P,

Table 16. Comparison of phosphorus accumulation in phosphorus pools for an ungrazed and a grazed microbial community.^{a,b,c}

Pool	Area-Specific		Cell-Specific	
	ng P cm ⁻² Ungrazed	Grazed	ng P cell ⁻¹ (x10 ⁻⁷) Ungrazed	Grazed
WC-P	76.8 ^c	72.0	34.5	54.9
L-P	14.2	12.3	6.4	9.4
MP-P	18.1	16.5	8.0	12.5
RNA-P	17.6	15.9	8.0	12.4
DNA-P	18.5	15.7	8.3	12.3

^aUngrazed and grazed microbial communities were significantly different with respect to phosphorus accumulation in each of the pools; $\alpha = 0.05$.

^bAccumulation of phosphorus for a period of 1178 h for ³³P (Phase 1 and Phase 2).

^cMean P incorporation for phosphorus pools.

Table 17. Distribution of ^{33}P at isotopic equilibrium for the intracellular pools as % of WC-P.^a

Intracellular Pool	% of WC-P	
	Ungrazed	Stream Grazed
L-P	19 \pm 3	17 \pm 3
MP-P	24 \pm 3	22 \pm 4
RNA-P	24 \pm 3	22 \pm 5
DNA-P	24 \pm 3	22 \pm 5
Total Recovery	91	83

^aMean \pm 1 S.D.; n = 16.

RNA-P, and DNA-P pools. No differences in the distribution of ^{33}P in the corresponding intracellular pools for the ungrazed and grazed microbial communities was observed (a non-statistical statement). The intracellular pools accounted for 91% and 83% of the WC-P for the ungrazed and grazed microbial communities, respectively.

Phosphorus Turnover Kinetics for an Oak CPOM

Microbial Community

To determine the phosphorus turnover rate constants for the various phosphorus pools, a double-labeling procedure was used. For this procedure, ^{33}P must be in isotopic equilibrium with ^{31}P (stable phosphorus isotope) of the various phosphorus pools prior to the addition of ^{32}P . Figures 42 to 45 show some representative examples of the incorporation of ^{33}P into various phosphorus pools. ^{33}P reached isotopic equilibrium in approximately 30 days (700 h). ^{32}P and ^{33}P were then simultaneously released into the stream and the ratio of ^{32}P to ^{33}P was determined at various times and used to calculate the phosphorus turnover rate constant.

Phosphorus Turnover Rate Constants for Synthesis

The phosphorus turnover rate constants for synthesis for an ungrazed and a grazed microbial community are shown in Table 18. The turnover rate constants for both community types (WC-P) were not significantly different from each other. The general trend, however, was that the grazed microbial community had a greater turnover rate constant than the ungrazed microbial community. The

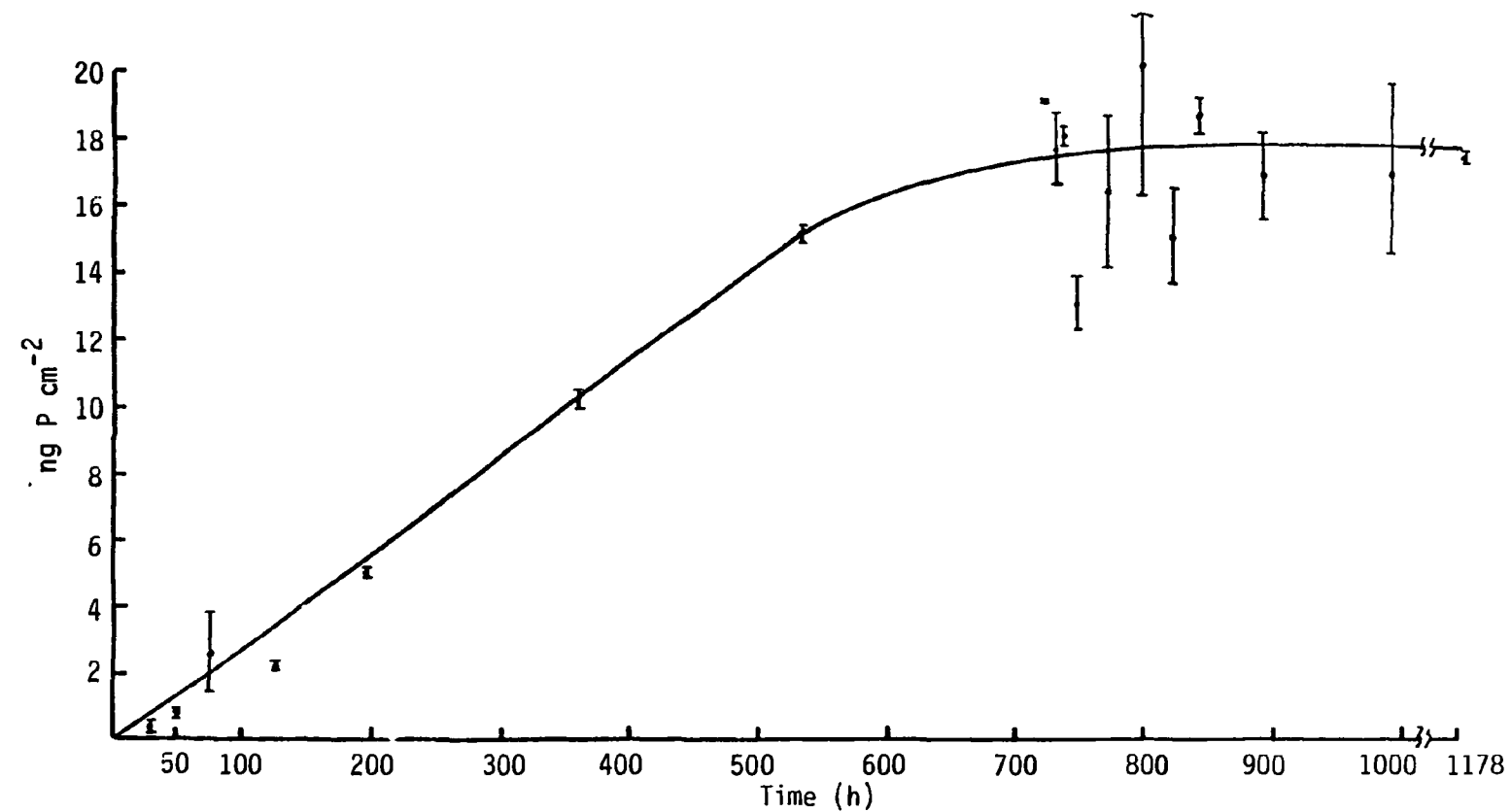


Figure 42. Incorporation of ^{33}P (as ng P cm^{-2}) into L-P pool of a grazed microbial community associated with oak CPOM before and after isotopic equilibrium was achieved. ^{33}P achieved isotopic equilibrium in the L-P pool by 700 h.

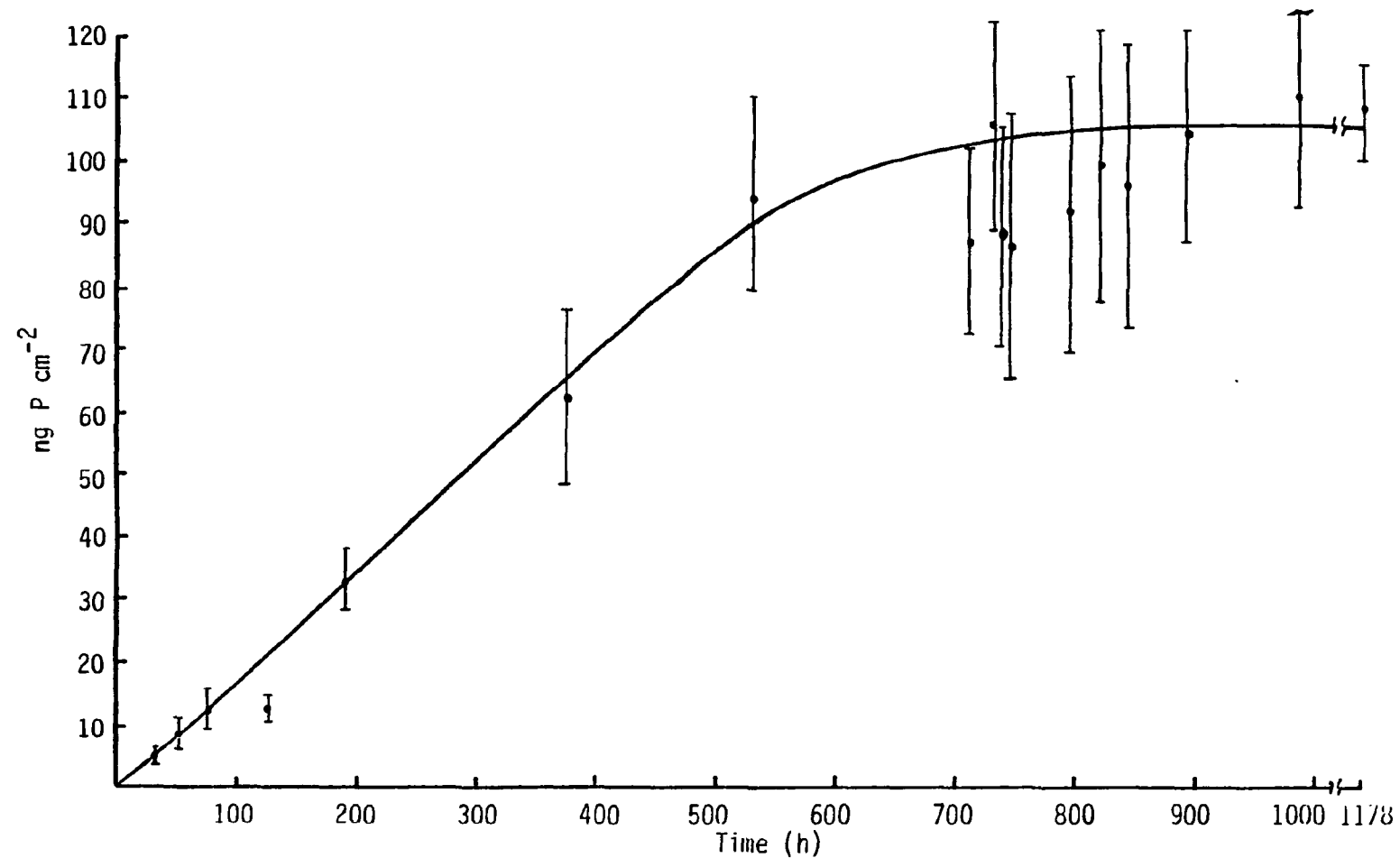


Figure 43. Incorporation of ^{33}P (as ng P cm^{-2}) in WC-P pool of a grazed microbial community associated with oak CPOM before and after isotopic equilibrium was achieved. Isotopic equilibrium was achieved in the WC-P pool by 700 h.

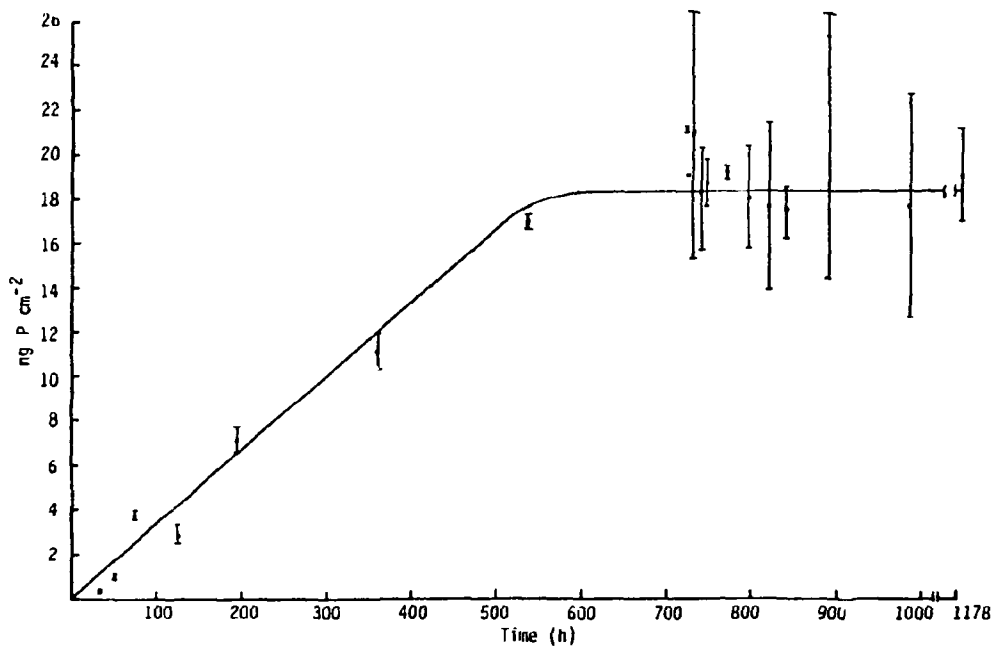


Figure 44. Incorporation of ^{33}P (as ng P cm^{-2}) into L-P pool of an ungrazed microbial community associated with oak CPOM before and after isotopic equilibrium was achieved. ^{33}P was in isotopic equilibrium in the L-P pool by 700 h.

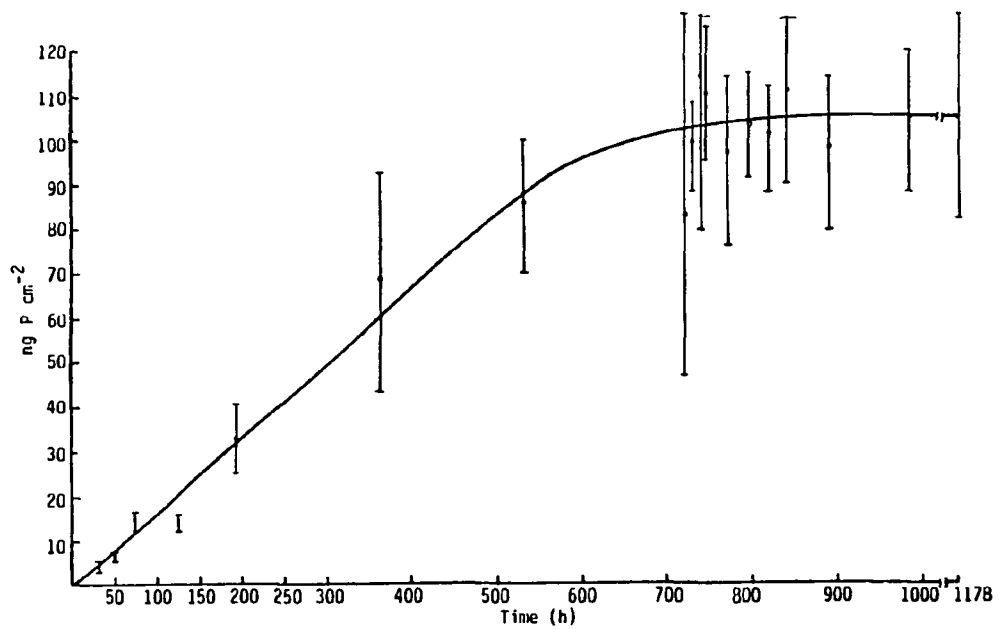


Figure 45. Incorporation of ^{33}P (as ng P cm^{-2}) into WC-P pool of an ungrazed microbial community associated with oak CPOM before and after isotopic equilibrium was achieved. Isotopic equilibrium was achieved by 700 h.

Table 18. Comparison of phosphorus turnover rate constants for synthesis for an ungrazed and a grazed oak leaf detrital microbial community.^a

Stream	Pool	Phosphorus Turnover Rate Constants for Synthesis									
		Turnover ^d		Area-Specific		ATP-Specific		Cell-Specific			
		h ⁻¹ ^b (x10 ⁻³)	r ^{2c}	Time (h)	cm ⁻² h ⁻¹ (x10 ⁻⁴)	r ²	pg ATP ⁻¹ h ⁻¹ (x10 ⁻⁷)	r ²	cell ⁻¹ h ⁻¹ (x10 ⁻¹¹)	r ²	
Ungrazed	WC-P	1.26 ± 0.05	0.96	0.126	794	4.09 ± 0.15	0.96	1.43 ± 0.84	0.91	1.65 ± 0.09	0.92
	L-P	0.96 ± 0.09	0.95	0.096	1042	0.62 ± 0.06	0.95	0.22 ± 0.33	0.89	0.25 ± 0.04	0.89
	MP-P	1.35 ± 0.18	0.91	0.135	741	0.88 ± 0.12	0.91	0.31 ± 0.04	0.90	0.36 ± 0.07	0.84
	RNA-P	1.94 ± 0.53	0.71	0.194	515	1.26 ± 0.35	0.71	0.48 ± 0.14	0.69	0.51 ± 0.14	0.71
	DNA-P	1.14 ± 0.17	0.90	0.114	877	0.74 ± 0.11	0.90	0.26 ± 0.04	0.91	0.30 ± 0.05	0.86
Grazed	WC-P	1.31 ± 0.06	0.94	0.131	763	4.25 ± 0.20	0.94	3.02 ± 0.21	0.88	3.72 ± 0.14	0.96
	L-P	1.11 ± 0.11	0.95	0.111	901	0.72 ± 0.07	0.95	0.51 ± 0.08	0.87	0.63 ± 0.04	0.98
	MP-P	1.80 ± 0.25	0.90	0.180	556	1.17 ± 0.16	0.90	0.90 ± 0.19	0.81	1.07 ± 0.16	0.89
	RNA-P	2.45 ± 0.71	0.68	0.245	408	1.59 ± 0.46	0.68	1.43 ± 0.38	0.72	1.56 ± 0.32	0.81
	DNA-P	1.34 ± 0.19	0.98	0.134	746	0.87 ± 0.12	0.90	0.73 ± 0.16	0.80	0.83 ± 0.15	0.85

^aAs determined by the change in $(^{32}\text{P}/^{33}\text{P})_{\text{pool}} / (^{32}\text{P}/^{33}\text{P})_{\text{stream water}}$.

^bRate ± 95% confidence limit; $\alpha = 0.05$.

^cCoefficient of determination.

^dTime required for a complete replacement of phosphorus.

phosphorus turnover times, the time required for a complete replacement of phosphorus in the community, was 763 h and 794 h for the grazed and ungrazed microbial communities, respectively. These results suggest that grazing increases phosphorus cycling, although phosphorus cycling in both of these communities was relatively slow.

The L-P rate constant of the ungrazed community was not significantly different from the DNA-P rate constant; however, it was significantly slower than the MP-P and RNA-P rate constants. The MP-P turnover rate constant was not significantly different from the RNA-P and DNA-P rate constants, but it was significantly greater than the L-P rate constant. The RNA-P rate constant for the ungrazed community was not significantly different from that of the MP-P, however, it was significantly greater than the L-P and DNA-P rate constants. The DNA-P rate constants for the ungrazed community was significantly less than the RNA-P constant, but not significantly different from the other phosphorus rate constants.

The grazed L-P turnover rate constant was not significantly different from DNA-P constant, but was significantly less than the MP-P and RNA-P phosphorus turnover rate constants. The MP-P rate constant was not significantly different from the RNA-P turnover rate constant, however, it was significantly greater than the L-P and DNA-P rate constants. The RNA-P rate constant for the grazed microbial community was not significantly different from the MP-P rate constant, but it was significantly greater than the L-P and DNA-P phosphorus turnover rate constants.

A comparison of the phosphorus turnover rate constants of the ungrazed and grazed oak CPOM microbial communities indicated that the L-P, RNA-P, and DNA-P phosphorus turnover rate constants were not significantly different from each other. The MP-P phosphorus turnover rate constants for the grazed microbial community was significantly faster than the ungrazed MP-P rate constant. The general trend for the grazed microbial community having faster rate constants was suggested, although the differences were not statistically significant.

The phosphorus turnover times for the intracellular pools for both ungrazed and grazed microbial communities are ranked as follows: RNA-P<MP-P<DNA-P<L-P, however, the grazed community turnover times are shorter than the ungrazed community (Table 18). These results indicated that the grazed microbial community is metabolically more active and growing faster compared to the ungrazed microbial community.

Area-specific phosphorus turnover rate constants for synthesis.

Table 18 shows the area-specific phosphorus turnover rate constants for the oak CPOM study. The WC-P (community) phosphorus turnover rate constant of the grazed and ungrazed microbial community were not significantly different from each other, although the rate constant for the grazed community was greater.

A comparison of the intracellular phosphorus turnover rate constant for the ungrazed and grazed microbial communities indicated

that the corresponding rate constants were not significantly different from each other. For both the grazed and ungrazed communities, the RNA-P and MP-P constants were significantly greater than the L-P and DNA-P rate constants; this suggests unbalanced metabolism. These results indicate that on an area basis there were no differences between the grazed and ungrazed communities with regards to phosphorus turnover.

Cell-specific phosphorus turnover rate constants for synthesis.

Cell-specific phosphorus turnover rate constants are shown in Table 18. The WC-P (community) phosphorus turnover rate constant of the grazed community was significantly greater than the rate constant for the ungrazed community. The rate constant for the grazed community was approximately two-fold greater than the rate constant for the ungrazed community.

The cell-specific phosphorus turnover rate constants for the intracellular phosphorus pools of the grazed microbial community were significantly greater than the rate constants for the corresponding pools of the ungrazed community. The L-P rate constant of the grazed community was about two and one-half-fold greater than the ungrazed L-P rate constant, while the MP-P, RNA-P, and DNA-P rate constants of the grazed community were approximately three-fold greater than those of the ungrazed community. These results indicate that bacteria of the grazed community were metabolically more active than the bacteria of the ungrazed community.

ATP-specific phosphorus turnover rate constants for synthesis.

ATP-specific phosphorus rate constants are shown in Table 18. The phosphorus turnover rate constant for the grazed community was significantly greater than the rate constant for the ungrazed community. The rate constant for the grazed community was about two-fold greater than that for the ungrazed community.

The phosphorus turnover rate constants for the intracellular phosphorus pools of the grazed microbial community were significantly greater than the corresponding rate constants for the ungrazed microbial community. The L-P turnover rate constant for the grazed community was approximately two-fold greater than the L-P rate constant for the ungrazed community, whereas the MP-P, RNA-P, and DNA-P turnover rate constants of the grazed community were about three-fold greater than those of the ungrazed community. These data suggest the grazed microbial community was metabolically more active than the ungrazed microbial community.

Turnover Rates

The turnover of phosphorus from the components was also followed after the input of tracer was stopped. Thus, two measurements of phosphorus turnover were possible, as determined by ^{32}P and ^{33}P loss from the pool.

Area-specific turnover rates. The WC-P phosphorus turnover rates (^{32}P) for the ungrazed and grazed microbial community were not significantly different from each other; however, the grazed

community had a greater turnover rate than the ungrazed community (Table 19). This suggests that grazing of the microbial community increases the metabolic activity of the microbial community. The ^{33}P -derived WC-P turnover rate had the same trend as for the ^{32}P -derived rate (Table 20). The ^{33}P -derived rate, however, was about two-fold greater than the ^{32}P -derived WC-P rate. The ^{33}P - and ^{32}P -derived rates, however, were not significantly different from each other.

The turnover rates for the intracellular phosphorus pools are shown in Tables 19 and 20. The turnover rates of the ungrazed community, both ^{32}P and ^{33}P derived, were not significantly different from the corresponding rate of the grazed community; however, the grazed microbial community had higher turnover rates than the ungrazed microbial community. The ^{33}P -derived rates for the intracellular pools were approximately two-fold greater than the ^{32}P -derived rates although the rates were not significantly different from each other.

Generally, grazing of the microbial community seems to increase the metabolic activity of the community in comparison to a non-grazed community.

Cell-specific turnover rate. The community (WC-P) turnover rate, ^{32}P - or ^{33}P -derived, for the grazed community was not significantly different from the ungrazed community turnover rate (Tables 19 and 20). The grazed community, however, had a faster turnover rate than the ungrazed community, suggesting that grazing increases

Table 19. Comparison of phosphorus turnover rates for degradation for an ungrazed and a grazed oak leaf detrital microbial community.^a

Phosphorus Turnover Rates ^b							
Stream	Pool	Area-Specific		Cell-Specific		ATP-Specific	
		ng P cm ⁻² h ⁻¹	(x10 ⁻²)	ng P cell ⁻¹ h ⁻¹	(x10 ⁻⁹)	r ²	ng P pg ATP ⁻¹ h ⁻¹
Ungrazed	WC-P	2.39 ± 0.82	0.53	1.08 ± 0.35	0.56	0.73 ± 0.41	0.30
	L-P	0.36 ± 0.17	0.77	0.17 ± 0.10	0.67	0.10 ± 0.11	0.41
	MP-P	0.56 ± 0.34	0.67	0.25 ± 0.11	0.81	0.17 ± 0.23	0.30
	RNA-P	1.04 ± 0.73	0.61	0.49 ± 0.23	0.78	0.30 ± 0.45	0.26
	DNA-P	0.80 ± 1.01	0.33	0.37 ± 0.37	0.43	0.25 ± 0.54	0.15
Grazed	WC-P	2.81 ± 0.66	0.71	1.81 ± 0.70	0.47	1.65 ± 0.86	0.33
	L-P	0.52 ± 0.17	0.88	0.35 ± 0.18	0.74	0.28 ± 0.27	0.45
	MP-P	0.58 ± 0.54	0.47	0.39 ± 0.64	0.22	0.40 ± 0.76	0.18
	RNA-P	0.77 ± 1.05	0.29	0.42 ± 1.12	0.10	0.61 ± 1.22	0.16
	DNA-P	0.68 ± 0.33	0.76	0.43 ± 0.56	0.32	0.46 ± 0.72	0.24

^aAs determined by ³²P loss from pools during Phase 2.

^bRate ± 95% confidence limit; $\alpha = 0.05$.

^cCoefficient of determination.

Table 20. Comparison of phosphorus turnover rates for degradation for an ungrazed and a grazed oak leaf detrital microbial community.^a

Phosphorus Turnover Rates ^b							
Stream	Pool	Area-Specific		Cell-Specific		ATP-Specific	
		ng P cm ⁻² h ⁻¹	(x10 ⁻²)	ng P cell ⁻¹ h ⁻¹	(x10 ⁻⁹)	r ²	ng P pg ATP ⁻¹ h ⁻¹
Ungrazed	WC-P	5.68 ± 1.98	0.52	2.68 ± 0.89	0.55	1.65 ± 0.99	0.27
	L-P	0.76 ± 0.43	0.71	0.40 ± 0.25	0.66	0.19 ± 0.30	0.24
	MP-P	1.22 ± 0.89	0.59	0.56 ± 0.28	0.76	0.38 ± 0.57	0.25
	RNA-P	0.73 ± 0.98	0.30	0.44 ± 0.30	0.62	0.16 ± 0.62	0.05
	DNA-P	0.97 ± 0.55	0.70	0.51 ± 0.15	0.90	0.25 ± 0.50	0.16
Grazed	WC-P	5.98 ± 1.71	0.62	3.54 ± 1.70	0.37	3.71 ± 2.10	0.30
	L-P	1.11 ± 0.65	0.69	0.67 ± 0.58	0.51	0.65 ± 0.74	0.37
	MP-P	1.25 ± 0.58	0.78	0.84 ± 0.85	0.43	0.76 ± 1.04	0.29
	RNA-P	0.96 ± 1.02	0.40	0.44 ± 0.90	0.16	0.66 ± 1.00	0.25
	DNA-P	1.16 ± 0.76	0.64	0.67 ± 1.06	0.24	0.84 ± 1.34	0.23

^aAs determined by ³³P loss from pools during Phase 3.

^bRate ± 95% confidence limit; $\alpha = 0.05$.

^cCoefficient of determination.

the metabolic activity of the bacteria. The ^{33}P -derived rates were approximately two-fold greater than the ^{32}P -derived rates.

The phosphorus turnover rates for the corresponding intracellular pools (derived from ^{32}P or ^{33}P) for the grazed community were not significantly different from those for the ungrazed community (Tables 19 and 20). A general trend of faster phosphorus turnover rates for the phosphorus pools of the grazed microbial community was observed.

ATP-specific turnover rates. The WC-P pool turnover rate (^{32}P - and ^{33}P -derived) for the grazed community was not significantly different from the WC-P rate of the ungrazed community. The grazed community had a greater turnover rate, however, than the ungrazed microbial community.

A comparison between the ungrazed and grazed communities phosphorus turnover rates for their corresponding intracellular phosphorus pools (^{32}P - or ^{33}P -derived) indicated that there was no significant difference between the rates. The turnover rates for the grazed community were greater than the turnover rates for the ungrazed microbial community, although not significantly faster.

Phosphorus turnover times were determined by following the loss in radioactivity of both ^{33}P and ^{32}P from the phosphorus pool after the tracer input was stopped. The turnover time was defined as the reciprocal of the slope of the curve obtained by plotting the log of percent of initial activity per cm^2 versus time. Turnover

times for the phosphorus pools for the ungrazed microbiota associated with oak CPOM for ^{33}P and ^{32}P , respectively, were: WC-P, 2174 h and 1887 h; L-P, 2941 h and 1818 h; MP-P, 2398 h and 2041 h; RNA-P, 6667 h and 2500 h; and DNA-P, 3846 h and 3448 h. The phosphorus turnover times for the grazed microbiota were: WC-P, 1852 h and 1449 h; L-P, 1692 h and 1111 h; MP-P, 1563 h and 2128 h; RNA-P, 2941 h and 4348 h; and DNA-P, 2632 h and 2041 h, respectively, for ^{33}P and ^{32}P .

VI. DISCUSSION

The goal of this investigation was to elucidate the physiological aspects of microbial community development and phosphorus dynamics associated with decomposing leaves in a lotic system. In order to accurately determine the role of the microbial community in stream phosphorus dynamics, it is necessary to ensure that detrital community biomass and activity are representative for detrital communities as reported by other investigators. The discussion and interpretation of the results will be done in regard to the river epilithon model of the microbial community (Lock, 1984), and the nutrient spiraling model (Elwood, 1981, 1983; Newbold, 1981, 1983; Mulholland, 1983, 1985).

Sessile (attached) microbial communities associated with rocks in stream ecosystems are enclosed in a highly hydrated fibrous anionic exopolysaccharide, termed glycocalyx, which may act as an ion exchange resin attracting and concentrating charged nutrients (Costerton, 1984; Geesey et al., 1977, 1978; Lange, 1976). A complex sessile microbial community (so called epilithon) develops and proliferates as distinct microcommunities within the glycocalyx matrix (Lock et al., 1984). The spatial organization of the epilithon plays an important role in the growth, energy transformation, and nutrient cycling of the community because of the possible interaction between neighboring organisms, such as competition, amensalism, and comensalism (Wimpenny, 1981). The glycocalyx also creates diffusion

gradients of nutrients and gases which are important to the growth of the epilithon (La Motta, 1976b). As the glycocalyx thickness increases, organisms near the bottom might become nutrient limited due to slow diffusion through the epilithon.

Although the epilithon model was developed to describe the sessile microbial community associated with river rocks, the concept is applicable to the development of the microbial community associated with decomposing leaves in streams (Figures 17-28, pages 78, 81, 83, 85, 88, 90, 92, 94, 96, 98, 101, 103, respectively). The development of the polysaccharide matrix associated with the microbial community does not appear to be extensive. This is likely due to the dehydration step of sample preparation resulting in the condensation of the polymer (Mackie et al., 1979; Davis, 1985).

Microbial Community Development and Activity

The colonization pattern observed in the present study indicated bacteria were the first to colonize followed by fungi. The fungi subsequently declined, but the bacteria and polysaccharide matrix continued to increase (Figures 17-28). The temporal pattern, however, was dependent on the leaf species; the more readily decomposable the species, the greater the development of the community (oak<maple<dogwood). Suberkropp (1976) reported that fungi were the first colonizers of leaf litter in streams, but since his first samples were taken 14 days after the leaves were placed in the stream, he missed the initial colonization period which may have been dominated by bacteria.

The temporal pattern for the development of the relative heterotrophic potential, determined by glucose uptake rates, for decomposing maple and oak leaves suggests that the sessile community was somehow limited (no further increase in the rate of glucose uptake) within two weeks, probably due to the reduction in the availability of readily labile organic substrates or inorganic nutrients as a result of the glycocalyx (Figure 12, page 70). The microbial community associated with dogwood leaves displayed a different response which probably represents the leaf's rate of decomposition; therefore, a greater supply of oxidizable organic substrate was probably available. The same phenomenon was observed for glucose assimilation for the dogwood, maple, and oak microbial communities (Figure 13, page 71). The temporal pattern observed for glucose mineralization rates indicated a bimodal trend of increasing mineralization for the dogwood, maple, and oak microbial communities (Figure 14, page 72), suggesting two periods of accelerated energy production. These data suggest that the heterotrophic potential of the microbiota on leaves in streams is dependent on the species of leaf colonized. The effect of leaf species seems to be related to the relative ease at which the leaf is decomposed.

Red maple leaves used for the ungrazed maple CPOM study are considered to be an intermediate species with regard to their rate of decomposition, whereas white oak leaves (oak CPOM study) are more resistant to decomposition due to their high content of polyphenols and lignin. Colonization of maple leaves was followed for a period of 51 days. By the time of the first sampling (15 days),

the biomass, as ATP, had established an approximate steady-state microbial community (Figure 29, page 107) with a mean biomass of about 15,000 pg ATP cm^{-2} of leaf surface. The mean ATP values for days 15 to 32 were generally lower than the grand mean, whereas the mean ATP for days 34 to 44 generally were greater than the grand ATP mean value. These results demonstrate a slight increase in microbial biomass with an increase in residence time of the leaves in the stream. The ATP biomass data reported here are in close agreement with the values reported by Mulholland (1984) and Fairchild (1983), although the trend of increasing biomass with residence time is not as pronounced.

In the oak CPOM study the ATP biomass remained relatively constant during the course of this study, as did the direct bacterial cell counts, for both the ungrazed and grazed oak CPOM (Figures 40 and 41, pages 134 and 135, respectively). This observation was not unreasonable since the oak leaves were colonized for a period of 112 days prior to the start of this study. Thus, a steady-state microbial community was associated with oak leaves. The total cell counts of the oak microbiota may be underestimated by as much as about 50% (see page 57). However, the trend observed is not affected by low estimates.

The ATP biomass and bacterial density associated with oak leaves fall within the range reported by Suberkropp for oak leaves (1976). Suberkropp also noted a greater biomass, measured as ATP, and bacterial density associated with hickory leaves than with oak

leaves. Hickory leaves are considered to be an intermediate species with regards to ease of decomposition, as are maple leaves. Thus, it seems that the more recalcitrant the leaf is to decomposition, the smaller the cell density.

The microbial biomass, as ATP, associated with the maple leaves was approximately three and one-half-fold greater than the ATP biomass associated with ungrazed oak leaves (Figures 29 and 40, pages 107 and 134, respectively). The higher ATP content of the microbial community associated with the maple CPOM was probably due to a higher population density of the fungal component of the microbial community, whereas the microbial community associated with the oak CPOM was probably bacterial. The microbial community of the maple CPOM study was approximately the same age as that for the colonization study (about 50 days), which had a developed fungal population (see SEM Figures 21-24, pages 88, 90, 92, and 94, respectively), whereas the microbial community associated with oak litter was 112 days old at the start and 191 days at the completion of the study. It has been observed by Suberkropp (1976) that the bacterial population of the microbial community associated with leaf CPOM becomes dominant as the residence time in the stream increased. Supporting evidence for the hypothesis of a community on oak CPOM dominated by bacteria comes also from the ATP content per bacterium data (Table 14, page 137) which were at the lower range of reported values. Thus, if fungi were an important component of the oak microbial community, the ATP per bacterium content would have been elevated due to the contribution of fungal ATP.

The difference between the biomass, as ATP, of maple and oak leaf litter may also be a reflection of the organic quantity and quality of the leaves. The maple study was conducted using relatively young (0 to 51 days) leaves (high organic matter) compared to the oak study which used old (112 to 191 days) leaves (low organic matter). Bott et al. (1984) demonstrated that the steady state bacterial biomass of precombusted sediment (to remove the organic matter) was approximately twenty-fold lower than compared to natural (uncombusted) sediments. Figure 16, page 76, shows the organic content of leaves does tend to decrease with the residence time in the stream; therefore, the microbiota associated with the oak CPOM may have been limited by the availability of utilizable organic matter.

Physiological Status

The calculated ATP content per cell, a measure of the physiological status, observed for the ungrazed microbiota associated with decomposing oak leaves ($0.19 \text{ fg cell}^{-1}$) was at the low end of the scale reported for laboratory grown cultures (Nuzback et al., 1983; Hamilton and Holm-Hansen, 1967); however, the ATP per cell value does fall within the range observed for bacteria in natural ecosystems (Wilson et al., 1981). The observations of the present study, like those of Wilson, were obtained by using direct cell counts, and showed that the ATP per cell content was low compared to laboratory grown cells. Direct cell counts, however, estimate

total cell numbers and therefore the proportion of viable cells may be less than 100% (Meyer-Reil, 1978; Faust and Correll, 1977), thus the ATP per cell values may be underestimated. The value for the oak microbiota represent a microbial community in which about 50% of the community were viable due to the possible underestimation of total cell counts (see page 57).

The synthesis rate of phospholipid, RNA and DNA has been suggested as a measure of the relative microbial growth in aquatic environments (White, 1977; Karl, 1979, 1981; Tobin and Anton, 1978; Fuhrman and Azam, 1982). The growth rates of microbial communities can also be estimated from the turnover of cellular components (White, 1983). Different organisms within a microbial community, however, grow at different rates; therefore, the growth rate estimate represents an average community growth rate. The rates observed in this study indicate that the microbial community associated with leaf CPOM are slowly growing.

The calculation of the mean generation time was determined in the following manner. The product of the percent phosphorus in DNA, 9.23% (Sober, 1968), and the amount of DNA per genome, 4.2×10^{-15} g (Kubitschek, 1971), yields the amount of phosphorus per genome. Assuming one genome per cell, at slow growth (Kubitschek, 1971), this product represents the amount of genome equivalent phosphorus per cell. Dividing this value by the product of the percent phosphorus in PO₄, 32.63%, and the cell-specific incorporation rate for DNA-P, 1.55×10^{-18} g PO₄ cell⁻¹ h⁻¹ (Table 15, page 138), will

yield the mean generation time for the microbial community. A mean generation time of about 32 days was determined for the ungrazed microbiota associated with oak CPOM which is in the upper end of reported generation times for natural systems (Gray, 1976; Jordan and Likens, 1979; Hagstrom, 1979; Karl, 1979; Newell and Christian, 1981; Van Es, 1982; Riemann et al., 1982).

The slow growth rate observed may reflect the nature of the system studied. The artificial streams used for these studies were designed to simulate a heterotrophic water stream, thus primary production was negligible, therefore, no autochthonous dissolved organic carbon (DOC) was produced. The DOC level in these streams was low, about 0.45 mg L^{-1} (Mulholland, unpublished data), and coupled with the low phosphorus level (approx. $2.3 \text{ } \mu\text{g L}^{-1}$), it is not surprising to find the microbial community slowly growing.

Detrital Community Phosphorus Dynamics

The distribution of phosphorus in the CPOM associated microbes (Tables 8 and 17, pages 118 and 142, respectively) was comparable to the pattern observed in laboratory cultures. Bolton (1956), using ^{32}P , reported a phosphorus distribution pattern of 20% in the metabolite pool, 15% in the phospholipids, and 63% associated with the nucleic acids (vs. 21%, 18%, and 65%, respectively, for the maple study, and 24%, 19%, and 48%, respectively, for the oak study). A phosphorus distribution pattern of 12%, 66%, and 19% was observed by Taylor (1946) for phospholipid, RNA, and DNA,

respectively, using standard chemical analysis. The lower percentage of ^{33}P associated with the RNA fraction for the oak study, compared to the maple microbiota (24% vs. 43%), probably reflects a slower growth rate of the community, since the RNA content has been shown to be proportional to the growth rate (Maaløe and Kjeldgaard, 1966). This is consistent with Taylor's results above, who used an 8-hour broth culture of E. coli (log phase); therefore, one would expect a higher RNA content.

The phosphorus turnover and incorporation rates determined for this study represent the average of all the organisms in the microbial community and the average of all the components in a specific phosphorus pool. The inorganic phosphorus incorporation rates determined are net rates since any efflux of phosphorus from the pool would not have been measured. The phosphorus incorporation rates, therefore, will be considered a minimum estimate of the actual rate at which phosphorus entered the phosphorus pool. The turnover rates were determined by following the decrease in radioactivity in the pool; however, the extent to which the tracer isotope was reincorporated into the pool should be determined to accurately estimate the true turnover rate (Swick et al., 1956). The rate measurements of the present study were not corrected for reincorporation of tracer isotope which probably is reflected by the extremely long turnover times determined using this procedure. The loss of radioactivity due to grazing and the sloughing or detachment of cells are other sources of error.

Neither the exponential (i.e., log transformed) nor the linear (i.e., untransformed) models fit (low r^2 values) the data for phosphorus turnover (radioactivity loss). It may be best to analyze the turnover data in a multiphasic approach; however, due to insufficient data, this was not possible. The results (Tables 10, 19, and 20, pages 127, 154, and 155, respectively) indicate that depending on which tracer (^{33}P or ^{32}P) was used to determine the turnover rate, a different value was obtained. The ^{33}P - and ^{32}P -derived turnover rates, however, generally were not significantly different from each other.

Another important consideration pertaining to phosphorus dynamics is the extent to which organic phosphorus contributes to the phosphorus metabolism of the microbiota of decomposing leaves. Only inorganic phosphate was used to determine the rate estimates in this study. If the microbiota acquire substantial quantities of phosphorus from organic phosphorus compounds, the phosphorus kinetics reported might be underestimated, the extent of which is not known.

The alkaline and acid hydrolysis procedure used to extract DNA might have resulted in an over estimation of the amount of tracer phosphorus associated with the DNA. This is because phosphate can be incorporated into polyphosphates which are hydrolyzed in the procedure used to extract DNA (Harold, 1966). The contribution of polyphosphate to the DNA phosphate for this study was considered to be negligible due to the low phosphate concentration in the stream

(Table 12, page 131) which is limiting to the synthesis of polyphosphates in bacteria and fungi (Harold, 1966; Beever and Burn, 1980; Dawes and Senior, 1973). Elwood et al. (1981) demonstrated that the microbiota associated with decomposing leaves in Walker Branch were phosphorus limited at these P levels (Table 12). Thus, it is not likely that the microbiota are storing polyphosphates since polyphosphates are not stored under P-limited conditions.

A comparison of the kinetic data of the maple and oak studies shows the microbiota associated with maple leaves to have higher rates, as well as biomass, compared to the oak microbiota. The differences are attributed to differences in the developmental age of the communities associated with the two leaf species. The microbial community of the maple leaves were 21 to 45 days old compared to 112 to 191 days old for the oak microbiota during the course of the study. The microbiota on maple leaves colonized for 19 days had a higher phosphate uptake rate than leaves colonized for 31 days (Figures 8 and 10, pages 59 and 62; also see page 60). The leaf species difference is also of importance since different species are colonized at different rates (Kaushik, 1971). This hypothesis is supported by the observations of a study by Mulholland et al. (1984), who examined the role of microbial conditioning (colonization and growth) of CPOM on inorganic phosphate uptake. They found that the phosphate uptake rate was rapid initially (first 20 days) and then declined to a relatively constant rate by day 30. Elwood et al.

(unpublished) found that the level of microbial activity on CPOM affected the phosphorus spiraling length by as much as a factor of two. The spiraling length reached a minimum after about 2 to 3 weeks of leaf conditioning.

The results of both Mulholland and Elwood suggest that phosphate uptake rate and phosphorus spiraling length are stabilized after CPOM was in the stream for about 3 to 4 weeks; however, the spiraling length will increase as leaves decompose and the community becomes less active. The SEM study and glucose metabolism data presented here were done in conjunction with the Mulholland study (1984). The decline in phosphorus and oxygen uptake he observed and the leveling off of glucose uptake (Figure 12, page 70) reported in the present study all coincided with the increase of polymer (polysaccharide build-up on the leaves) suggesting that a diffusion gradient might be limiting community metabolism. La Motta (1976b) has shown that the thickness of the microbial film and the concentration of substrate affect the diffusion of nutrients into the slime matrix, thus affecting the microbial metabolism.

The phosphorus turnover rate constants for synthesis (double-labeling procedure) determined for the ungrazed microbial community on maple leaves were two- to four-fold greater than the phosphorus turnover rate constants of the oak microbiota (Tables 9 and 18, pages 122 and 148, respectively). However, the ATP-specific phosphorus turnover rate constants for synthesis of the oak microbiota were greater (one and one-half to eleven-fold) than corresponding constants for the maple microbial community (Tables 9 and 18).

This indicates that per unit biomass the microbiota associated with the oak CPOM turned over phosphorus faster than the microbiota associated with the maple CPOM. This suggests that the developmental age of the community might be an important factor influencing phosphorus turnover.

Berman and Skyring (1979), using a double-labeling (^{32}P and ^{33}P) procedure, reported phosphorus turnover rates of synthesis for intact cells and MP-P for laboratory cultures of algal and bacterial cells which were about three to four orders of magnitude greater than the turnover rates observed for the microbiota associated with decomposing leaves (Table 18, page 148). This indicates that the microbiota associated with decomposing leaves are not very metabolically active and are slowly growing. This hypothesis is supported by the work of White and his colleagues on detrital microbiota who estimated an increase in bacterial biomass of 0.024% to 0.0096% per 2h based upon total muramic acid and 0.11% per 2h based on ATP (Morrison et al., 1977), slow phosphorus lipid turnover ($t_{1/2}$ of 110 hours for glycerol phosphate esters of phospholipids) (King and White, 1977), and slow turnover of muramic acid ($t_{1/2}$ 78h) (King and White, 1977).

Influence of Grazing

Grazing by snails resulted in approximately a two-fold depression in the microbial biomass, as ATP, and the bacterial cell density associated with the oak CPOM compared to the ungrazed

microbiota (Figures 40 and 41, pages 134 and 135, respectively). It was assumed that the percent ATP extracted and the percent cell dislodgement from the leaf surface was the same for the ungrazed and grazed microbial communities associated with the oak CPOM. Mulholland (1983) also observed a reduction in aufwuch biomass in response to snail grazing compared to an ungrazed community. Thus, snail grazing seems to play a role in controlling the size of the microbial community.

The calculated ATP content per cell for the grazed microbiota associated with oak CPOM was approximately 1.3 times greater than that of the ungrazed microbial oak community (Table 14, page 137). The mean generation time calculated for the grazed microbiota associated with oak CPOM (see page 164 for details) was 12 days which was about 2.8 times faster than that of the ungrazed oak microbial community.

A comparison of the area-specific and cell-specific phosphorus accumulation in the phosphorus pools for the ungrazed and grazed oak microbial communities (Table 16, page 141) indicates that on an area-specific basis the ungrazed community accumulated a significantly greater amount of phosphorus than did the grazed community. On a cell-specific basis, however, the grazed community accumulated a significantly greater amount of phosphorus than the ungrazed community. The reason for these results was due to differences in the bacterial cell density associated with the ungrazed and grazed microbial communities (Table 13, page 133). Although the bacteria

of the grazed community had more phosphorus per cell than the bacteria of the ungrazed community, the ungrazed community accumulated more phosphorus per unit surface area than did the grazed community due to greater cell density (1.7x). This suggests that grazing by snails results in less retention of phosphorus in the stream. It should be noted, however, that there was no alternative food source, such as an autotrophic component, for snails to graze; therefore, food switching by snails could not have occurred, as a consequence the CPOM might have been over-grazed by the snails.

These results are similar to those of Mulholland (1983) who observed that a reduction in the aufwuch biomass, primary productivity, and phosphorus uptake occurred in response to snail grazing. In the autotrophic stream used by Mulholland, the periphyton served as the only food source (no CPOM); thus food switching could not have occurred. Overcropping was suspected to be the reason for the increase in uptake length (reduction in P uptake).

The area-specific rates (incorporation and turnover) for the grazed oak microbiota were about the same as the corresponding rates for the ungrazed oak community (Tables 15, 19, 20, pages 138, 154, 155, respectively). On a biomass-specific basis, however, the rates for the grazed microbiota were approximately two-fold greater than the corresponding rate for the ungrazed oak microbiota. Thus, the biomass reduction due to grazing is offset by an increased uptake of phosphorus per unit biomass resulting in no change in uptake per unit area.

An increase in metabolism for aquatic autotrophic and heterotrophic microbiota in response to grazing has been previously reported (Hargrave, 1970; Barsdate et al., 1974; Fenchel and Harrison, 1976; Smith et al., 1982; Morrison and White, 1980). There also appears to be an optimum grazing level above which microbial metabolism declines (Hargrave, 1970; Cooper, 1973). The reason for the increase in phosphorus metabolism as a result of the grazing may be due to (1) a phosphorus enrichment due to nutrient regeneration by the grazer; (2) grazers consuming bacteria thereby increasing available surface area for further colonization which prevents the microbiota from becoming self-limiting; (3) the possible synthesis of stimulatory products by the grazers; (4) the reduction in the diffusion gradient for phosphorus or the nutrients by break-up or reduction of the thickness of the glycocalyx.

The hypothesis of a reduction in the diffusion gradient is reasonable since Ladd et al. (1977) have reported that dispersed epilithic populations had significantly higher metabolic activity (glutamic acid uptake) than did the undisturbed epilithic community. They suggest that the metabolism of bacteria enclosed in polysaccharide matrix are rate-limited by the diffusion of nutrients through the matrix. The concentration of phosphate (SRP) in the oak study is very low, about $2.3 \mu\text{g L}^{-1}$, and this tended to limit the phosphorus availability to the community due to the diffusion barrier of the glycocalyx. The diffusion coefficient of the slime layer has been reported to be dependent upon the nutrient concentration (Ladd, 1977).

Contribution to Phosphorus Spiraling

The uptake and regeneration (turnover) of phosphorus by the microbial community, in addition to hydrologic transport, are important processes controlling phosphorus spiraling. Any process, such as grazing or storms, which affect uptake and turnover will also influence spiraling.

In the autumn the microbial biomass would be expected to be at its highest density due to the increase in colonizable surface area. The concentration of available P should also increase as a result of leaching from leaves. The microbiota associated with CPOM represent a large storage reservoir of phosphorus, preventing the rapid loss of the pulse of phosphorus from the stream headwaters to the downstream reaches. Due to the slow turnover of phosphorus, and low biological activity of the microbiota, the phosphorus remains in the headwater; therefore, downstream biota may be influenced by the spiraling of phosphorus (slowly recycling P). On a short-term basis, the microbiota associated with leaves will generally tend to have a shortening effect on the distance between spiral loops (i.e., the nutrient nearly completes a cycle at any one point within the stream)(Figure 46). Grazing of the microbiota by snails increases the turnover rate (hence decreasing the retentiveness) and increases the uptake rate, thus reducing the spiraling length (the distance between loops).

On the long-term basis the standing stock of CPOM and microbial biomass will be reduced due to the hydrologic transport of CPOM downstream (Mulholland, 1985). As a result, the uptake

ORNL-DWG 86-9467

Mechanism	Retention	Biological Activity	Effect on Nutrient Recycling	Distance Between Spiral Loops	Ecosystem Response to Nutrient Addition
				FAST	SHORT
A. HIGH	HIGH	HIGH			CONSERVATIVE (I>E)
				SLOW	SHORT
B. HIGH	LOW	LOW			STORING (I>E)
				FAST	LONG
C. LOW	LOW	HIGH			INTERIMEDIATELY CONSERVATIVE (A but > D)
				SLOW	LONG
D. LOW	LOW	LOW			EXPORTING (I=E)

Figure 46. Postulated effects of different interactions between nutrient spiraling and biological activity. I = import, E = export. The smaller the diameter of a loop, the faster the rate of recycling of a nutrient. The distance between the loops represents the extent of downstream displacement of a cycle by the unidirectional flow of water. The effect of flow can be offset by retention mechanisms so that the higher the retention, the shorter the distance between loops (i.e., the more nearly complete the cycle at any one point in the stream). Adapted from G. W. Minshall et al. 1983. Ecological Monographs 53(1):1-25; Figure 18).

and turnover lengths will be increased resulting in an increase in the spiraling length, thus decreasing stream productivity. Furthermore, any mechanism that will reduce the loss of CPOM from the system, e.g., debris dams, will shorten the spiraling length and increase stream productivity.

This investigation points out many new avenues for continued study concerning phosphorus metabolism of the microbiota associated with CPOM. Some other questions and aspects which could be addressed in future studies are:

1. What influence does grazing intensity have on the phosphorus metabolism of the microbiota on CPOM?
2. What effect does the colonization period have on phosphorus metabolism?
3. What effect does the leaf species colonized have on the intracellular microbial phosphorus metabolism?
4. What effect does the thickness of the sessile microbial community of CPOM have on phosphorus metabolism?
5. Is the utilization of organic phosphate compounds (phospholipid, RNA, DNA, sugar phosphates, etc.) by the microbiota important to the phosphorus dynamics of lotic ecosystems?
6. What enzymatic activities (phosphatase, 5'-nucleotidase, DNase, RNase) do the microbiota possess and what is its importance to the phosphorus dynamics of lotic ecosystems?
7. An in-depth SEM study describing the colonization of leaf CPOM would aid in the interpretation of phosphorus utilization patterns.

8. What effect do elevated levels of nutrient (phosphorus or nitrogen) and dissolved organic carbon concentration have on phosphorus metabolism of CPOM associated microbiota?

9. A study of the microbiota associated with CPOM using the biochemical approaches developed by White and his colleagues.

10. A study of the energetics of CPOM associated microbiota using microcalorimetry.

The answers to these points would further our understanding of the structure and function of the microbiota associated with CPOM, and the importance of this microbial community to the stability of lotic ecosystems.

VII. SUMMARY

The objective of this ecological investigation was to examine the dynamics of phosphorus of a microbial community associated with decomposing leaf CPOM in a lotic ecosystem. Two studies were conducted: the first used ungrazed red maple CPOM, while the second was a comparative study to examine the effect of snail grazing on the microbiota associated with oak CPOM.

The microbial biomass, expressed as ATP, for the red maple CPOM, remained relatively constant over a period of 15 to 44 days; however, a modest increase in ATP occurred during the latter stage of the study period (days 34 to 44). The mean ATP concentration was about 15,000 pg ATP cm^{-2} of leaf surface and ranged from 5820 pg to 20,586 pg. The mean biomass (as ATP) estimated for the red maple CPOM was approximately 3.5-fold and 4.5-fold greater than the ungrazed and grazed microbiota, respectively, on the white oak CPOM.

The biomass, as ATP, and bacterial cell density associated with both the ungrazed and grazed oak CPOM remained relatively constant during the 69-day period examined (colonization period, days 112 to 191). The microbial community on the oak CPOM, therefore, was in a steady-state. The ungrazed CPOM microbiota had a significantly greater biomass (ATP) and bacterial density than did the grazed microbial community. The ungrazed microbiota on oak CPOM had a mean ATP biomass of approximately 4200 pg ATP cm^{-2} of leaf

surface, and a mean bacterial density of 2.37×10^7 cells cm^{-2} of leaf surface, whereas the grazed microbial community had a mean ATP biomass of approximately 3300 pg ATP cm^{-2} of leaf surface, and a mean bacterial cell density of 1.40×10^7 cells cm^{-2} of leaf surface.

ATP content per bacterium was used as an index of the physiological status of the microbiota associated with the oak CPOM. The microbiota of the ungrazed oak CPOM had a calculated mean ATP content per cell of approximately 0.19 fg ATP bacterium $^{-1}$, while the grazed CPOM microbiota had 0.25 fg ATP bacterium $^{-1}$. This suggests that the grazed microbial community was metabolically more active than the ungrazed microbiota.

Bacteria were the first population to colonize the leaf CPOM. The fungal population was next to develop and then subsequently declined, while the bacterial population continued to be present.

The heterotrophic community was enclosed in a polysaccharide matrix (glycocalyx) which increased with residence time in the stream. The development of the glycocalyx has important implications concerning the availability of phosphate for utilization by the microbiota with the glycocalyx.

The kinetic data for the maple and oak studies indicate that the microbiota associated with CPOM were not metabolically very active and were slowly growing. The calculated generation time was 12 days for the grazed oak microbiota and 32 days for the ungrazed oak microbiota. The microbial community associated with the maple CPOM recycled phosphate about two-fold faster than the oak microbiota,

and it should be noted that the maple microbiota were much younger relative to the oak microbiota.

The presence of snails significantly reduced the amount of phosphate accumulated by the microbiota on an area-specific basis, but snail grazing significantly increased the amount of cell-specific phosphate accumulated. Grazing of the oak microbiota by snails also stimulated the microbial activity as evidenced by the elevated biomass-specific phosphorus turnover and incorporation rates for the intracellular phosphorus pools (L-P, MP-P, RNA-P, DNA-P). The microbiota recycled phosphorus about two-fold greater per cell in the presence of snails; however, the increased recycling was not enough to counter-balance the reduction in biomass. Thus, on an area-specific basis the grazed microbiota did not significantly recycle phosphorus at a greater rate than the ungrazed microbiota.

VIII. CONCLUSIONS

The general conclusions that can be drawn from this investigation are:

1. The microbial community was principally composed of bacterial and fungal populations which were enclosed in a glycocalyx matrix. The bacteria were the first colonizers of the CPOM followed by the fungi.
2. The microbiota are slowly growing (generation time 12 days to 32 days) and are not metabolically very active.
3. Snail grazing reduces the microbial biomass and increases the metabolic activity and generation time of the community.
4. The microbiota associated with CPOM seems to play a damping or buffering role, slowly releasing phosphorus, and slowing down the loss of phosphorus from the ecosystem.
5. As a result of the reduced retention of phosphorus due to grazing, the spiraling length is increased indicating a decrease in the efficiency of phosphorus utilization.
6. The developmental age of the microbiota associated with CPOM is inversely related to phosphorus spiraling, i.e., the younger the community, the shorter the spiraling length.

LIST OF REFERENCES

Ball, R. C., and F. F. Hooper. 1963. Translocation of phosphorus in a trout stream ecosystem. In: Radioecology, eds. V. Schultz and A. W. Klement, Jr., Reinhold, NY. pp. 217-228.

Bärlocher, F., and B. Kendrick. 1973. Fungi in the diet of Gammarus pseudolimnaeus (Amphipoda). Oikos 24: 295-300.

Bärlocher, F., and B. Kendrick. 1974. Dynamics of the fungal population on leaves in a stream. J. Ecology 62(3): 761-791.

Barsdate, R. J., and R. T. Prentki. 1974. Phosphorus cycle of model ecosystems; significance for decomposer food chains and effect of bacterial grazers. Oikos 25: 239-251.

Beever, R. E., and D.J.W. Burns. 1980. Phosphorus uptake, storage and utilization by fungi. In: Advances in Botanical Research. Academic Press, Inc., London 8: 127-219.

Berg, B. 1975. Cellulase location in Cellvibrio fulvus. Can. J. Microbiol. 21: 51-57.

Berman, T., and G. W. Skyring. 1979. Phosphorus cycling in aquatic microorganisms studied by phased uptake of ³³P and ³²P. Current Microbiology 2: 47-49.

Boling, R. H., Jr., E. D. Goodman, J. A. Van Sickle, J. O. Zimmer, K. W. Cummins, R. C. Petersen, and S. R. Reice. 1975. Toward a model of detritus processing in a woodland stream. Ecology 56: 141-151.

Bolton, E. T., R. J. Britten, D. B. Cowie, E. H. Creaser, and R. B. Roberts. Carnegie Institution of Washington Yearbook 1955-1956. pp. 110-136.

Bott, T. L., L. A. Kaplan, and F. T. Kuserk. 1984. Benthic bacterial biomass supported by streamwater dissolved organic matter. Microb. Ecol. 10: 335-344.

Brown, E. J., and R. F. Harris. 1978. Kinetics of algal transient phosphate uptake and the cell quota concept. Limnol. Oceanogr. 23(1): 35-40.

Brown, E. J., R. F. Harris, and J. F. Koonce. 1978. Kinetics of phosphate uptake by aquatic microorganisms: Deviations from a simple Michaelis-Menten equation. Limnol. Oceanogr. 23(1): 26-34.

Burmaster, D. E., and S. E. Chisholm. 1979. A comparison of two methods for measuring phosphate uptake by Monochrysis lutheri droop grown in continuous culture. *J. Exp. Mar. Biol. Ecol.* 39: 187-202.

Cavari, B. 1976. ATP in Lake Kinneret: Indicator of microbial biomass or of phosphorus deficiency? *Limnol. Oceanogr.* 21(2): 231-236.

Chen, M. 1974. Kinetics of phosphorus absorption by Corynebacterium bovis. *J. Microb. Ecol.* 1(3): 164-175.

Cooper, D. C. 1973. Enhancement of net primary productivity by herbivore grazing in aquatic laboratory microcosms. *Limnol. Oceanogr.* 18: 31-37.

Costerton, J. W. 1984. Mechanisms of microbial adhesion to surfaces. In: *Current Perspectives in Microbial Ecology*, eds. M. J. Klug and C. A. Reddy. Amer. Soc. Microbiol.

Cowen, W. F., and G. F. Lee. 1973. Leaves as source of phosphorus. *Environm. Sci. Technol.* 7: 53-54.

Cuhel, R. L., H. W. Janasch, and C. D. Taylor. 1983. Microbial growth and macromolecular synthesis in the northwestern Atlantic Ocean. *Limnol. Oceanogr.* 29(1): 1-18.

Cuhel, R. L., and J. B. Waterbury. 1984. Biochemical composition and short term nutrient incorporation patterns in a unicellular marine cyanobacterium, Synechococcus (WH7803). *Limnol. Oceanogr.* 29(2): 370-374.

Cummins, K. W. 1974. Structure and function of stream ecosystems. *Bioscience* 24: 631-641.

Currier, D. J., and J. Kalff. 1984. The relative importance of bacterioplankton and phytoplankton phosphorus uptake in freshwater. *Limnol. Oceanogr.* 29: 311-321.

Daley, R. J., and J. E. Hobbie. 1975. Direct counts of aquatic bacteria by a modified epifluorescence technique. *Limnol. Oceanogr.* 20: 875-882.

Davis, J. W. 1985. Biological mediated removal of dissolved organic carbon from coal slurry wastewater. Ph.D. Dissertation, Univ. of Tennessee, Knoxville.

Dawes, E. A., and P. J. Senior. 1973. The role and regulation of energy reserve polymers in microorganisms. In: *Advances in Microbial Physiology*. A. H. Rose and D. W. Tempest, eds. Academic Press, London and New York. 10: 135-266.

Downes, M. T., and H. W. Paerl. 1978. Separation of two dissolved reactive phosphorus fractions in lake water. *J. Fish. Res. Br. Can.* 35(12): 1636-1639.

Elwood, J. W., and D. J. Nelson. 1972. Periphyton production and grazing rates in a stream measure with a ^{32}P material balance method. *Nikos* 23: 295-303.

., J. D. Newbold, R. V. O'Neil, R. W. Stark, and P. T. Singley. 1981. The role of microbes associated with organic and inorganic substrates in phosphorus spiralling in a woodland stream. *Verh. Int. Ver. Limnol.* 21: 818-824.

Elwood, J. W., J. D. Newbold, A. F. Trimble, and R. W. Stark. 1981. The limiting role of phosphorus in a woodland stream ecosystem: Effects of P enrichment on leaf decomposition and primary producers. *Ecology* 62(1): 146-158.

Elwood, J. W., J. D. Newbold, R. V. O'Neil, and W. Van Winkle. 1983. Resource spiralling: An operation paradigm for analyzing lotic ecosystems. In: *The Dynamics of Lotic Ecosystems*. DOE Symposium Series, eds. R. D. Fontaine III and S. M. Bartell, Ann Arbor Science Publisher.

Eppley, R. W., et al. 1973. A study of plankton dynamics and nutrient cycling in the central gyre of N. Pacific Ocean. *Limnol. Oceanog.* 18: 534.

Fairchild, J. F., T. P. Boyd, E. Robinson-Wilson, and J. R. Jones. 1983. Microbial action in detrital leaf processing and the effects of chemical perturbation. In: *Dynamics of Lotic Ecosystems*, T. D. Fontaine III and S. M. Bartell, eds. Ann Arbor Science Publishers, Ann Arbor, Michigan.

Faust, M. A., and D. L. Correll. 1977. Autoradiographic study to detect metabolically active phytoplankton and bacteria in the Rhode River Estuary. *Marine Biol.* 41: 293-305.

Fenchel, T., and P. Harrison. 1976. The significance of bacterial grazing and mineral cycling for the decomposition of particulate detritus. In: *The Role of Terrestrial and Aquatic Organisms in Decomposition Processes*, J. M. Anderson and A. Macfadyen, eds. Blackwell Scientific Publication, Oxford, England.

Fisher, S. G., and G. E. Likens. 1972. Stream ecosystem: Organic energy budget. *Bioscience* 22: 33-35.

Francko, D. A., and R. T. Heath. 1979. Functionally distinct classes of complex phosphorus compounds in lake water. *Limnol. Oceanogr.* 24(3): 463-473.

Francko, D. A., and R. T. Heath. 1982. UV-sensitive complex phosphorus: Association with dissolved humic material and iron in a bog lake. *Limnol. Oceanogr.* 27(3): 564-569.

Fuhrman, J. A., and F. Azam. 1982. Thymidine incorporation as a measure of heterotrophic bacterioplankton production in marine surface waters: Evaluation and field results. *Marine Biology* 66: 109-120.

Fuhs, G. W. 1969. Phosphorus content and rate of growth in the diatoms Cyclotella nana and Thalassiosira fluviatilis. *J. Phycol.* 5: 412-421.

Fuhs, G. W., and E. Canelli. 1970. Phosphorus-33 autoradiography used to measure phosphate uptake by individual algae. *Limnol. Oceanogr.* 15: 962-967.

Garen, A., and C. Levinthal. 1960. A five structure genetic and chemical study of the enzyme alkaline phosphatase of E. coli I. Purification and characterization of alkaline phosphatase. *Biochem. Biophys. Acta* 38: 470-483.

Geesey, G. G., W. T. Richardson, H. G. Yeomans, R. T. Irvin, and J. W. Costerton. 1977. Microscopic examination of natural sessile bacterial populations from an alpine stream. *Can. J. Microbiol.* 23(12): 1733-1736.

Geesey, G. G., R. Mutch, J. W. Costerton, and R. B. Green. 1978. Sessile bacteria: An important component of the microbial population in small mountain streams. *Limnol. Oceanogr.* 23(6): 1214-1223.

Gray, T.R.G. 1976. Survival of vegetative microbes in soil. In: *The Survival of Vegetative Microbes*. T.R.G. Gray and J. R. Postgate, eds. Cambridge University Press. pp. 327-364.

Green, D. B., T. J. Logan, and N. E. Smeck. 1978. Phosphate adsorption-desorption characteristics of suspended sediments in the Maumee River Basin of Ohio. *J. Environ. Qual.* 7(2): 208-212.

Gregory, S. V. 1978. Phosphorus dynamics on organic and inorganic substrates in streams. *Verh. Internat. Verin. Limnol.* 20: 1340-1346.

Hagstrom, A., U. Larsson, P. Horstedt, and S. Normak. 1979. Frequency of dividing cells, a new approach to the determination of bacterial growth rates in aquatic environments. *Appl. Environm. Microbiol.* 37: 805-812.

Hamilton, R. D., and O. Holm-Hansen. 1967. Adenosine triphosphate content of marine bacteria. *Limnol. Oceanogr.* 12: 319-324.

Hanson, R. S., and J. A. Phillips. 1981. Chemical composition. In: *Manual of Methods for General Bacteriology*. American Society for Microbiology, Washington, D.C.

Hargrave, B. T. 1970. The utilization of benthic microflora by Hyalella azteca (Amphipoda). *J. Anim. Ecol.* 39: 427-437.

Hargrave, B. T. 1972. Aerobic decomposition of sediment and detritus as a function of particle surface area and organic content. *Limnol. Oceanogr.* 17(4): 583-596.

Harold, F. M. 1963. Accumulation of inorganic polyphosphate in Aerobacter aerogenes. I. Relationship to growth and nucleic acid synthesis. *J. Bacteriol.* 86: 216-221.

Harold, F. M., and S. Sylvan. 1963. Accumulation of inorganic polyphosphate in Aerobacter aerogenes. II. Environmental control and the role of sulfur compounds. *J. Bacteriol.* 86: 222-231.

Harold, F. M. 1966. Inorganic polyphosphates in biology: Structure, metabolism, and function. *Bacteriol. Rev.* 30(4): 772-794.

Hawkes, H. A. 1975. River Zonation and Classification in River Ecology. B. A. Whitton, ed. Univ. California Press, Berkeley and Los Angeles, CA.

Helwig, J. T., and K. A. Council (eds.). 1982. Statistical Analysis System. SAS Institute, Inc., Cary, North Carolina.

Hill, A. R. 1982. Phosphorus and major cation mass balances for two rivers during low summer flows. *Freshwater Biol.* 12: 293-304.

Hobbie, J. E., and C. C. Crawford. 1969. Respiration corrections for bacterial uptake of dissolved organic compounds in natural waters. *Limnol. Oceanogr.* 14: 528-532.

Holm-Hansen, O., W. H. Sutcliffe, Jr., and J. Sharp. 1968. Measurement of deoxyribonucleic acid in the ocean and its ecological significance. *Limnol. Oceanogr.* 13: 501-514.

Holm-Hansen, O. 1970. ATP levels in algal cells as influenced by environmental conditions. *Plant and Cell Physiol.* 11: 689-700.

Hynes, H.B.N. 1961. The invertebrate fauna of a Welsh mountain stream. *Arch. Hydrobiol.* 57: 344-388.

Hynes, H.B.N. 1963. Imported organic matter and secondary productivity in streams. *Internat. Congr. Zool., Proc. 16th.* 4: 324-329.

Jackson, T. A., and D. W. Schindler. 1975. The biogeochemistry of phosphorus in an experimental lake environment: Evidence for the formation of humic-metal-phosphate complexes. *Verh. Internat. Verein. Limnol.* 19: 211-221.

Johannes, R. E. 1965. Influence of marine protozoa on nutrient regeneration. *Limnol. Oceanogr.* 10: 443-450.

Johnson, J. L. 1981. Genetic Characterization. In: *Manual of Methods for General Bacteriology*. American Society for Microbiology, Washington, D.C.

Jordan, M. J., and G. E. Likens. 1980. Measurement of planktonic bacterial production in an oligotrophic lake. *Limnol. Oceanogr.* 25(4): 719-732.

Karl, D. M. 1979. Measurement of microbial activity and growth in the ocean by rates of stable ribonucleic acid synthesis. *Appl. Environm. Microbiol.* 38(5): 850-860.

Karl, D. M. 1980. Cellular nucleotide measurements and applications in microbial ecology. *Microbiol. Rev.* 44(4): 739-796.

Karl, D. M., C. D. Winn, and D.C.L. Wong. 1981. RNA synthesis as a measure of microbial growth in aquatic environments. I. Evaluation, verification and optimization of methods. *Marine Biology* 64: 1-12.

Kaushik, N. K., and H.B.N. Hynes. 1968. Experimental study on the role of autumn-shed leaves in aquatic environments. *J. Ecol.* 56: 229-243.

Kaushik, N. K., and H.B.N. Hynes. 1971. The fate of the dead leaves that fall into streams. *Arch. Hydrobiol.* 68: 465-515.

King, J. D., and D. C. White. 1977. Muramic acid as a measure of microbial biomass in estuarine and marine samples. *Appl. Environm. Microbiol.* 33(4): 777-783.

King, J. D., D. C. White, and C. W. Taylor. 1977. Use of lipid composition and metabolism to examine structure and activity of estuarine detrital microflora. *Appl. Environm. Microbiol.* 33(5): 1177-1183.

Koch, A. 1962. The evaluation of the rates of biological processes from tracer kinetic data. I. The influence of labile metabolic pools. *J. Theoret. Biol.* 3: 283-303.

Kubitschek, H. E., and M. L. Freedman. 1971. Chromosome replication and the division cycle of Escherichia coli B/r. *J. Bacteriol.* 107(1): 95-99.

Ladd, T. I., J. W. Costerton, and G. G. Geesey. 1979. Determination of the heterotrophic activity of epilithic microbial populations. In: *Native Aquatic Bacteria: Enumeration, Activity, and Ecology*. ASTM STP 695, J. W. Costerton and R. R. Colwell, eds. American Society for Testing Materials. pp. 180-195.

La Motta, E. J. 1976a. Kinetics of growth and substrate uptake in a biological film system. *Appl. Environm. Microbiol.* 32(2): 286-293.

La Motta, E. J. 1976b. Internal diffusion and reaction in biological films. *Environm. Sci. and Technol.* 10(8): 765-769.

Lang, W. K., K. Glassey, and A. R. Archibald. 1982. Influence of phosphate supply on teichoic acid and teichuronic acid content of Bacillus subtilis cell walls. *J. Bacteriol.* 151(1): 367-375.

Lange, W. 1976. Speculations on a possible essential function of the gelatinous sheath of blue-green algae. *Can. J. Microbiol.* 22: 1181-1185.

Lean, D.R.S. 1973a. Movements of phosphorus between its biologically important forms in lake water. *J. Fish. Res. Brd. Can.* 30: 1525-1536.

Lean, D.R.S. 1973b. Phosphorus dynamics in lake water. *Science* 179: 678-680.

Lean, D.R.S., and C. Nalewajko. 1976. Phosphate exchange and organic phosphorus excretion by freshwater algae. *J. Fish. Res. Brd. Can.* 33: 1312-1323.

Lean, D.R.S., and E. White. 1983. Chemical and radiotracer measurements of phosphorus uptake by lake plankton. *Can. J. Fish. Aquat. Sci.* 40: 147-155.

Lehman, J. T. 1980. Release and cycling of nutrients between planktonic algae and herbivores. *Limnol. Oceanogr.* 25: 620-632.

Lien, T., and G. Knutsen. 1973. Phosphate as a control factor in cell division of Chlamydomonas reinhardtii, studied in synchronous culture. *Exptl. Cell Res.* 78: 79-88.

Lock, M. A., et al. 1984. River epilithon: Toward a structural-functional model. *Oikos* 42: 10-22.

Lorenz, M. G., B. W. Aardema, and W. E. Krumbein. 1981. Interaction of marine sediment with DNA and DNA availability to nucleases. *Mar. Biol.* 64: 225-230.

Lutkenhaus, J., J. Ryan, and M. Konrad. 1973. Kinetic of phosphate incorporation into adenosine triphosphate and guanosine triphosphate in bacteria. *J. Bacteriol.* 116: 1113-1123.

Maaløe, O., and N. O. Kjeldgaard. 1966. Control of macromolecular synthesis. A study of DNA, RNA, and protein synthesis in bacteria. W. A. Benjamin, Inc., New York.

Mackie, E. B., K. N. Brown, J. Lam, and J. W. Costerton. 1979. Morphological stabilization of capsules of group B streptococci, types Ia, Ib, II, and III, with specific antibody. *J. Bacteriol.* 138(2): 609-617.

McCallister, D. L., and T. J. Logan. 1978. Phosphate adsorption-desorption characteristics of soils and bottom sediments in the Maumee River Basin of Ohio. *J. Environ. Qual.* 7(1): 87-92.

Meyer, J. L. 1979. The role of sediments and bryophytes in phosphorus dynamics in a headwater stream ecosystem. *Limnol. Oceanogr.* 24(2): 365-375.

Meyer, J. L., and G. E. Likens. 1979. Transport and transformation of phosphorus in a forest stream ecosystem. *Ecology* 60(6): 1255-1269.

Meyer, J. L. 1980. Dynamics of phosphorus and organic matter during leaf decomposition in a forest stream. *Oikos* 34: 44-53.

Meyer-Reil, L-A. 1978. Autoradiography and epifluorescence microscopy combined for the determination of number and spectrum of actively metabolizing bacteria in natural waters. *Appl. Environm. Microbiol.* 36(3): 506-512.

Minear, R. A. 1972. Characterization of naturally occurring dissolved organophosphorus compounds. *Environ. Sci. Technol.* 6(5): 431-437.

Minshall, G. W. 1967. Role of allochthonous detritus in the trophic structure of a woodland springbrook community. *Ecology* 48(1): 139-149.

Minshall, G. W., R. C. Petersen, K. W. Cummins, T. L. Bott, J. R. Sedell, C. E. Cushing, and R. L. Vannote. 1983. Interbiome comparison of stream ecosystem dynamics. *Ecol. Monogr.* 53(1): 1-25.

Mitchell, P., and J. Moyle. 1953. Paths of phosphate transfer in Micrococcus pyogenes: Phosphate turnover in nucleic acids and other fractions. *J. Gen. Microbiol.* 9: 257-272.

Mitchell, P., and J. Moyle. 1954. The gram reaction and cell composition: Nucleic acids and other phosphate fractions. *J. Gen. Microbiol.* 10: 533-540.

Morrison, S. J., J. D. King, R. J. Bobbie, R. E. Bechtold, and D. C. White. 1977. Evidence for microfloral succession on allochthonous plant litter in Apalachicola Bay, Florida, USA. *Marine Biol.* 41: 229-240.

Morrison, S. J., and D. C. White. 1980. Effects of grazing by estuarine gammaridean amphipods on the microbiota of allochthonous detritus. *Appl. Environm. Microbiol.* 40(3): 659-671.

Mulholland, P. J., J. D. Newbold, J. W. Elwood, and C. L. Hom. 1983. The effect of grazing intensity on phosphorus spiraling in autotrophic streams. *Oecologia* 58: 358-366.

Mulholland, P. J., J. W. Elwood, J. D. Newbold, J. R. Webster, L. A. Ferren, and R. E. Perkins. 1984. Phosphorus uptake by decomposing leaf detritus: Effect of microbial biomass and activity. *Verh. Internat. Verein. Limnol.* 22: 1899-1905.

Mulholland, P. J., J. D. Newbold, J. W. Elwood, and L. A. Ferren. 1985. Phosphorus spiraling in a woodland stream: Seasonal variations. *Ecology* 66(3): 1012-1023.

Murphy, J., and J. P. Riley. 1962. A modified single solution method for the determination of phosphate in natural waters. *Analytica Chimica Acta* 27: 31-36.

Nannipieri, P., R. L. Johnson, and E. A. Paul. 1978. Criteria for measurement of microbial growth and activity in soil. *Soil Biol. Biochem.* 10: 223-229.

Nelson, D. J., and D. C. Scott. 1962. Role of detritus in the productivity of a rock-outcrop community in a piedmont stream. *Limnol. Oceanogr.* 7: 396-413.

Nelson, D. J., N. R. Kevern, J. L. Wilhm, and N. A. Griffith. 1969. Estimates of periphyton mass and stream bottom area using phosphorus-32. *Water Res.* 3: 367-373.

Newbold, J. D., J. W. Elwood, R. V. O'Neil, and W. Van Winkle. 1981. Measuring nutrient spiraling in streams. *Can. J. Fish. Aquat. Sci.* 38(7): 860-863.

Newbold, J. D., J. W. Elwood, R. V. O'Neil, and A. L. Sheldon. 1983. Phosphorus dynamics in a woodland stream ecosystem: A study of nutrient spiraling. *Ecology* 64(5): 1249-1265.

Newell, S. Y., and R. R. Christian. 1981. Frequency of dividing cells as an estimator of bacterial productivity. *Appl. Environm. Microbiol.* 42(1): 23-31.

Newman, R. H., and K. R. Tate. 1980. Soil phosphorus characterization by ³¹P nuclear magnetic resonance. *Commun. Soil Sci. and Plant Anal.* 11(9): 835-842.

Nuzback, D. E., E. E. Bartley, S. M. Dennis, T. G. Nagaraja, S. J. Galitzer, and A. D. Dayton. 1983. Relation of rumen ATP concentration to bacterial and protozoal numbers. *Appl. Environm. Microbiol.* 46(3): 533-538.

Odum, E. E., P. W. Kirk, and J. C. Zieman. 1979. Non-protein nitrogen compounds associated with particles of vascular plant detritus. *Oikos* 32: 363-367.

Overbeck, V. J., and D. Toth. 1978. The influence of phosphate on the uptake rate of glucose in bacteria. *Arch. Hydrobiol.* 82: 114-122.

Paerl, H. W. 1974. Bacterial uptake of dissolved organic matter in relation to detrital aggregation in marine and freshwater systems. *Limnol. Oceanogr.* 19(6): 966-972.

Paerl, H. W., and D.R.S. Lean. 1976. Visual observation of phosphorus movement between algae, bacteria, and abiotic particles in lake waters. *J. Fish. Res. Bd. Can.* 33: 2805-2813.

Paerl, H. W., and M. T. Downes. 1978. Biological availability of low versus high molecular weight reactive phosphorus. *J. Fish. Res. Bd. Can.* 35(12): 1639-1643.

Paerl, H. W., and S. M. Merkel. 1982. Differential phosphorus assimilation in attached vs. unattached microorganisms. *Arch. Hydrobiol.* 93: 125-134.

Parsons, T. R., and J.D.H. Strickland. 1962. On the production of particulate organic carbon by heterotrophic processes in sea water. *Deep Sea Res.* 8: 211-222.

Patterson, H., R. Irvin, J. W. Costerton, and K. J. Cheng. 1975. Ultrastructure and adhesion properties of Ruminococcus albus. *J. Bacteriol.* 122(1): 278-287.

Paul, R. W., Jr., D. L. Kuhn, J. L. Plafkin, J. Cairns, Jr., and J. G. Croxdale. 1977. Evaluation of natural and artificial substrate colonization by scanning electron microscopy. *Trans. Amer. Micros. Soc.* 96(4): 506-519.

Perry, M. J., and R. W. Eppley. 1981. Phosphorus uptake by phytoplankton in central N. Pacific Ocean. *Deep Sea Res.* 28: 39.

Peters, R. H. 1977. Availability of atmospheric orthophosphate. *J. Fish. Res. Brd. Can.* 34: 918-924.

Peters, R. H. 1978. Concentrations and kinetics of phosphorus fractions in water from streams entering Lake Memphremagog. *J. Fish. Res. Brd. Can.* 35: 315-328.

Petersen, R. C., and K. W. Cummins. 1974. Leaf processing in a woodland stream. *Freshwat. Biol.* 4: 343-368.

Pomeroy, L. R. 1960. Residence time of dissolved phosphate in natural waters. *Science* 131(3415): 1731-1732.

Reice, S. R. 1974. Environmental patchiness and the breakdown of leaf litter in a woodland stream. *Ecology* 55: 1271-1282.

Rhee, G-Yull. 1972. Competition between an alga and an aquatic bacterium for phosphate. *Limnol. Oceanogr.* 17(4): 505-514.

Riemann, B., J. Fuhrman, and F. Azam. 1982. Bacterial secondary production in freshwater measured by 3-H-thymidine incorporation method. *Microb. Ecol.* 8: 101-114.

Rigler, F. H. 1956. A tracer study of the phosphorus cycle in lake water. *Ecology* 37(3): 550-562.

Rigler, F. H. 1964. The phosphorus fractions and the turnover time of inorganic phosphorus in different types of lakes. *Limnol. Oceanogr.* 9: 511-518.

Rigler, F. H. 1966. Radiobiological analysis of inorganic phosphorus in lake water. *Int. Ver. Theor. Angew. Limnol. Verh.* 16: 465-470.

Roberts, R. B., D. B. Cowie, P. H. Ableson, E. T. Bolton, and R. J. Britten. 1957. Studies of biosynthesis in *Escherichia coli*. Carnegie Inst. of Washington, Publication 607, Washington, D.C.

Rodina, A. G. 1963. Microbiology of detritus of lakes. *Limnol. Oceanogr.* 8: 388-393.

Sayler, G. S., L. C. Lund, M. P. Shiaris, T. W. Sherrill, and R. E. Perkins. 1979. Comparative effects of Aroclor 1254 (polychlorinated biphenyls) and phenanthrene on glucose uptake by freshwater microbial populations. *Appl. Environm. Microbiol.* 37: 878-885.

Schumacher, G. J., and L. A. Whitford. 1965. Respiration of 32-P uptake in various species of freshwater algae as affected by a current. *J. Phycol.* 1: 78-80.

Shilo, M. 1970. Lysis of Blue-Green algae by Myxobacter. *J. Bacteriol.* 104(1): 453-461.

Slack, K. V., and H. R. Feltz. 1968. Tree leaf control on low flow water quality in a small Virginia stream. *Environm. Sci. Technol.* 2: 126-131.

Smith, G. A., J. S. Nickels, W. M. Davis, R. F. Martz, R. H. Findlay, and D. C. White. 1982. Perturbations in the biomass, metabolic activity, and community structure of the estuarine detrital microbiota: Resource partitioning in amphipoda grazing. *J. Exp. Mar. Biol. Ecol.* 64: 125-165.

Sober, H. A., ed. 1970. CRC Handbook of Biochemistry, Selected Data for Molecular Biology. The Chemical Rubber Co., Cleveland, Ohio.

Sokal, R. R., and F. J. Rohlf. 1969. Biometry. W. H. Freeman and Co., San Francisco.

Stumm, W., and J. J. Morgan. 1970. Aquatic chemistry: An introduction emphasizing chemical equilibrium in natural waters. Wiley-Interscience, New York.

Suberkropp, K. F., and M. J. Klug. 1974. Decomposition of deciduous leaf litter in a woodland stream. I. A scanning electron microscopic study. *Microbial Ecol.* 1: 96-113.

Suberkropp, K. F., and M. J. Klug. 1976(a). Fungi and bacteria associated with leaves during processing in a woodland stream. *Ecology* 57(4): 707-719.

Suberkropp, K. F., G. L. Godshalk, and M. J. Klug. 1976(b). Changes in the chemical composition of leaves during processing in a woodland stream. *Ecology* 57: 720-727.

Suberkropp, K. F., and M. J. Klug. 1980. The maceration of deciduous leaf litter by aquatic hyphomycetes. *Can. J. Bot.* 58: 1025-1031.

Swick, R. W., A. L. Koch, and D. T. Handa. 1956. The measurement of nucleic acid turnover in rat liver. *Arch. Biochem. Biophys.* 63: 226-242.

Taylor, A. R. 1946. Chemical analysis of the T2 bacteriophage and its host, Escherichia coli (B strain). *J. Biol. Chem.* 165: 271-284.

Tobin, R. S., and D.H.J. Anthony. 1978. Tritiated thymidine incorporation as a measure of microbial activity in lake sediments. *Limnol. Oceanogr.* 23: 161-165.

Torriani, A. 1960. Influence of inorganic phosphate in the formation of phosphatases by Escherichia coli. *Biochim. Biophys. Acta* 38: 460-469.

Triska, F. J., J. R. Sedell, and B. Buckley. 1975. The processing of conifer and hardwood leaves in two coniferous forest streams: II. Biochemical and nutrient changes. *Verh. Internat. Verein. Limnol.* 19: 1628-1639.

Van Es, F. B., and L.-A. Meyer-Reil. 1982. Biomass and metabolic activity of heterotrophic marine bacteria. In: *Advances in Microbial Ecology*, Vol. 6. K. C. Marshall, ed. Plenum Press, New York. pp. 111-170.

Vannote, R. L., G. W. Minshall, K. W. Cummins, J. R. Sedell, and C. E. Cushing. 1980. The river continuum concept. *Can. J. Fish. Aquat. Sci.* 37: 130-137.

Webster, J. R. 1975. Analysis of potassium and calcium dynamics in stream ecosystems on three southern Appalachian watersheds of contrasting vegetation. Ph.D. dissertation, Univ. of Georgia, Athens, GA.

Webster, J. R., and B. C. Patten. 1979. Effects of watershed perturbation on stream potassium and calcium dynamics. *Ecol. Monogr.* 49: 51-72.

Wetzel, R. G. 1975. Limnology. W. B. Saunders Co. Philadelphia, PA. p. 743.

Wetzel, R. G., and G. E. Likens. 1979. Limnological Analysis. W. B. Saunders Co., Philadelphia, PA.

White, D. C., R. J. Bobbie, S. J. Morrison, D. K. Oosterhof, C. W. Taylor, and D. A. Meeter. 1977. Determination of microbial activity of estuarine detritus by relative rates of lipid biosynthesis. *Limnol. Oceanogr.* 22(6): 1089-1099.

White, E., and G. Payne. 1980. Distribution and biological availability of reactive high molecular weight phosphorus in natural waters in New Zealand. *Can. J. Fish. Aquat. Sci.* 37: 664-669.

White, E., G. Payne, S. Pickmere, and F. R. Pick. 1981. Orthophosphate and its flux in lake waters. *Can. J. Fish. Aquat. Sci.* 38: 1215-1219.

White, E., G. Payne, S. Pickmere, and F. R. Pick. 1982. Factors influencing orthophosphate turnover times: A comparison of Canadian and New Zealand lakes. *Can. J. Fish. Aquat. Sci.* 39: 469-474.

White, D. C. 1983. Analysis of microorganisms in terms of quantity and activity in natural environments. In: *Microbes in their natural environments. Symposium 34.* J. H. Slater, R. Whittenbury and J.W.T. Wimpenny, eds. Society for General Microbiology Ltd., Cambridge University Press.

Whitford, L. A., and G. J. Schumacher. 1961. Effect of current on mineral uptake and respiration by a freshwater alga. *Limnol. Oceanogr.* 6: 423-425.

Whitford, L. A., and G. J. Schumacher. 1964. Effect of a current on respiration and mineral uptake in Spirogyra and Oedogonium. *Ecology* 45(1): 168-170.

Wilson, C. A., L. H. Stevenson, and T. H. Chrzanowski. 1981. The contribution of bacteria to the total adenosine triphosphate extracted from the microbiota in the water of a salt-marsh creek. *J. Exp. Mar. Biol. Ecol.* 50: 183-195.

Wimpenny, J.W.T. 1981. Spatial order in microbial ecosystems. *Biol. Rev.* 56: 295-343.

Wright, R. T., and J. E. Hobbie. 1965. The uptake of organic solutes in lake water. *Limnol. Oceanogr.* 10: 22-28.

INTERNAL DISTRIBUTION

1. S. I. Auerbach	17. R. V. O'Neill
2. S. M. Bartell	18. A. V. Palumbo
3. H. L. Boston	19. W. M. Post
4. D. L. DeAngelis	20. D. E. Reichle
5-9. J. W. Elwood	21. A. J. Stewart
10. C. W. Gehrs	22. W. Van Winkle
11. S. G. Hildebrand	23. Central Research Library
12. M. A. Huston	24-38. ESD Library
13. D. W. Johnson	39-40. Laboratory Records Department
14. B. L. Kimmel	41. Laboratory Records, RC
15. J. M. Loar	42. ORNL Patent Office
16. P. J. Mulholland	43. ORNL Y-12 Technical Library

EXTERNAL DISTRIBUTION

44. Dewey Bunting, Graduate Program in Ecology, The University of Tennessee, Knoxville, TN 37916
45. J. Thomas Callahan, Associate Director, Ecosystem Studies Program, Room 336, 1800 G Street, NW, National Science Foundation, Washington, DC 20550
46. C. E. Cushing, Ecosystems Department, Battelle-Northwest Laboratories, Richland, WA 99352
47. G. J. Foley, Office of Environmental Process and Effects Research, U.S. Environmental Protection Agency, 401 M Street, SW, RD-682, Washington, DC 20460
48. C. R. Goldman, Professor of Limnology, Director of Tahoe Research Group, Division of Environmental Studies, University of California, Davis, CA 94616
49. J. W. Huckabee, Manager, Ecological Studies Program, Electric Power Research Institute, 3412 Hillview Avenue, P.O. Box 10412, Palo Alto, CA 94303
50. George Y. Jordy, Director, Office of Program Analysis, Office of Energy Research, ER-30, G-226, U.S. Department of Energy, Washington, DC 20545
51. Harry Leland, Department of the Interior, Geological Survey, 345 Middlefield Road, Menlo Park, CA 94025
52. Helen McCammon, Director, Ecological Research Division, Office of Health and Environmental Research, Office of Energy Research, MS-E201, ER-75, Room E-233, Department of Energy, Washington, DC 20545
53. J. Denis Newbold, Stroud Water Research Center, Avondale, PA 19311
- 54-58. R. E. Perkins, Department of Microbiology, School of Medicine, East Carolina University, Greenville, NC 27834
59. Irwin Remson, Department of Applied Earth Sciences, Stanford University, Stanford, CA 94305

- 60-64. Gary S. Sayler, Department of Microbiology, The University of Tennessee, Knoxville, TN 37916
65. R. J. Stern, Director, Office of Environmental Compliance, MS PE-25, FORRESTAL, U.S. Department of Energy, 1000 Independence Avenue, SW, Washington, DC 20585
66. Wayne T. Swank, Coweeta Hydrologic Laboratory, U.S. Forest Service, Franklin, NC 28734
67. Jackson R. Webster, Biology Department, Virginia Polytechnic Institute and State University, Blacksburg, VA 24060
68. Leonard H. Weinstein, Program Director of Environmental Biology, Cornell University, Boyce Thompson Institute for Plant Research, Ithaca, NY 14853
69. Raymond G. Wilhour, Chief, Air Pollution Effects Branch, Corvallis Environmental Research Laboratory, U.S. Environmental Protection Agency, 200 SW 35th Street, Corvallis, OR 97330
70. Frank J. Wobber, Ecological Research Division, Office of Health and Environmental Research, Office of Energy Research, MS-E201, Department of Energy, Washington, DC 20545
71. M. Gordon Wolman, The Johns Hopkins University, Department of Geography and Environmental Engineering, Baltimore, MD 21218
72. Office of Assistant Manager for Energy Research and Development, Oak Ridge Operations, P. O. Box E, Department of Energy, Oak Ridge, TN 37831
- 73-99. Technical Information Center, Oak Ridge, TN 37831